Utrecht University

A digital twin model for congestion management and market optimization

A case-study of industry park Wetering-Haarrijn and Lage Weide in Utrecht, the Netherlands

Name: Hasko Schortinghuis
Student number: 6858953
Course code: GEO4-2510

Main supervisor: Dr. Ir. Ioannis Lampropoulos
Daily supervisor: Simone Coccato M.Sc.

2nd Reader: Prof. Dr. Wilfried van Sark

Utrecht University

Abstract

The electricity grid is increasingly burdened as energy demand rises and various renewable energy generation technologies are integrated. These technologies become more economically profitable, and so are battery energy storage systems (BESS). Renewable energy generation is subjected to tempo-spatial weather conditions and peaks in generation require large grid connections for limited amount of time. This leads to increased grid contract costs for end-users. Besides, the grid becomes satiated with high grid contracts, while the contract size is not often fully utilized. Sizing down grid connection while not controlling energy power flow can lead to congestion, where power flow exceeds nominal capacity.

In this research, a case study is conducted on two industrial sites using a digital twin approach and finds the optimal utilization of a BESS in a trade-off between self-consumption, grid fees, battery degradation, and subsidy schemes. While these factors are researched on individual basis, the combination of those is not found in research. Multiple battery control strategies are proposed using case-study data and developed in Python, using Gurobi optimization. Results show degradation is decisive for model behavior, nevertheless, still results in economical attractive solutions. Photovoltaic (PV) generation peaks combined with insufficient BESS capacity raise grid connection, despite raising grid tariff costs. This only applies when there is a large difference in local PV generation and demand and as a result, the system encounters excessive PV generation, which is required to flow through the grid connection. Considering grid fees, self-consumption is deemed not the optimal control strategy, as it pushes the battery to charge and discharge to the grid at non-ideal times and with non-ideal quantity. Subsidies based on grid injection change model behavior and show potential but can only be feasible with sufficient surplus PV generation. This research shows that multiple aspects determine the optimal economic benefits and shows that these aspects are case study specific, and lead in particular to case study specific recommendations. This research also shows that ideal BESS operation is determined by multiple monetary flows as grid fees, subsidy schemes, electricity costs, and that degradation is a decisive factor.

Keywords: battery energy storage system, congestion, digital twin, control strategy, Gurobi, battery degradation, self-consumption, grid fees, subsidy, renewable energy, photovoltaic

Nomenclature

Acronym	Definition
BESS	battery energy storage system
CO2	carbon dioxide
CPB	congestion management & power balancing
DoC	depth of cycle
DT	digital twin
EFR	enhanced frequency response
ENTSOE	european network of transmission system operators for electricity
ESS	energy storage systems
ETPA	energy trading platform Amsterdam
EV	electric vehicle
FCR	frequency containment reserve
FRR	frequency restoration reserve
GBM	generic battery model
GFM	grid fees model
GHG	greenhouse gas
GOPACS	grid operators platform for congestion solutions
HV	High voltage
ID	intraday
IoT	internet of things
IV	Intermediate voltage
LFC	load frequency control
LFP	lithium iron phosphate
LER	limited energy reservoir
LV	Low voltage
IPCC	intergovernmental panel on climate change
LDC	load duration curve
MV	Middle voltage
NP	net dependency
PV	photovoltaics
RES	renewable energy sources
RR	replacement reserves
SCM	Self-consumption model
SoC	state of charge

Parameters		Meaning
η_c		battery charging efficiency
η_d		battery discharging efficiency
Δt		duration of timestep
b		number of cycles under full cycle depth
C_{bat}	[€]	battery investment costs
$C_{demanddata}$	[€]	dataset demand electricity costs
$C_{SDEbasic}$	[€/kWh]	basic SDE costs
C_{STpmax}	[€/kW/month]	stedin peak grid power costs
C_{STcont}	[€/kW/month]	stedin grid contract costs
Cap_{bat}	[kWh]	battery capacity
E_{FCR}	[€/kWh]	FCR price
E_{price}	[€/kWh]	electricty price
$f_{alertdown}$	[Hz]	alertband lower boundary
$f_{alertup}$	[Hz]	alertband upper boundary
$f_{deadhigh}$	[Hz]	deadband upper boundary
$f_{deadlow}$	[Hz]	deadband lower boundary
f_{grid}	[Hz]	grid frequency
$freq_{nom}$	[Hz]	nominal grid frequency
m	[-]	curvature line full equivalent cycles vs cycle depth
P_{alert}	[kW]	alertband power

P_{batmax}	[kWh]	
P_{demand}	[kWh]	demand dataset
P_{FCRmax}	[kW]	maximum allocated FCR power
$P_{gridmax}$	[kWh]	grid max power
$P_{gridmaxdata}$	[kWh]	dataset maximum grid power
P_{PV}	[kWh]	PV generation
$R_{SDEbase}$	[€/kWh]	SDE base amount
SDE_{maxPV}	[€/kWh]	SDE based on PV generation
$SDE_{maxgrid}$	[€/kWh]	SDE based on grid injection
SoC_{lb}	[€]	state of charge lower boundary
SoC_{ub}	[€]	state of charge upper boundary
WF_A		group A weight factor
WF_B		group B weight factor
$WF_{surplus}$		surplus weight factor

Variables		**Meaning**
C_{elgrid}	[€]	grid electricity costs
C_{deg}	[€]	degradation costs
C_{GFpmax}	[€]	grid fees maximum grid power costs
C_{GFcont}	[€]	grid fees contract costs
C_{GFsum}	[€]	grid fees sum costs
Cyc_{deg}	[%]	degradation cyclic
Con_{grid}	[%]	congestion grid
Con_{contr}	[%]	congestion contract
DSoC	[%]	delta state of charge
E_{req}	[kWh]	total BESS power delivery during congestion
E_{tot}	[kWh]	total consumed power
NP	[%]	net dependency
P_{ch}	[kWh]	power battery in
P_{disch}	[kWh]	power battery out
P_{FCR}	[kW]	FCR power
P_{grid}	[kWh]	grid power
$P_{gridext}$	[kWh]	grid extract power
$P_{gridextmax}$	[kWh]	grid extract maximum power
$P_{gridinj}$	[kWh]	grid inject power
$P_{gridinjmax}$	[kWh]	grid inject maximum power
$P_{gridnew}$	[kWh]	new grid power
$P_{gridnewmax}$	[kWh]	new grid maximum power
$P_{surplus}$	[kWh]	surplus power
$P_{conpeaknoBESS}$	[kWh]	peak congestion no BESS
$P_{conpeakBESS}$	kWh	peak congestion BESS
SC	[%]	self consumption
SS	[%]	self sufficiency
SoC	[%]	state of charge
SoC_d	[%]	delta state of charge
SoC_{dabs}	[%]	absolute delta state of cahrge
R_{FCR}	[€/kWh]	FCR revenues
R_{sub}	[€/kWh]	subsidy revenues
R_{SDE}	[€/kWh]	SDE total revenues
R_{SDEPV}	[€/kWh]	SDE PV revenues
$R_{SDEgrid}$	[€/kWh]	SDE grid inject revenues
R_{tot}	[€/kWh]	total revenues

Utrecht University

Contents

1. Introduction

1.1 Background research

Over the last years, the severity of human-induced global warming caused by anthropogenic climate change has been pronounced (Höök & Tang, 2013). The annual carbon dioxide (CO_2) emissions of 2021 were the highest ever recorded, and the latest Intergovernmental Panel on Climate Change (IPCC) report showed that humankind is running out of time to prevent irreversible processes regarding the current climate (IEA, 2022; IPCC, 2022). With continuing economic growth and increasing energy demand, energy generation without fossil fuels such as renewable energy is inevitable (Höök & Tang, 2013).

While renewable generation does not produce CO_2 emissions, the amount of energy generated by renewables is entirely dependent on tempo-spatial weather conditions such as the amount of solar irradiation or wind velocity (Gowrisankaran et al., 2016). Because of intermittency, renewables do not provide the constant power output generated by fossil fuel-based power plants, and a mismatch in demand and supply can occur (Idem).

There are different methods and places to generate renewable energy. A single PV (Photovoltaics) panel can be placed in a variety of places, but PV parks require large surface areas. Due to growing food demand, many rural regions are used for agricultural purposes (Calvert & Mabee, 2015). However, placing PV panels on rooftops and facades in urban areas lowers the burden on the climate by increasing local generation (Kobashi et al., 2021). In 2019, in the Netherlands, the greenhouse gas (GHG) emissions CO_2-eq were attributed by 12.34% to the built environment and 30% to the industry (PBL Netherlands Environmental Assessment Agency, 2020).

A PV-based system is currently the least-cost option for domestic distributed electricity generation (IRENA, 2021). With prices expected to fall further, the popularity of PV can only be seen as increasing further in the future (Vartiainen et al., 2020). However, the issue hindering the diffusion of solar power is the intermittency, with generation varying both on daily, seasonal, and annual timescales (Engeland et al., 2017). There are several ways the mismatch between generation and consumption can be solved. For instance, if a grid connection is available, this connection can be used to balance consumption by allowing the purchase of electricity when needed and selling surplus electricity when available. Another option is to store surplus energy for later use with suitable energy storage methods (Puranen et al., 2021).

Battery energy storage systems (BESS) can balance the intermittency of renewable energy sources (RES) and increase self-consumption, allowing the storage of energy produced during peak solar activity to be used during peak demand hours. Currently, in the Netherlands, the net metering rule is in effect, allowing consumers to sell back electricity to the grid and contributing to residential PV deployment (IEA, 2020). This rule will be abolished in 2031 and revenues start to decrease from 2025 (Rijksoverheid, 2022). Therefore, selling energy back to the grid might not be appealing soon, incentivizing self-consumption. This will mainly affect residential customers because net-metering applies to clients connected to the grid through a connection with a value smaller or equal to 3*80A (RVO, 2022b). Industrial sites with larger grid connections are not affected by the net metering rule.

A new technology that can increase the potential of a BESS is a model created in a digital environment, so called a digital twin (DT). This digital entity is tied to a real-life counterpart in which a process or system is described with (live) data (Palensky et al., 2021). Since the DT uses (live) data, development of the Internet of Things (IoT) increases the connectivity between the physical component and its digital counterpart. DT applications can be categorized in three perspectives: data related technologies, high-fidelity modeling technologies, and model-based simulation technologies (Liu et al., 2021). Data related technologies focus on data collecting, data mapping, data processing and data transmission. High-fidelity modeling means a physical model is recreated in a digital environment, with thorough understanding of physical properties and mutual interactions. By having this understanding, some parts of the model can be modeled in greater detail than others. Because model-based simulation enables interaction with the physical entity in real-time, this perspective can be applied to the energy system. This can result in optimized regulation in grid voltage distribution and congestion levels (Palensky et al., 2021). Using a DT, grid-tied appliances can optimize their operations since they can anticipate environmental situations and peer behavior (Idem). This can lead to reduction in environmental footprint and carbon emissions (Yu et al., 2022).

1.2 Research gap

Research has shown that the continuing development of BESS and therefore reduction in cost, makes the technology a favorable solution for grid applications (Gundogdu et al., 2017). BESS can be used for frequency regulation, electricity arbitrage, ancillary services, and reserve services (Idem). Earlier research shows that using a BESS as an Enhanced Frequency Response (EFR) mechanism can generate revenues, and that these revenues are highly dependet on maintaining a certain State of Charge (SoC) and controlling degradation costs (Xu et al., 2014). A certain SoC can be controlled by a battery control scheme, which regulates charging and discharging of the battery. An example of this is by selling or buying electricity on the intraday market. If a BESS is combined with a PV forecast model, revenues increase (Choi et al., 2021).

While the research by Xu et al. (2014) demonstrates the ability to use BESS as a revenue source, it is unclear whether the operating strategies proposed are feasible while minimizing congestion in a similar time frame.

Other research has shown that when the objective function is to minimize congestion, this can be reduced if the BESS operates with this strategy (Mohamed et al., 2020). This means the battery can mitigate grid congestion and serve to lower grid connection. Tiemann et al. (2020) demonstrates BESS are economically attractive for grid fee reduction when used for peak shaving. The payback period of BESS is determined by capacity based on load profile. Bloch et al. (2019) shows battery degradation can determine the battery control scheme and degradation costs should be included into the model objective function. The self-consumption control scheme is widely used in PV-BESS systems (Nair et al., 2020). If self-consumption is combined with a model predictive controller, grid congestion and battery degradation reduce (Idem). However, no trade-off is made with grid fees.

From research it is not clear what control scheme can be applied which lowers the grid connection, and finds a trade-off between self-consumption, grid fees, battery degradation, and subsidy schemes.

A case study investigation in this field of research is relevant because by minimizing grid congestion, the energy transition towards renewables is less constrained by mismatch in PV and demand. In practice this means the grid contracts of energy consumers can be lowered, and more room on the grid is created for new consumers. High grid contracts are mandatory because mismatch in PV and demand causes high peak grid power.

Meanwhile, BESS that can minimize grid connections need to be economically competitive. The case-study can be used as an example for industrial sites with large surplus in PV generation over energy demand, and when demand is higher than PV generation.

1.3 The case-study

This thesis is performed within the Congestion-management & Power Balancing (CPB) project. The CPB project is part of a European support scheme, REACT-EU regeling 2021. This support scheme incentives regional economies on a green and digital basis (EFRO, 2021). The CPB project involves two industry complexes in Utrecht, Lage Weide and De Wetering-Haarijn. The partners involved are EnergieCollectief Utrechtse Bedrijven, Berenschot, Friday Energy, REConvert, Stamhuis, Warmtebouw, University Utrecht and University of Applied Sciences Utrecht. Jointly the net congestion problem is targeted. What the congestion problem entails, is that for industry complexes an increase in energy demand results in overload of the local network. Therefore, entrepreneurs located on these industry complexes are not able to install solar panels or stimulate electrical vehicles (EVs) by placing charging stations, which inhibits growth of the energy transition and retards sustainable economic growth. The solution used to solve this problem in the CPB project is to coordinate supply and demand on the industry complex by using smart technologies (ECUB, 2021). These smart technologies are combined in a DT, which is the final delivery of the CPB project. Through the development of a DT the congestion problem is solved, using smart technologies installed a Warmtebouw and Stamhuis, such as cloud camera and sustainable energy generation and storage, with a battery storage capacity of 390 kWh and 1.3 MWh respectively. By using sustainable local generated energy, self-sufficiency increases, and grid reinforcement is avoided.

1.4 Problem definition and research aim

A better balance of generation and sustainable energy use can be achieved using smart digital techniques and BESS. The goal is to take advantage of more renewable energy by storing it into a BESS, or to inject it into the grid. This goal can be achieved by using a BESS control scheme. If this control scheme is not in place or, if there is no BESS installed, large surplus in PV generation over demand can lead to congestion. Congestion occurs if the power flow through a cable/network is above its nominal capacity. It does not necessarily mean that large surplus in PV generation over demand does not create congestion, yet more power is injected into the grid, which could be above the connection nominal capacity.

Because of this, there must be a thorough understanding of the placement and capacity of the renewable generation technologies in the industrial parks. In this case-study, the renewable energy technology is PV. The location and orientation of PV panels could also play a role in leveling out energy generation with PV panels distributed over the east and west side of building facades. This research aims to find optimization, using the programming language Python and optimizer module Gurobi, for battery usage while considering battery efficiency, degradation, and minimizing grid congestion. Python is a programming language which emphasizes readability (van Rossum, 2007). Gurobi is a solver for linear mathematical optimization problems (Meindl & Templ, 2012).

According to the previously mentioned points and the need for a deeper understanding of the specific field, the following research question is formulated.

What is the optimal utilization of a BESS using a digital-twin model?

To answer the main question, this is broken down into the following sub-research questions to include aspects such as technical, economic performances, and scenario analysis:

1. **Which are relevant applications for BESS?**
2. **Which different scenarios can be developed which are in-line with the case-study?**
3. **What are the requirements for a functioning generic model?**
4. **What knowledge is required to transform the generic model to a case-study applicable model?**
5. **How can a digital-twin model be developed in Python and to what constraints is it subjected?**
6. **How can BESS be modeled regarding efficiency, aging, and degradation?**
7. **Which results and provision of recommendations are produced in this research?**

1.5 Research scope and boundaries

In this thesis a multi-revenue costs analysis will be conducted on a distribution network with an installed BESS and local PV generation. This thesis mainly focuses on local services (Table 1), and on one balancing service, FCR. There are several boundaries to this project. The battery specifications are fixed and provided by Friday Energy. This means there are pre-defined boundaries for battery power and capacity. The installed PV generation is not analyzed on orientation and tilt. Historical data is used, that means there is no use of solar forecasting data. This concept is later added to the project and is not part is this research. By using historical data, the BESS cannot be optimized on real time data e.g. weather conditions and electricity market updates. Therefore, it is not possible to determine ideal scenarios based on large variation in data with use on artificial intelligence. Within the scope of this thesis is the creation of a model which has diverse battery strategies using Python, that can be used by external parties and where the input parameters can be easily modified. These strategies are based on subsidy scheme, battery degradation and grid fees. As a result, an economic analysis is made over a certain duration of historical data.

2. Theoretical background

2.1 Literature review on BESS

In this section, a literature review is conducted on BESS to get an understanding of the technology by answering the first research question;
- Which are relevant applications for BESS and what is their working principle?

Another part of understanding BESS is a literature review in which the current state of the technology will be mapped. The libraries and keywords used are provided in Appendix A.

A BESS can fulfill different services in the electricity grid. These services, as can be seen in Table 1, Overview of BESS servicesare local services, national services, and network services. As described in the research scope, Utrecht University will focus on local scale and therefore local services. However, multiple sources of income are required for BESS-business cases to be successful (Invest NL, 2021). Therefore, a combination of local and network services might be mandatory to improve the revenue streams of BESS (Invest NL, 2021). Because of the significant BESS' capacity, the BESS can be divided into smaller parts which are each allocated to a unique service. Another option could be that different services run simultaneously. In the first section, local services are explained. In the second section, network services are explained.

Table 1 Overview of BESS services

Service layer	***Service type***	***Source***
Local services	Increase self-consumption PV	(Sevilla et al., 2015)
	Decreasing net dependency & net costs	(Shayeghi, 2020)
	Increase net capacity	(Nair et al., 2020)
	Congestion management	(Invest NL, 2021)
National market and services	Day-ahead	(Invest NL, 2021)
	Intraday	(Invest NL, 2021)
	System balancing (FCR/FRR)	(Tennet, 2022)
	Generation optimization	(Invest NL, 2021)
Grid services	System adequacy	(Dratsas et al., 2021)
	Congestion management (GOPACS)	(Invest NL, 2021)
	Grid capacity management	(Invest NL, 2021)

2.1.1 Local services

Demand side management (DSM) is a working principle in which demand sided energy flow is altered to enhance demand response and energy efficiency (Behrangrad, 2015). Figure 1 shows the DSM options demand response, energy efficiency and self-consumption (Lampropoulos et al., 2020). Except for one, all DSM options are relevant in this case-study, as industry site installed energy technologies are unable to influence the industrial sites' energy efficiency. Relevant DSM options are combined with the service types from Table 1 and discussed in the sections below.

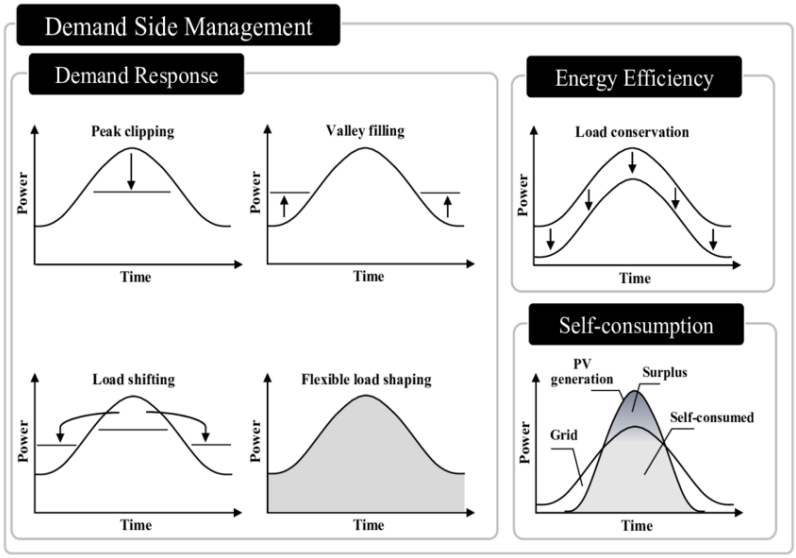

Figure 1 DSM options from (Lampropoulos et al., 2020)

Increase self-consumption and decrease net dependency

Self-consumption can be expressed as the amount of local generated and consumed electricity in respect to the local amount of PV generation, see equation 1 (Ciocia et al., 2021). This prevails grid dependency and decreases grid electricity costs (Nyholm et al., 2016).

$$SC^t = \frac{E^t_{local}}{E^t_{gen}} \qquad eq.(1)$$

In case of mismatch in PV supply and industry site demand, excessive energy can be stored in the BESS. Stored energy can be used at a later moment in time to fulfill the demand of the industry site. Energy can also be bought from the grid and stored in the BESS. By doing so, the industry site load is shifted to another moment in time. Therefore, the peak of the demand is removed. Self-consumption is incentivized by grid electricity prices as this drives the costs. When grid electricity prices are high it is beneficial to increase self-consumption (Castillo-Cagigal et al., 2011). From the BESS perspective, this can only happen temporarily as the level of DSM is limited by storage characteristics. The battery SoC can only operate between certain thresholds. These thresholds can be set to prevent deep cycle events, or to reserve capacity for other services, for example net capacity. On the other hand, early full charging on the day of BESS results in high SOC dwell time. This leads to feed-in of peak PV power into the grid. If this happens simultaneously across many PV systems, this can lead to grid congestion and voltage rise (Resch et al., 2015). Self-consumption can be increased by introducing a two-price grid scheme (Sevilla et al., 2015). A high grid price incentives direct use of energy from the BESS and in case of a low electricity price, energy is bought from the grid. If demand is lower than PV generation, energy is stored in the battery for later usage. If for a prolonged period demand is higher than PV generation, operation with a self-consumption scheme is not sustainable as the battery SoC decreases.

Self-sufficiency is the level of which the local generation is sufficient to fill the local demand, see equation 2 (Luthander et al., 2015). It quantifies user independence from the grid.

$$SS^t = \frac{E^t_{local}}{E^t_{load}} \qquad eq.(2)$$

Net dependency (ND) differs from these concepts in a way that it expresses the local power generation in respect to the sum of local power generation and grid electricity (Shayeghi, 2020). A lower NP leads to lower grid electricity costs. See equation 3 for net dependency.

$$NP^t = \frac{E^t_{gen}}{E_{gen} + E_{grid}} \qquad eq.(3)$$

Net capacity and congestion management

A BESS with DSM load shifting strategy induces a lower peak demand. A BESS can provide temporary local energy injection of peak demand through DSM, acting as peak shaving load control. If the BESS is considered a microgrid, the BESS increases net capacity. If the grid limitation is exceeded, congestion occurs. The time congestion occurs can be expressed as the time the load exceeds the grid threshold (Chua et al., 2016). This is depicted in Figure 2**Error! Reference source not found.** as grey surface area between t_a and t_b. The level of congestion and simultaneously required peak power of the BESS is the difference between P_{max} and P_{UTh} (Figure 2). Without BESS, congestion should be as low as possible. With a BESS installed, the BESS can provide power in the congestion zone. In this case, the value expresses the time the BESS and possible forced higher grid connection provides uninterrupted power delivery. A load duration curve (LDC) gives insight into the amount of time a certain load occurs. With use of LDC's the level of congestion is determined in the results.

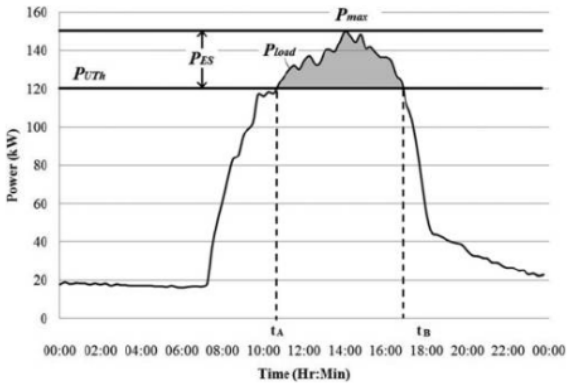

Figure 2 Generic load profile from (Chua et al., 2016)

The mandatory power delivery form BESS can be expressed as follows (5):

$$P^t_{ES} = P^t_{load} - P^t_{UTh} \qquad eq.(5)$$

The total energy required from the BESS during congestion can be expressed as (6):

$$E_{req} = \int_{t_1}^{t_2} P^t \Delta t \qquad eq.(6)$$

Congestion can therefore be quantified as a percentage of the total energy consumption over a given period, equation 7.

$$Congestion\ (\%) = \frac{E_{req}}{E_{tot}} \qquad eq.(7)$$

There are several key performance indicators (KPI) to quantify the model results, see Table 7. From this theory section these are; equation 5, 6 and 7.

2.1.2 System balancing

A BESS can provide balancing services as can be seen in Table 1. These services can be offered to grid operators and the economic potential lies in stacking several revenue streams (Invest NL, 2021). These revenue streams include system adequacy services such as Grid Operators Platform for Congestion Solutions (GOPACS), frequency containment reserve (FCR), frequency regulation reserve (FRR) and grid capacity management. Services with the most economically attractive potential are FCR and passive balancing (Invest NL, 2021). The grid frequency varies depending on the load and supply and therefore, several load frequency control (LFC) systems are in place. LFC systems are categorized in primary, secondary and tertiary control systems, also known as FCR, FRR and replacement reserves (RR) (Ersdal et al., 2016)

FCR

There are strict requirements by the European Network Transmission System Operator for Electricity (ENTSO-E) to which a system providing balancing services must adhere. BESSs have a limited energy reservoir (LER) compared to other energy storage systems (ESS). These could be chemical bonding based, such as hydrogen storage, or work with kinetic energy, e.g. hydro storage. The service FRR is regulated to require a minimum bid size of 5 MW. Due to their LER, BESS are often used to provide FCR, which requires a minimum bid size of 1 MW (Marchgraber et al., 2020). FCR services require continuous SoC management. A stand-alone BESS, which means it is separated from other ESS and thus limited in capacity, requires to have at least 125% rated power against contracted power (ENTSO-E, n.d.). In case of a grid frequency deviation of > 200 mHz, 1 MWh capacity per 1 MW contracted power is required to have sufficient energy capacity. Also, with a grid deviation > 200 mHz the allocated volume needs to be injected into the grid in 30 seconds. See Table 2 for the annual average FCR price (TenneT, 2021). FCR services are usually delivered for 4 hours (ENTSOE, 2022a). The total FCR power in the Netherlands available by TenneT is 111 MW (TenneT, 2022).

Table 2 Average historical FCR price (TenneT, 2022)

€/MWh	2019	2020	2021
Yearly average FCR price Dutch auction	15.5	20.4	24.0
Yearly average FCR price common auction	9.4	7.3	17.8

Another way of maintaining system balance is passive balancing (Koch & Maskos, 2019). This service enables participants to sell their services on the intraday (ID) market against actual imbalance prices and works parallel with services from grid operators, such as FRR. Given a certain market price and lower imbalance price, there is incentive for a portfolio to fill energy shortage with the lower imbalance price. Imbalance in this portfolio can be caused by incorrect weather forecasts, such as reduced PV generation. The difference between market price and imbalance price is called the imbalance price delta. This concept enables market parties to make revenues. See Table 3 for the historical imbalance price delta in the Netherlands (TenneT, 2021). On the ID market the minimal tradable volume is 0.1 MW.

Table 3 Average historical imbalance price NL (TenneT, 2021)

€/MW/h	2019	2020	2021
Average imbalance price delta short system	16.4	27	27
Average imbalance price delta long system	16.4	25.4	25.4

In contrast to FCR, selling energy on the ID market requires smaller quantities of trading volume. The BESS at Stamhuis and Warmtebouw can serve both services.

Congestion management (GOPACS)

Another service both BESS systems are eligible for is GOPACS. This is a collaboration between grid operators where local congestion is tackled by placing an order to produce local energy on the COPACS wholesale market. To prevent regional frequency disturbances, a sell order is placed elsewhere outside the local area. A difference in price between buy and sell orders is paid by the grid operator. Taking part in COPACS can be done via the ID market of energy trading platform Amsterdam (ETPA). Using the ID market, the minimal trading volume is 0.1 MW. See Table 4 for the historical average price of ID Congestion Spreads (IDCONS) (TenneT, 2021).

Table 4 Average historical price IDCONS (TenneT, 2021)

€/MWh	2019	2020	2021
Sell price	115	107	280

2.2 Digital twin design

In the this section, a literature review on the DT is conducted, and the DT is designed. The libraries and keywords used are provided in Appendix A. By doing this, the fifth sub-research question is answered:

- How can a digital-twin model be developed in Python and to what constraints is it subjected?

Once the industry park is recreated into a digital environment, the DT should be able to replicate the real-life counterpart. At first, this is done with historical data and eventually live data will be used to determine optimal solutions. It needs to be identified what type of DT is required to gain the desired outcome, since a more detailed model does not guarantee more accurate results. Yu et al. (2022) proposes a framework which classifies different DT families, see Figure 3.

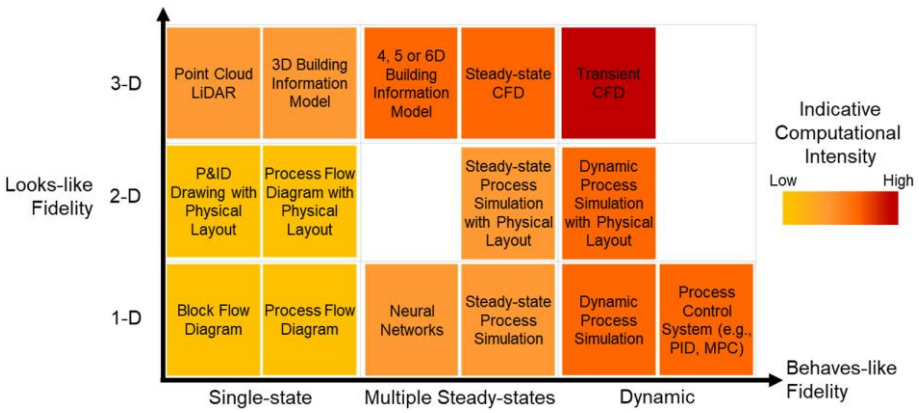

Figure 3 Digital twin families from Yu et al. (2022)

With the introduction of industry 4.0 (4th industrial revolution), the DT is a foundation of digital transformation (Pang et al., 2021). Typical for industry 4.0 is the integration of software and physical systems in sectors and industries (Lasi et al., 2014). In this thesis the focus will be on the energy sector. A DT is not only a digital counterpart of a real-life entity, but also a whole new way of exploring limits and decision making at system operations of existing technologies (Palensky et al., 2021). A challenge from a technical point of view is the digitalizing legacy of products, as it is resource intensive whilst there is generally a lack of information. This is not applicable to the CPB project as it is completely new. However, the DT in the CPB project requires data flow from sensors, and this data flow must be monitored which requires workforce. Because the DT concept is new, the switch from conventional models and data to a new truth can create social challenges. In the CPB project this is not applicable because there is deliberately chosen to use a DT technology from the start.

Limits that can be explored using a DT can include pushing the efficiency of the system or predicting mistakes. These can also be described as the goal or purpose of the DT. In Moghadam et al. (2021) the DT is used as a measure of observable characteristic performance of PV energy conversion. Because in real life, PV panel systems are prone to ways of reduced energy output e.g. dirty panels, interconnect failures, capacitor or inductor deterioration ect., a fault analysis method is performed in a matrix to measure a residual error. In this case, the DT is used to predict the difference between expected and calculated output. This is an interesting way of using the DT, because it not only encompasses a digital system, but mimics it in a much more detailed way. This proposed level of detail will not be applied in the CPB project at this moment in time.

The DT model can be expanded into the future with error calculations included. In the CPB project the aim is to have a virtual test bed that can predict optimized scenarios without using real life counterparts. Thereby, components are not put into use, and in case of a BESS, prevent degradation and extend lifetime. Unrealistic or potentially dangerous situations can be simulated, by pushing certain components of the system. These could be grid connections or asking maximum power from the BESS for prolonged periods, which can lead to heat building up. According to the EU, digitalization of the BESS application sector is directly linked with DT systems. Those systems will provide forecasting, optimal operation and preventive maintenance whilst improving safety and reliability. The BESS of an industrial park can be utilized as efficiently as possible. The DT in the CPB project is an aid in finding a trade-off between monetary flow and system hardware characteristics based on energy efficiency. Industry site specific characteristics are described in section 4. Based on the framework by Yu et al. (2022), the DT is a dynamic process simulation with physical lay-out.

3. Methodology

3.1 Methodological steps

To answer the research question, a model is developed to create an optimum between market revenues and congestion management. From the research question, sub-research questions are created which are linked to methodological steps, see Figure 4. The sub-research questions will be answered by a literature review, an assessment on the functionality of the model, or by gathering case-study specific data. Some sub-research questions will be answered in the theoretical background. The theoretical background is presented in the next chapter and consists of a literature review and elaborates concepts used in this thesis. The methodology is presented after the theoretical background and will answer several sub-research questions as well. In the methodology the process of data collection and model building is described. Besides, the aim of the models and pathway towards the results are described. In the results the flow charts of models as well as model results are presented, answering the last sub-research question.

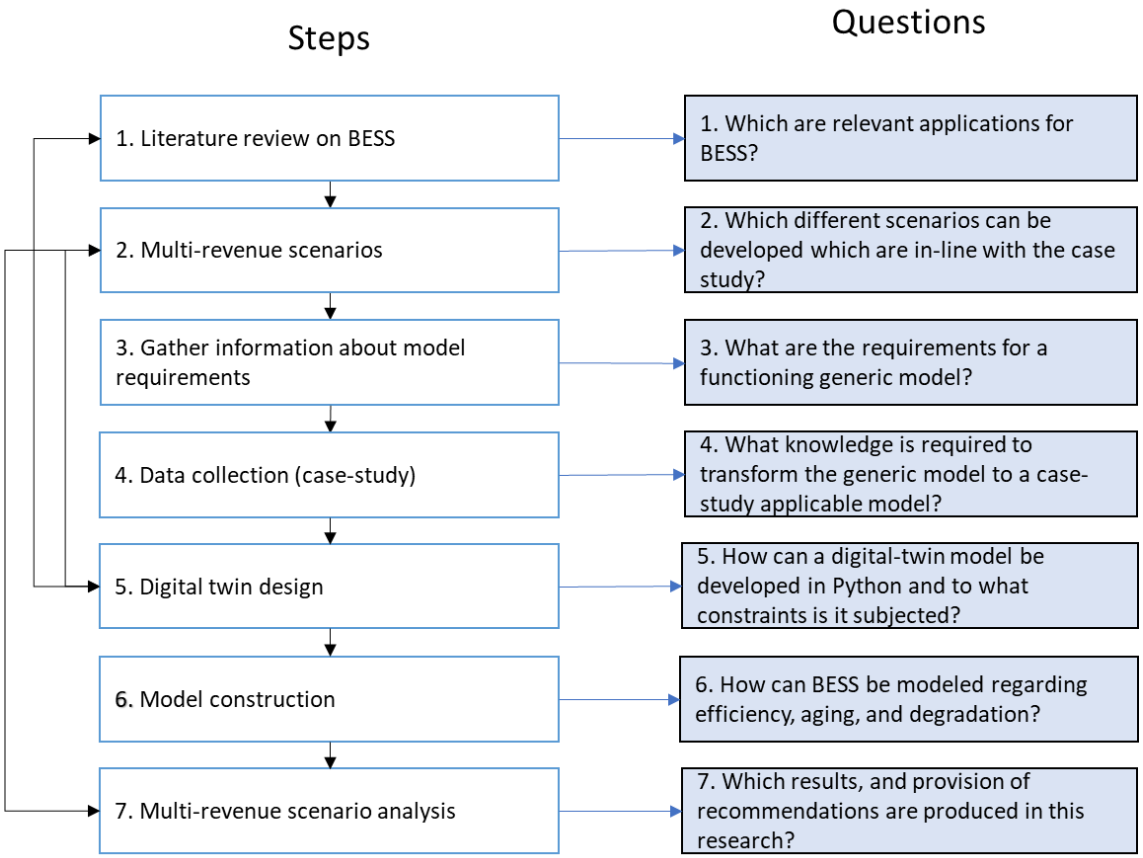

Figure 4 Top-down chart methodological steps

3.1 Data collection

To calculate the economic assessment of a BESS installed in the industrial sites, input data from the user is required. There are several partners involved in the CPB project, but for this thesis not all partners play a part to the same extent. An overview of contact persons and level of involvement is given in Table 43. Once per 2 months there is a partner meeting where partners give an update on their progress and questions can be asked directly. Because most of the time partners are working simultaneously but independently, the progress is supervised by John Eisses. If a partner is in need of contact information or an immediate answer, John Eisses can be contacted. Seen from the perspective of the thesis, the most important contact persons are Harald Kor working for Stamhuis, and Rik Hartog working for Warmtebouw. They provide datasets, subsidy contracts and Stedin contracts of the specific industry site and grid connections. The data is not shared outside the supervisor, reviewer, and partners.

3.2.1 Data types

Industry specific data

From the industry side, two types of data can be gathered. First, there is data used in the model which updates each timestep. This data consists of local PV generation, energy demand and power extracted from and delivered towards the grid (P_{grid}). The data has a 15-minute resolution. The PV power generation, energy demand and exchange with the grid P_{grid} are measured for Stamhuis and Warmtebouw with a sensor linked to a local installed transformer. Second, there is data depending on contracts and topology of the industrial sites. The industrial sites have contracts regarding subsidies, electricity price and grid infrastructure. This later used data can vary from time to time, but is obliged to a contract, and not limited to periodic solar generation or demand. The topology determines the location of grid connections and placement of batteries and solar panels.

The first type of data is retrieved from the year 2020. In the second type of data, subsidies and electricity prices are retrieved from the year 2020, whilst topology data is used from the current state of the industry parks.

Grid data

The historical national grid frequency [Hz] used to determine FCR is retrieved from RTE (RTE, 2020). The retrieved data is in intervals of 10 seconds and is scaled towards 15-minute intervals.

The historical FCR price is retrieved from European network of transmission system operators for electricity (ENTSOE) and is available from 21-04 onwards in the year 2020 (ENTSOE, 2022b). FCR prices [€/MWh] are fixed in 4-hour bidding blocks and in 15-minute resolution. Frequency data is analyzed using SPSS 29 (IBM Corp., 2022) to highlight outliers and calculate averages. Grid fees gathered from Stamhuis over the year 2020 apply to both industrial sites (Stedin, 2022b).

An overview of data and units is given in Table 5.

Table 5 Overview data and units

Type	**Unit**	**Source**
PV generation	kW	Industry site
Demand	kW	Industry site
Pgrid	kW	Industry site
Subsidy	€/kWh	Industry site
Electricity price	€/kWh	Industry site
Topology		Industry site
Grid frequency	Hz	RTE

FCR price	€/kWh	ENSTOE

3.2 Multi-revenue scenarios

In this step, an assessment is made on possible multi-revenue scenarios by answering the second research question.

- Which different scenarios can be developed which are in line with the case-study?

Because the model is used in an industrial site, economical solutions are key in terms of cost-effectiveness. The model can determine these revenues for multiple scenarios. Because, at the same time, grid congestion also needs to be minimized, optimization in Python using the module Gurobi will be used to determine tradeoffs between revenues and grid congestion and will be elaborated further on in part five of the methodology. The grid congestion problem is researched by designing a DT of the industrial complex in Python. This model mimics the industrial complex in grid capacity constraints and uses historical data regarding generation, balance, grid load, and consumption measurements.

There are multiple control strategies feasible for the case-study and associated BESS. Several scenarios are compiled, as a scenario can fit the general characteristics of a case study more than another scenarior. It could be that the BESS's capacity is not completely utilized by a control scheme, but this can also be in line with the industrial sites' perspective. Another possibility is a control scheme where there are simultaneously multiple objectives. The division of these services can change from time to time and determining this requires machine learning. It is unlikely that this level of complexity is reached in the thesis, albeit the scenarios will increase in complexity during the project duration.

The scenarios are divided into two main categories: local services and balancing services. Local services determine the local economic benefits. An overview of the scenarios is presented in Table 6. As seen in the theoretical background these are; increase in self-consumption, decreasing net dependency & net costs, increase net capacity and congestion management. It is not mandatory for these services to be treated separately, as they can be combined to a certain extent. First, a generic model is built which acts as a foundation for model extensions, subsidies and degradation. In scenario 2, subsidies are added and in scenario 3, subsidies and degradation are added. In section 3.4 the generic model is elaborated further upon.

Table 6 Overview of multi-revenue scenarios

Scenario	Service	Model type	Model extensions
1		Generic model	
2		Generic model	+ subsidies
3		Generic model	+ subsidies + degradation
4	Local services	Congestion management	+ subsidies
5		Congestion management	+ subsidies + degradation
6		Self-consumption	+ subsidies
7		Self-consumption	+ subsidies + degradation
8	Balancing services	FCR	
9		FCR	+ degradation

After scenarios 1-3, another model is created. Scenarios 4-7 focus on local services and are divided in a congestion management model and self-consumption model. In scenario 4, the congestion management model is extended with subsidies, and in scenario 5 degradation is added on top of subsidies. Self-consumption is treated in scenarios 6 with subsidies and 7 with subsidies and degradation. The balancing service FCR is in scenario 8 treated without degradation and in scenario 9 with degradation.

3.3 Multi-revenue scenario analysis

In this step, a multi-revenue scenario analysis is conducted to give results to the research by answering sub-research question 7:
- Which results and provision of recommendations are produced in this research?

Model results are quantified with performance indicators to allow comparison between scenarios (see Table 7). The performance indicators are categorized by type. Indicators based on grid connection give insight in demand/supply ratio, and whether the current grid connection is sufficient. If $P_{gridxextmax}$ is larger than $P_{gridinjmax}$, the industry site is dependent on grid energy, with insufficient PV generation. Vice versa, there is surplus in PV generation compared to demand. For the size of the grid connection, $P_{gridmax}$ is determined based on $P_{gridinjmax}$ or $P_{gridxextmax}$. In case of insufficient grid connection, $P_{surplus}$ energy is needed. This $P_{surplus}$ energy sets the $P_{gridnewmax}$. Indicators based on monetary value give insight in revenues based on subsidies, and costs streams based on grid electricity costs. Congestion indicators show if a certain set power threshold is exceeded, and with which value. Con_{contr} shows the amount of time $P_{surplus}$ is needed. $P_{gridmaxdata}$ shows the largest P_{grid} value in the dataset. From this value can be derived if the model succeeds in finding a smaller grid connection compared to historical data. The indicator $P_{conpeaknoBESS}$ compares $P_{gridmaxdata}$ to $P_{gridmax}$. This value can be compared to $P_{conpeakBESS}$, and if $P_{conpeakBESS}$ is lower than $P_{conpeaknoBESS}$, the BESS succeeded in lowering the required grid connection. If the physical limits of the grid connection cables are exceeded, there is Con_{grid}. Degradation is measured in C_{deg} and in Cyc_{deg}, based on the degradation per delta SoC. For reference, $C_{demanddata}$ are calculated if the system would not have BESS and PV installed. Grid fees are added to calculate the costs based on max P_{grid}, C_{GFpmax}, and the contract costs, C_{GFcont}. In the results, the industrial sites are given recommendations based on the performance parameters. Not all indicators are calculated in Gurobi, and as a result not included in the model construction section. Therefore, these equations are presented here. Please note that the units of the power key performance indicators are in kW and not as in the nomenclature, in kWh. The model works with kWh values, however because this research is interested in congestion and therefore peak power, these variables are converted to kW.

Table 7 Key performance indicators

Type	Key performance indicators	Unit	Equation
Grid connection	$P_{gridxextmax}$	kW	-
	$P_{gridinjmax}$	kW	-
	$P_{gridmax}$	kW	-
	$P_{surplus}$	kW	9
	$P_{gridnewmax}$	kW	9
Monetary value	C_{elgrid}	€	15
	R_{sub}	€	18,19
	R_{tot}	€	21,23
Reference	$C_{demanddata}$	€	15
Congestion	Con_{contr}	%	7
	$P_{conpeakBESS}$	kW	-
	$P_{conpeaknoBESS}$	kW	-
	Con_{grid}	kW	7
Reference	$P_{gridmaxdata}$	%	-
Degradation	C_{deg}	€	25
	Cyc_{deg}	%	26
Grid fees	C_{gfpmax}	€	27
	C_{gfcont}	€	28
	C_{gfsum}	€	-

3.4 Generic model

In this step, the model is constructed, and the sixth sub-research question is answered:
- How can BESS be modeled regarding efficiency, aging, and degradation?

The final products are several models written in Python version 3.8.15 (Python Software Foundation, 2022). Optimization is done using the Gurobi optimizer module version 9.1.2 for academics (Gurobi Optimization, 2022). In this part the building of the models is described. First, a generic model is considered and described in section 3.4.1. This model is connected to the grid with a single connection point and provides a foundation for the grid fees model (GFM) and self-consumption model (SCM). In section 3.4.2, an SDE subsidy scheme is added to the generic model and in section 3.4.3 battery degradation. After section 3.4, the generic model construction, in section 3.5 the local service models are constructed. These are the models for congestion management and self-consumption and are applied to the case study.

The balancing service FCR is elaborated in section 3.5. The desired amount of timesteps per model and result is determined and explained in the result section as some concepts come to light in a time duration of 4-hours, per 1 day or per 2 weeks.

3.4.1 Generic model requirements

In this section, a first assessment is made of the generic model requirements by answering the third research question;
- What are the requirements for a functioning generic model?

A foundation is made by considering a generic model. After data collection, this generic model is detailed further with case study specific data. The generic model consists of three blocks: local demand, local generation and local storage. These blocks are connected with the grid by a single connection node (Figure 5). A literature review on modeling BESS is conducted to be aware of the current state. The libraries and keywords used are provided in Appendix A.

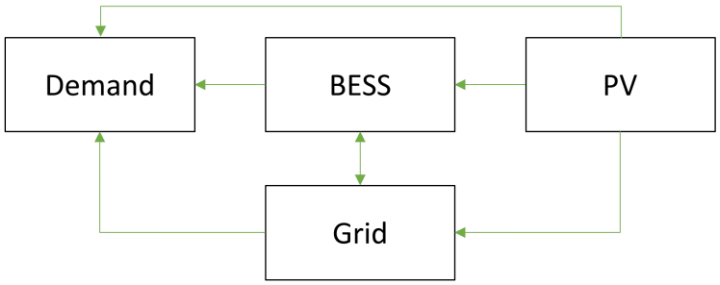

Figure 5 Block diagram power flow generic model

The input data for the model consists of PV generation, demand, grid power and the electricity price. The generic model is slightly detailed in regard to the objective function and optimizes to low grid electricity costs. By doing so, variables such as battery SoC and Pgrid change over time, but there is no incentive for economic benefits. These economic benefits are important because the full model determines a trade-off between BESS degradation and revenues. With optimization towards electricity costs, the BESS will discharge when the grid prices are high, and charge when the grid prices are low. This optimization also maximizes the use of PV energy. When the BESS is full SoC or near, the PV generated energy cannot be stored in the BESS and is fed directly into the grid. This concept is maximized when the grid costs are high at that given moment in time. The actual BESS specifications are used in the generic model, see Table 17.

Limitations on grid power, battery capacity, battery power, and battery efficiency determine the model boundaries. Because these limitations are industry site specific, they are presented in the industry section of the results. In the model are variables created to represent the nodes given in Figure 5. These variables are: $P_{gridinj}$, $P_{gridext}$, SoC, P_{ch}, P_{disch}, $P_{surplus}$, $P_{gridnew}$, and $P_{gridnewmax}$, and are subjected to the power boundaries of the system. The constraints (1-8) of the generic battery model (GBM) are:

$$0 \geq P_{gridinj}^{t} \geq P_{gridmax} \; \forall t \qquad constr.(1)$$

$$0 \geq P_{gridext}^{t} \geq P_{gridmax} \; \forall t \qquad constr.(2)$$

$$SoC_{lb} \geq SoC^{t} \geq SoC_{ub} \; \forall t \qquad constr.(3)$$

$$P_{ch}^{t} \geq Charge_{nom} \; \forall t \qquad constr.(4)$$

$$P_{disch}^{t} \geq Discharge_{nom} \; \forall t \qquad constr.(5)$$

$$0 \geq P_{surplus}^{t} \geq \infty \; \forall t \qquad constr.(6)$$

$$P_{gridnew} = Continuous\ variable \qquad constr.(7)$$

$$P_{gridnewmax} = Continuous\ variable \qquad constr.(8)$$

The grid power is constrained to the maximum power flow from and towards the grid. The level of congestion is linked to these values. The lower boundary of battery SoC is 20%, and upper boundary is 95%, as these values represent the range of usable capacity. The charge and discharge battery power are the maximum power flow in and out the battery. Surplus energy can only be positive, as it can only be added to the current P_{grid} limitation, to create a new limit called $P_{gridnew}$.

These variables are linked with the following power equations.

The battery SoC is at timestep t a function of P_{ch} and P_{disch} at timestep [t-1]. The charge and discharge efficiency are represented respectively with η_c and η_d. In the result section the initial value of SoC can change because it has influence on the results.

$$SoC^{t} = SoC^{t-1} + \frac{\left(\eta_{ch} Pch^{t-1} - \frac{1}{\eta_d} Pdisch^{t-1}\right)}{CAP_{bat}} \qquad eq.(8)$$

$$Newpgrid^{t} = P_{gridmax} + Surplus^{t} \qquad eq.(9)$$

$$P_{gridextr}^{t} \cdot P_{gridinj}^{t} = 0 \qquad eq.(10)$$

$$P_{ch}^{t} \cdot P_{disch}^{t} = 0 \qquad eq.(11)$$

For the first timestep there is no change in battery SoC allowed. This results in an alteration of equation 8.

$$SoC^{0} = SoC^{0} + \frac{\left(\eta_{ch} P_{ch}^{0} - \frac{1}{\eta_d} P_{dis}^{t0}\right)}{CAP_{bat}} \qquad eq.(12)$$

The power balance formula:

$$P^t_{demand} = -P^t_{surplus} + P^t_{PV} - P^t_{ch} + P^t_{disch} - P^t_{gridinj} + P^t_{gridext} \qquad eq.(13)$$

The optimization function is focused on the minimization of costs, this leads to the following objective function.

$$minimize \quad \sum_{t=1}^{T} E^t_{price}\, P^t_{grid}(P^t_{surplus} \cdot WF_{Surplus})\Delta t \qquad eq.(14)$$

In the objective function $P_{surplus}$ is included with a weight factor. This is because in case the grid connection is too small, a larger grid connection can be created, $P_{gridnew}$. For the model this must be the least attractive option, as it is intended in the GBM as an escape clause. Therefore, no monetary value is linked to this variable in the GBM. In the congestion management model, this can be used to determine a new minimal required grid connection for the model to work and will be elaborated in section 3.4.4.

Income can be generated by selling electricity when the C_{elgrid} is high and charging the battery when C_{elgrid} is low. The costs can be expressed as follows, and are considered negative revenues:

$$\sum_{t=1}^{T} C^t_{elgrid} = E^t_{price} P^t_{gridext} \cdot -1 \qquad eq.(15)$$

Other variations of the GBM can generate positive revenues by subsidy scheme.

The generic model is first used to exploit the potential of local services. The reference scenario has no battery degradation included. After the generic model has provided results for scenario 1 and 2, these scenarios are compared to a model with battery degradation. Using the battery degradation linked to a cost penalty in the objective function in Gurobi determines an optimal solution, and therefore using a Pareto front is obsolete.

3.4.2 Generic model SDE

Costs analysis

If SDE is in place, two types of income flows can be generated, depending on the type of SDE scheme. This is elaborated in section 4.1.5, contracts.

If there are revenues based on the maximum subsidy tariff ($R_{SDEbase}$), the SDE subsidy is calculated in the model according to the following equation (RVO, 2022a):

$$SDE_{max} = R^t_{SDEbase} - C^t_{SDEbasic} \qquad eq.(16)$$

In this equation the base amount ($R_{SDEbase}$) is the allocated subsidy amount by the Rijksdienst voor ondernemend Nederland (RVO). This *base amount* represents the cost of technology that produces the energy. The basic energy price ($C_{SDEbasic}$)is the market energy price set at a given period at the beginning of the contract. This value can change over the years, the so-called correction value, if the market or contract electricity prices changes. In case of an energy price contract with an energy supplier, this value is used. This value can be changed in the model or DT environment.

As a result, the SDE revenues are:

$$\sum_{t=1}^{T} R_{SDEPV} = SDE_{maxPV}^{t} \cdot P_{PV}^{t} \qquad eq.(18)$$

If there are revenues based on the electricity supplied from the system towards the grid, the income flow can be expressed as:

$$\sum_{t=1}^{T} R_{SDEgrid} = SDE_{maxgrid}^{t} \cdot P_{gridinj}^{t} \qquad eq.(19)$$

As the industrial sites have different SDE subsidies, per industrial site the objective function and the revenues will be elaborated upon.

Case study SDE

Stamhuis

Stamhuis has a subsidy scheme based on equation 18. See equation 20 for the objective function. Note the negative sign in front, as the subsidy scheme generates positive revenues.

$$minimize \quad \sum_{t=1}^{T} (E_{price}^{t} P_{gridext}^{t} - SDE_{maxPV}^{t} P_{PV}^{t} + (Surplus^{t} \cdot WF_{Surplus}))\Delta t \qquad eq.(20)$$

The revenues can be expressed as:

$$Revenues = E_{price}^{t} P_{gridextr}^{t} - SDE_{max}^{t} P_{PV}^{t} \cdot -1 \qquad eq.(21)$$

Warmtebouw

Warmtebouw has two subsidy schemes, one is based on equation 19 and one on equation 18 and are applied using weight factors. See equation 21 for the objective function. Note the negative sign in front, as the subsidy scheme generates positive revenues.

$$minimize \quad \sum_{t=1}^{T} (E_{price}^{t} P_{gridext}^{t} - WF_A \, SDE_{maxgrid}^{t} P_{gridinj}^{t} - WF_B \, SDE_{maxPV}^{t} PV_{gen}^{t} + (Surplus^{t} \cdot WF_{Surplus}))\Delta t \qquad eq.(22)$$

The revenues can be expressed as:

$$Revenues = E_{price}^{t} P_{gridext}^{t} - WF_A \, SDE_{maxgrid}^{t} P_{gridinj}^{t} - WF_B \, SDE_{maxPV}^{t} PV_{gen}^{t} \cdot -1 \qquad eq.(23)$$

In this case, revenues are generated by injecting energy into the grid. The SDE price is always below the grid contract price, so it is likely this energy is generated by PV. Due to this concept, it can occur that the battery in case of Warmtebouw will not be charged by PV generation, as it generates more positive revenues to feed this energy directly into the grid.

3.4.3 Generic model battery degradation

Due to time and usage, batteries age and show reduction in performance regarding capacity and power capability. The latter is caused by an increase in internal resistance (Schuster, 2016). Battery degradation can be described in different levels of complexity. There are models which calculate several battery variables in detail, for example particle surface concentration [mol/m^3] or electrolyte potential [V] (Sulzer et al., 2021). Examples of complex modelling software are Python Battery Mathematical Modelling (PyBaMM) or COMSOL (Sulzer et al., 2021). The level of complexity used in this software is considered too detailed for this thesis, and the focus will be on one ageing mechanism, cyclic ageing. PyBaMM solves physics-based electrochemical models, and details as current density, negative particle surface concentration and electrolyte concentration are not deciding for control schemes when other parameters are not equally detailed. Calendric ageing is not relevant in this study, as it is not linked to the actual usage of the battery. Calendric ageing is a linear reduction in capacity over time and is mainly dominated by cell temperature and storage SoC (Schuster, 2016). Whether the BESS is placed on a heated environment out exposed to environmental temperatures does have influence on the calendric ageing constant but is not included in this study. The battery type is lithium iron phosphate (LFP) (Friday Energy, 2022).

Cyclic ageing is dominated by the depth of discharge for each cycle. Wöhler curves express the relationship between Stress and Number of cycles and describe the influence of cycle depth on lifetime (Ecker et al., 2014). Given an equal energy output, a battery with small capacity will be subjected to a larger depth of cycle (DoC) compared to a large capacity battery. Small batteries will degrade faster due to a larger variation in DoC (Magnor et al., 2009). Swings in SoC due to unmanaged BESS behavior could lead to increased degradation and ultimately replacement of the battery, increasing the costs and questioning the economic feasibility (Shen et al., 2017).

Gurobi cannot optimize a variable that is unknown at *t* and *t-1*. In other words, delta SoC is dependent on two SoC^t and SoC^{t-1}, and this difference is unknown in the model. Therefore, it is not possible to use a standalone battery degradation model, which can be applied on the results of any of the proposed models and uses the output delta SoC to determine the degradation over these timesteps, which results in a remaining battery capacity. To include degradation into Gurobi, it is added to the objective function.

Gurobi

Two variables need to be created: SoC_d (delta SoC) and SoC_{dabs} (delta SoC absolute). These are constraints 9 and 10. The absolute values of SoC_d are required because the difference in delta SoC works vice versa, and only positive numbers are allowed the way the objective function is set up. This is done using equation 24.

$$-1 \geq DSoC^t \geq 1 \; \forall t \qquad constr.(9)$$

$$DSoC_{abs} = Continuous\ variable \qquad constr.(10)$$

$$DSoC_{abs}^t = abs(DSoC^t) \qquad eq.(24)$$

In each timestep the model is required to make a tradeoff in using the battery. As the model expresses the optimization problem in monetary flow, the battery system must be expressed using the same concept. This is achieved by expressing the investment costs (C_{bat}) of the battery as degradation function (equation 25) (Brinkel et al., 2020). Charging and discharging of the battery is only feasible if it exceeds the degradation costs.

$$C_{deg} = C_{batt} \sum_{t=1}^{T} \Phi(SoC_d)\, \forall t \qquad eq.(25)$$

From Brinkel et al. (2020) battery degradation parameters for lithium-ion batteries are retrieved. These are for b and m respectively 4084 and -0.7514. B is the number of cycles under a full cycle depth and m determines the curvature of the line representing numbers of full equivalent cycles vs cycle depth. Using these parameters, a monetary value is linked to 100 delta SoC steps. Using a piecewise linear constraint, this concept is added to the objective function.

From equation 25 the degradation per cycle of the battery can be derived and is the dimensionless degradation function $\Phi(\delta^t)$:

$$\Phi(\delta^t) = \frac{0{,}5}{bSoC_d^{m-1}} \qquad eq.(26)$$

3.5 Local services

3.5.1 Congestion management

Before the modelling of congestion management, grid fees are explained. Besides the fact that the national electricity network can be physically full at certain places, using a BESS can cause the required grid connection to be smaller. A smaller grid connection leads to lower grid fees, as there are several cost drivers based on the size of grid connection.

Grid fees

There are two types of grid fees; variable grid fees and fixed grid fees. Fixed grid fees are fees based on periodic consumption or the ability to have a grid connection. These costs are fixed per month and consist of; transport independent fee (€/month), periodical connection fee (€/month), transport fee (€/kWh) and metering fee (€/connection/month). There is also a one-time payment-based on grid connection size. A smaller grid connection can lead to lower fixed grid fees, but fixed grid fees are not the main driver of the congestion management problem. The two variable grid fees are grid fees for peak power consumed (€/kW/month), and grid fees for peak power contracted (€/kW/month). A consumer has a certain peak power contracted, and exceeding this peak power leads to significantly more costs, as the contract cannot be lowered for the next 12 months. Peak power on the other hand occurs on a few occasions annually, so lowering the peak power contracted can result in significant economic benefits. On top of the peak power contracted, there are also grid fees for peak power consumed. This fee is a monthly payment, so a lower monthly peak power results in a lower contracted peak power. Therefore, the variable grid fees are the main costs driver. See equation 27 and 28 for grid fees for peak power consumed and grid fees for peak power contracted respectively. The price of the electricity contract is based on the contracted transport power. This data is included in the data result section.

$$\sum_{t=1}^{T} C_{GFpmax} = P_{gridextmax}^{t} \cdot C_{STpmax} \qquad eq.(27)$$

$$\sum_{T=1}^{T} C_{GFcont} = P_{gridextmax}^{t} \cdot C_{STcont} \qquad eq.(28)$$

Modelling

The model uses grid tariff categories provided by Stedin, and finds an optimal grid connection in a certain range of grid tariffs, combined with the minimal possible grid connection for the model to work. As a result, load shifting will take place, as the battery will have to mitigate grid power. The smallest value of peak power consumed known, and a slightly higher peak power contract can be set up. This concept is modeled by setting a constraint on the maximum grid connection by creating two new variables called Pgridinjectmax and Pgridextractmax (constraint 11, 12).

$$P_{gridinjmax}^{t} = P_{gridinj}^{t} \qquad constr.(11)$$

$$P_{gridextmax}^{t} = P_{gridext}^{t} \qquad constr.(12)$$

$$P_{gridinjmax}^{t} = P_{gridextmax}^{t} \qquad constr.(13)$$

The value of this constraint is however unknown and minimized in the objective function (equation 29 and 30). The objective function from equation 20 and 22 are altered. As a result, the model minimizes towards minimal costs by minimizing $P_{gridextmax}$ and $P_{gridmax}$. The model is an iteration on the generic battery model and other concepts are unchanged.

Stamhuis

Objective function Stamhuis

$$minimize \quad \sum_{t=1}^{T} (E_{price}^{t} P_{gridextract}^{t} - SDE_{maxPV}^{t} P_{PV}^{t} + P_{gridextmax}^{t} \cdot \sum (C_{GFpmax} + C_{GFcont}) + (P_{surplus}^{t} \cdot WF_{Surplus})) \Delta t \qquad eq.(29)$$

Warmtebouw

Objective function Warmtebouw

$$minimize \quad \sum_{t=1}^{T} (E_{price}^{t} P_{gridext}^{t} - WF_{A} SDE_{maxgrid}^{t} P_{gridinj}^{t} - WF_{B} R_{SDEPV} PV_{gen}^{t} + P_{gridextmax}^{t} \cdot \sum (C_{GFpmax} + C_{GFcont}) + (P_{surplus}^{t} \cdot WF_{Surplus})) \Delta t \qquad eq.(30)$$

3.5.2 Self-consumption

The service is modeled by using the battery specifications as provided in Table 17, grid constraints 1-8 and equations 8-12. Furthermore, the power balance in equation 13 is used.

There can only be self-consumption if local generated electricity is available. Therefore, to maximize self-consumption, the locally stored electricity from local generation should also be maximized. This maximization is done by a battery control management that restricts energy exchange between BESS and the grid (Castillo-Cagigal et al., 2011). The BESS is incentivized to only discharge by the local load, and charge with excess PV energy, see constraint 14 and 15. However, P_{grid} always remains an option, but this option is never preferred.

$$P_{ch}^{t} = PV_{gen}^{t} \qquad constr.(14)$$

$$P_{disch}^{t} = P_{demand}^{t} \qquad constr.(15)$$

If the SoC reaches 100%, no more energy can be stored in the BESS. PV generated electricity is fed directly back into the grid, against a feed in tariff. This leads to the following constraint:

$$IF\ SOC_{100} \rightarrow P_{grid}^{t} = PV_{gen}^{t} + P_{demand}^{t} \qquad constr.(16)$$

As the SoC cannot drop below 20% SOC, no more energy can be extracted from the battery. Any demand will be supplied by the grid electricity, despite a possible unfavorable electricity price. This leads to the following constraints:

$$IF\ SOC_{20} \rightarrow P_{demand}^{t} = P_{grid}^{t} + PV_{gen}^{t} \qquad constr.(17)$$

Between SoC 20% and 95%, the control management maximizes self-consumption by constraining grid electricity. This results in the following objective function:

$$minimize \quad \sum_{t=1}^{T} P_{grid}^{t} \Delta t \qquad eq.(31)$$

This objective function varies from the objective function used in the base model. There, the objective is to find an optimum with P_{grid} and C_{elgrid}, and in this case the function is not dependent on the price. As stated earlier, an increase in self consumption leads to a decrease in net dependency and net costs. However, net dependency and net costs are not simultaneously optimized with self-consumption. The optimization of decreasing net dependency and net costs is done by minimizing the net costs, which is the base model. As self-sufficiency is another way of expressing the same concept, the optimization of self-sufficiency is therefore obsolete. Revenues are determined in a similar way as in the GBM.

3.5 Grid services

In this section the grid balancing service FCR is modeled. This service operates independently of the generic battery model and is considered a stand-alone model. While the aim of the generic battery model is the incentivization of local services due to different operating strategies, the aim of the FCR model is to maximize revenues from this service.

FCR model

The service is modeled by using the battery specifications as provided in Table 17, and constraints 1-5. The grid frequency can slightly deviate from 50 Hz and there are two critical zones, the alertband and the dead-band. The alertband is in the range of 49.8-50.2 Hz, the dead-band is in the range of 49,99-50,01 Hz. From the steady-state frequency of 50 Hz, the maximum droop to the alertband is 0,2 Hz. When this alertband is activated and the frequency deviation exceeds 200 mHz, the full FCR power must be activated in 30 seconds. The FCR power is defined by the following equation:

$$P_{FCR}^{t} = \frac{|freq^{t} - freq_{nom}|}{\Delta freq_{max}} P_{FCR_{max}} \qquad eq.(32)$$

The grid frequency f^t of each timestep is loaded into the model. The value of the deviation from the steady-state frequency is $freq^t$-$freq_{nom}$, this is called Δf from now on. The magnitude of Δf, whether it activates the alertband or is a normal deviation, is determined with the following constraints:

$$freq^{t} \geq f_{alert_{down}} \qquad constr.(18)$$

$$f_{alert_{up}} \geq freq^{t} \qquad constr.(19)$$

The alertband power, P^t_{alert}, is:

$$P_{alert}^{t} = P_{FCR_{max}} \Delta t \qquad eq.(33)$$

The main driver factor behind the power injected or taken out of the grid on time step t, P^t_{fcr}, is determined by Δf. If the grid frequency is higher than 50 Hz, energy needs to be taken out of the grid. The grid needs to be adjusted down, and the BESS is charged. This process happens the other way around if the grid frequency is lower than 50 Hz. It is assumed that P^t_{fcr} is positive if the BESS is discharged, and vice-versa.

There is also a FCR battery control management in place. There are three SOC management options; dead-band utilization, FCR over fulfillment, and scheduled market transactions. From these options, dead-band utilization and FCR over fulfillment are free of charge. Scheduled market transactions cost money which increases the BESS operational costs, but electricity sold on-the-spot market generates income. In this research, only dead-band utilization is considered. This is done because research has shown dead-band utilization is the largest contribution in SOC management (Groza et al., 2022).

When the grid frequency is in the dead-band, the BESS can be charged and discharged without additional costs and there is no need to provide FCR service. This principle is constrained by the time the grid frequency is in the dead-band zone:

$$f_{dead_{low}} \geq freq^{t} \geq f_{dead_{high}} \qquad constr.(20)$$

This results in a power flow charge and discharge equation:

$$P_{FCR}^{t} = \frac{|freq^{t} - freq_{nom}|}{\Delta freq_{max}} P_{FCR_{max}} \qquad eq.(34)$$

In which P^t_{FCRsoc} is the power flow to charge and discharge the battery. If the BESS would only charge and discharge using FCR, the SOC would vary with large amounts, and near the upper and lower boundaries of the SOC and with higher frequency deviations, FCR would not be possible.

Ideally a SOC management would be applied which charges the battery using dead-band from 20 to 50% SOC and discharges the battery from 100 to 60% SOC (Groza et al., 2022). Using Gurobi, I was not able to apply this concept, and it is therefore left out of the model.

The total energy flow of the BESS is:

$$P^t_{FCR} = P^t_{BESS} \qquad constr.(21)$$

The BESS cannot charge using the dead-band and discharge providing FCR service simultaneously:

$$P^t_{ch} P^t_{dis} = 0 \qquad constr.(22)$$

The BESS' SOC is updated with the following equation:

$$SoC^t = SoC^{t-1} + \frac{\left(\eta_c P^t_{ch_{FCR}} - \frac{1}{\eta_d} P^{t-1}_{disch_{FCR}}\right)}{CAP_{bat}} \qquad eq.(35)$$

This results in the objective function:

$$maximize \quad \sum_{t=1}^{T} (P_{ch_{FCR}} + P_{disch_{FCR}})\,\Delta t \qquad eq.(36)$$

Using this objective function, the power flow through the BESS will be maximized. This is because the power flow is related to using the dead-band, alertband and steady-state frequency. This model creates revenues by taking the P^t_{fcr} and FCR price:

$$R_{FCR} = P^t_{FCR} * FCR_{price} \qquad eq.(37)$$

3.6 Initial model conditions and variable values

Initial conditions are given to parameters and variables before the model can produce results. Conditions can change between industrial sites. First, conditions applicable to all models are presented. After that, model specific conditions are discussed.

3.6.1 Local models

In Table 8 the initial conditions of parameters and variables are presented. In the result section, it can be seen how most values are obtained. Exceptions are:

- WF_A, WF_B: These weight factors are applied using the annual generation distribution between group A and group B. Group A produces 41,907% of annual site generation, and group B produces 58,092%.
- $SF_{surplus}$: This weight factor is used because it is the least desirable option in the model. When the grid connection or grid contract are set too low, the model can become infeasible, because there is excess energy in the system. As this variable acts as an escape clause, the model must not be incentivized to use the variable.
- SoC^0: The battery starts the beginning of the simulation at SoC 0,5. By doing so, the battery can charge or discharge, and the model is not limited by reaching the lower or upper SoC boundary.
- Δt: Revenues are based on kWh, and the model computes in 15-minute resolution. This value is used to match units.
- P_{batmax}, $P_{gridmax}$: The model computes in 15-minute resolution and uses kWh for the amount of energy. Therefore, to match kWh with 15-minute resolution, the constraints are divided by 4 e.g., Stamhuis: P_{batmax} 522 kWh -> 130,5 kWh per 15 minutes.

Table 8 Initial condition local models

Parameters / variables	All models	Stamhuis	Warmtebouw
η_c	0,95		
η_d	0,95		
Δt	0,25		
SoC_{lb}	0,2		
SoC_{ub}	0,95		
P_{batmax}		130,5	39
$P_{gridmax}$		64	157,5
C_{bat}		615384	184615
C_{elgrid}		0,0423	night: 0,03326 day: 0,04624
CAP_{bat}		1300	390
C_{GFpmax}	1,457		
C_{GFcont}	0,9577		
$R_{SDEbase}$		0,112	0,074
SoC^0	0,5		
SoC_{lb}	0,2		
SoC_{ub}	0,95		
WF_A			0,41907
WF_B			0,58092
$WF_{surplus}$	1000000		

3.6.2 FCR model

In Table 9 the initial conditions for the FCR model can be seen.

Table 9 Initial conditions FCR model

Parameters / variables	All
η_c	0,95
η_d	0,95
Δt	0,25
SoC_{lb}	0,2
E_{FCR}	0,95
$f_{alertdown}$	49,8
$f_{alertup}$	50,2
$f_{deadhigh}$	50,01
$f_{deadlow}$	49,99
$freq_{nom}$	50

3.7 Sensitivity analysis

A method to illustrate the impact of the relative change of a parameter to the model output is a sensitivity analysis (Cacuci et al., 2005). There are several types of sensitivity analysis. While a sensitivity analysis can be conducted in Gurobi, this process takes up time to understand and not is not in scope of the research (Gurobi Optimization L, 2022). For this research, the one-factor-at-a-time analysis by Haghnegahdar et al. (2017) is used.

Parameters subject to change in the sensitivity analysis are: electricity price, PV generation and demand. Parameters of the year 2020 are a snapshot in time and in reality, change due to changing markets, weather influence or industry intensity. The relative parameter change is determined per case study.

The current electricity price differs in an order of magnitude compared to year 2020. Compared to ~0,04 €/kWh in 2020, prices in December 2022 are in the range of ~0,4 €/kWh (Energiemarktinformatie, 2022). For Stamhuis and Warmtebouw, the sensitivity analysis is performed with 0,4 €/kWh. Because Warmtebouw has a varying price scheme, the same relative difference as in the 2020 price is applied, resulting in a low tariff of 0,244 €/kWh and high tariff of 0,4 €/kWh.

PV generation can change due to varying solar intensity, change in installed capacity, or change with panel characteristics. In year 2020 there were 12% less solar hours compared to the year 2022 on location de Bilt (KNMI, 2022).

Electricity demand can vary due to higher industry intensity or using more energy efficient appliances. Demand is changed by -40% and +40% for Stamhuis and Warmtebouw.

4. Results

This research yields different results. The results are based on; data gathering, the structure of the models, the outcomes of the models and the recommendations given to the industrial sites.

4.1 Data

In the fourth step, data is collected about the case study with the use of the fourth research question;
- What knowledge is required to transform the generic model to a case-study applicable model?

First, grid frequency and FCR price are discussed in 4.1.1. Second, grid fees are discussed in section 4.1.2. After grid fees, top-down overview of the two industrial sites is given in section 4.1.3. This overview includes the grid and transformer constraints. In section 4.1.4 are load duration curves presented and in section 4.1.5 subsidy and grid electricity contracts are discussed.

4.1.1 Grid frequency/ FCR price

Grid frequency data

In Figure 6 Histogram grid frequency (IBM Corp., 2022)Figure 6 a histogram of the grid frequency can be seen. The depicted distribution of the data is not in the middle since the left outlier is lower in value than the right outlier. The maximum value of these outliers can be seen in Figure 7**Error! Reference source not found.**.

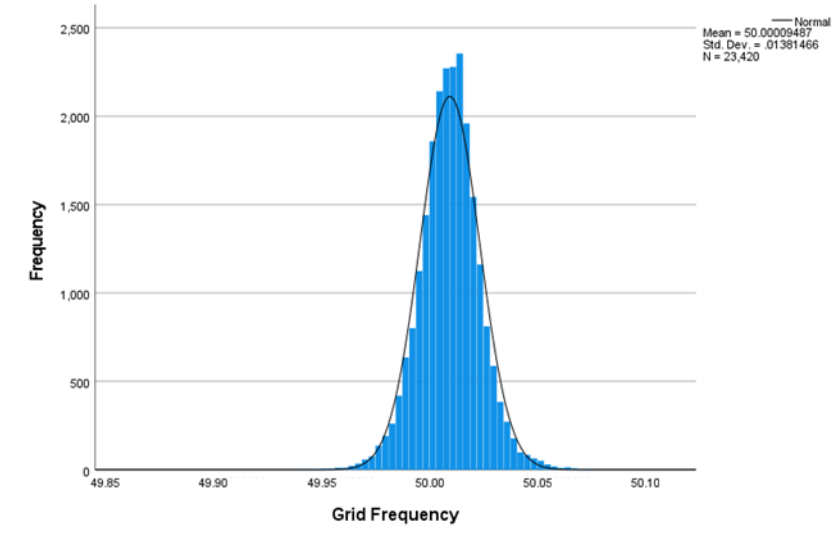

Figure 6 Histogram grid frequency (IBM Corp., 2022)

Statistics

Grid Frequency

N	Valid	23420
	Missing	0
Mean		50.000094869
Median		50.000248335
Minimum		49.89902778
Maximum		50.07619889
Percentiles	1	49.965577136
	2.5	49.972191748
	25	49.991732220
	50	50.000248335
	75	50.008394163
	97.5	50.027824750
	99	50.036152631

Figure 7 Results analysis dataset (IBM Corp., 2022)

This analysis shows that grid frequency deviates a small amount from 50 [Hz]. 95% Percentile of the data set is in a range between 49,97219 [Hz] and 50,02782 [Hz]. 98% Percentile of the data set is in a range between 49,96557 [Hz] and 50,03615 [Hz]. Further monthly analysis of the monthly data is shown in Table 10. The absolute minimum and maximum frequency per month are outside 98%

percentile for each month. In the result section these values are linked to available FCR power, as the goal is to find an upper and lower frequency limit in which the BESS system must operate.

Table 10 Grid frequency data set

	Min	Max
January	49,9446	50,0634
February	49,9339	50,0587
March	49,9413	50,0549
April	49,9414	50,0576
May	49,9447	50,0647
July	49,8992	50,0761
August	49,9277	50,0593
September	49,9326	50,0616
Absolute max	**49,8992**	**50,0761**

FCR prices

The FCR prices can vary throughout the dataset as can be seen in Table 11. This also means the FCR prices can change throughout the day in 4-hour timeslots. The price is equal between balancing services up and down.

Table 11 FCR prices dataset

FCR prices [€/MWh] 21-04-2020 / 31-12-2020		
Min	Max	Average
2,75	121,25	24,59

4.1.2 Grid fees

There are 6 grid operators in the Netherlands from which Stedin controls the province Utrecht, Zeeland and partly South-Holland (Energievergelijk, 2022). High voltage lines connect smaller electricity networks with each other. Stedin offers different connection sizes, dependending on the needs of the consumer or size of the company. Low profile electricity consumers and high-profile electricity consumers have different grid tariffs, as their consumption differs in an order of magnitude. As discussed in part 3.5 of the methodology there are variable grid fees and fixed grid fees. Only variable grid fees are presented here as those values are used in the models. Fixed grid fees are included in appendix B, as they can influence the recommendations given to the industrial sites.

Variable grid fees

Grid fees are based on grid connection size, as they require different types of hardware. The larger the capacity of the transformer, the more expensive the required hardware and grid cables. The different categories are; low voltage (LS), middle voltage (MS), high voltage (HS) and intermediate voltage (IV). See Table 12 Tariffs transport services 2020Table 12 for the 2020 tariffs (Stedin, 2020).

Table 12 Tariffs transport services 2020 (Stedin, 2020)

Transport category	Contracted power	kW contract €/month	kW max €/month
LV	to 50 kW	0.6574	-
Trafo MV/LV	51 to 150 kW	1.7229	1.4570
MV	151 to 1500 kW	0.9577	1.4570
Trafo HV+IV/MV reserve	> 1500 kW	0.926	0.8183
Trafo HV+IV/MV	> 1500 kW	1.8473	2.3640
IV reserve	> 1500 kW	0.8157	0.7930
IV	> 1500 kW	1.6314	2.2908

4.1.3 Industry site topology

A topology from the industrial sites of Stamhuis and Warmtebouw is created. This overview shows the physical grid connection and contract. The installed amount and placement of solar power. The placement of transformer and connection, and the placement of the BESS and connection. The values of these connections are presented in Table 13. With this data the industry park can be closer matched to the digital counterpart, the DT. For Stamhuis and Warmtebouw the transformer output power is rated in kilovolts ampere [kVA]. In alternating current, the rated transformer power in [kW] is equal to [kVA] because the power factor is 1.0 (Bhattacharyya et al., 2011). The grid connection can be seen in Figure 9 and Figure 11 (Stedin, 2022a).

Table 13 Case study specifications

	Stamhuis	Warmtebouw
Grid connection		
Physical	1500 kW	1000 kW
Contracted	256 kW	630 kW
Max extracted	204 kW	154,8 kW
Max injected	1416 kW	111 kW
PV		
Installed	1770 kW	174,6 kW
Contracted	1770 kW	273,7 kW
Max value	1454,2 kW	128 kW

Stamhuis

In Figure 8 below, the position of the battery, the solar panels and grid connection is shown. The industry site is connected to the grid with a connection of 1500 [kVA]. Solar panels located on building 5 have a capacity of 845 [kW]. The address of building 5 is Fermiweg 28, 3542CB Utrecht. A second transformer with a capacity of 1000 [kVA] connects building 5 to building 1, 2 and 3. The address of building 1, 2 and 3 is Fermiweg 24, 3542 CB Utrecht. Solar panels located on buildings 1 and 2 are connected to this transformer.

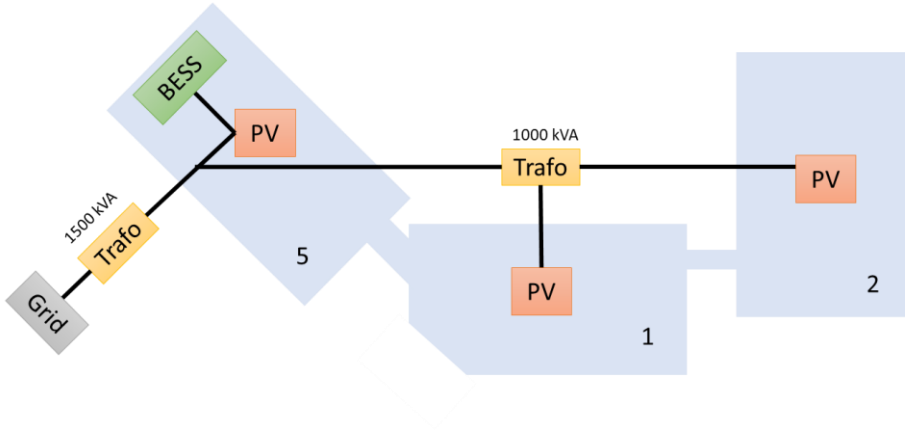

Figure 8 Topology Stamhuis

As can be seen from Table 13, the contracted grid connection is smaller than physical installed PV capacity, and the maximum power injected to the grid is larger than the contracted grid connection., This is due to the large amount of installed PV. The installed and contracted PV are equal.

In Table 14 the capacity and production of the installed solar panels per building is shown. While PV group building 1+2 has a larger capacity than PV building group 5, the maximum annual production is not proportionally larger. This could be due to the orientation of PV panels.

Table 14 Stamhuis PV capacity

Year 2020	Stamhuis production	Capacity
Solar panels building 1+2 Total annual Max annual	 876.917 kWh 765,7 kW	 - 925 kW
Solar panels building 5 Total annual Max annual	 434.902 kWh 721,7 kW	 - 845 kW

The grid map is retrieved from Stedin, see Figure 9 (Stedin, 2022a). A middle voltage station connections Stamhuis with the grid. Connected to this station are 4 low voltage cables, and 2 middle voltage cables.

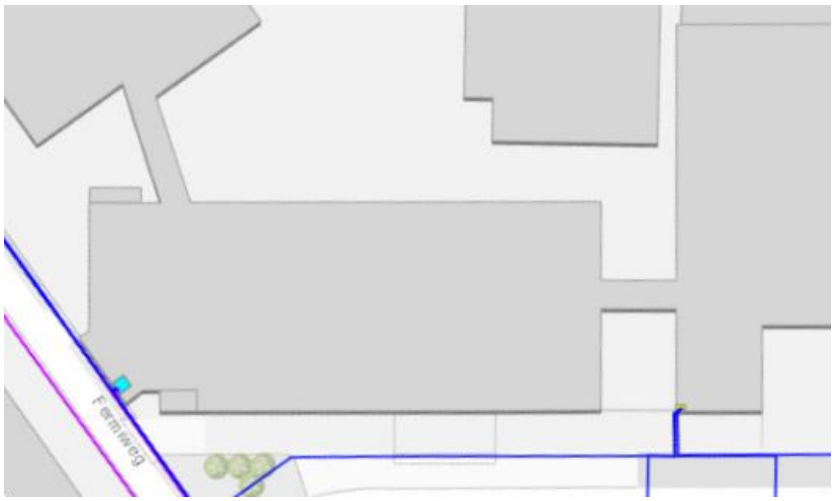

Figure 9 Stedin grid connections Stamhuis. Purple: Middle voltage line. >400V <50kV
Blue: Low voltage line <=400V
Light blue: Middle voltage station >400V <50kV
Yellow: Low voltage station <= 400V (Stedin, 2022a)

Warmtebouw

In Figure 10 below the position of the battery, the solar panels and grid connection is shown.. The industry site is connected to the grid by a transformer with a capacity of 1000 [kVA]. The address of Warmtebouw is Middenwetering 1, 3543 AR Utrecht. As can be seen from Table 13, the physical grid connection is larger than contracted which creates headroom for expansion in PV capacity and more demand. Even a doubling of installed PV would not create problems regarding grid connection. However, Wamtebouw has a relatively small rooftop area, so it is not likely the grid connection will be fully utilized in the future with conventional PV panels.

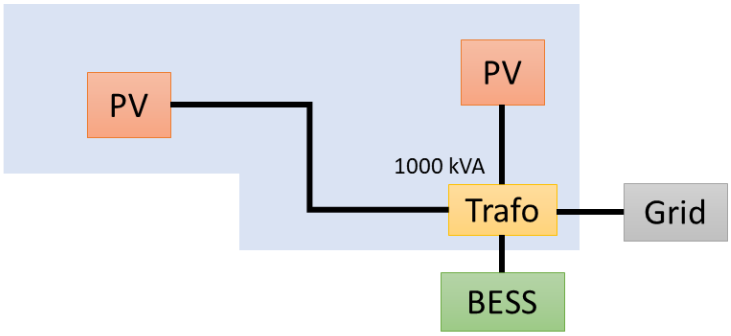

Figure 10 Topology Warmtebouw

There are two groups of solar panels installed on the rooftop area, see Table 15 for the production and capacity. Group A is located on the right side of the building, group B is located on the left side of the building. Because the left side of the building has a larger rooftop area compared to the right side, the difference in capacity can be derived from this.

Table 15 Warmtebouw PV capacity

Year 2020 [kWh]	Warmtebouw production	Capacity
Group A Total annual Max annual	 67.194 kWh 50,84 kW	 - 102,2 kW
Group B Total annual Max annual	 93.145 kWh 77,2 kW	 - 171,1 kW

The grid map is retrieved from Stedin, see Figure 11Figure 9 (Stedin, 2022a). Warmtebouw is connected to the grid with a middle voltage station. Connected to this station are 2 middle voltage cables.

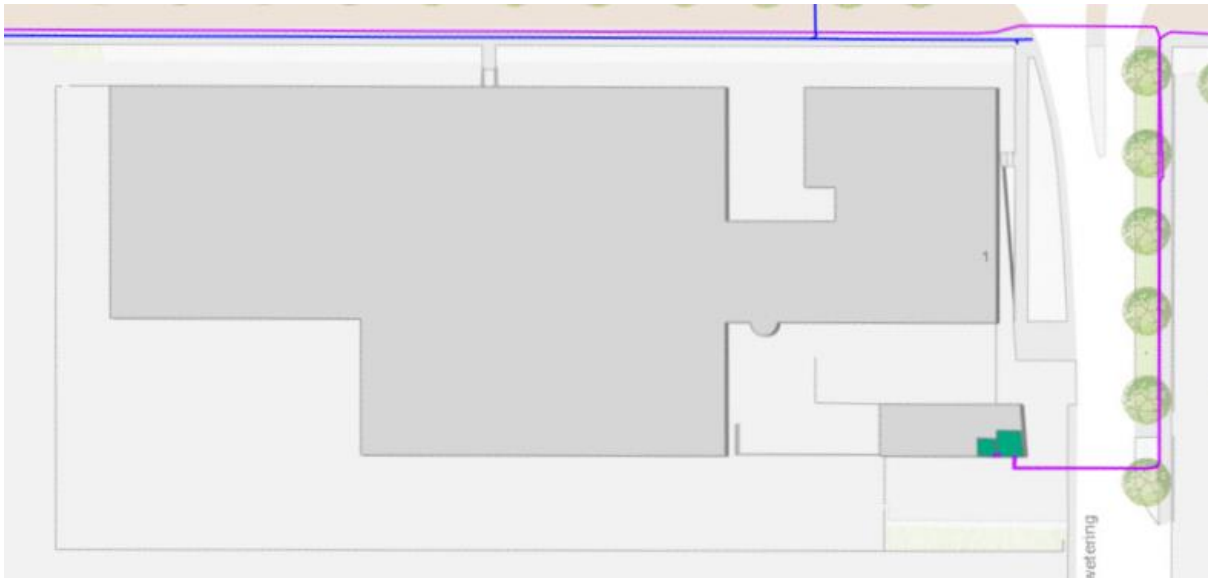

Figure 11 Stedin grid connections Warmtebouw. Purple: Middle voltage line. >400V <50kV Green: Middle voltage station. >400V <50kV (Stedin, 2022a)

Comparison industrial sites

In Table 16 an overview is given of industry site PV generation, demand and grid power data. This is done to give an understanding about the magnitude of the values. Specifications of the BESS are presented in Table 17 (Friday Energy, 2022).

Table 16 Industry site generation, demand and grid power data

Year 2020	Stamhuis	Warmtebouw
PV generation Total Max	 1.311.820 kWh 1454,2 kW	 160.339 kWh 128 kW
Energy demand Total Max	 475.593 kWh 283,1 kW	 449.130 kWh 194,9 kW
Pgrid Total extract Max	 229.392 kWh 204 kW	 321.561 kWh 154,8 kW
Pgrid Total inject Max	 1.065.619 kWh 1416 kW	 32.836 kWh 111,2 kW

Table 17 BESS specifications (Friday Energy, 2022)

	Warmtebouw	**Stamhuis**
Capacity	390 kWh	1,3 MWh
Number of cells	26	87
Round trip efficiency	95 %	
Max. charge – min. discharge	95% - 20%	
Voltage	400 V	
Maximum charge-/discharge rate	260 kW	870 kW
Nominal charge-/discharge rate	156 kW	522 kW

4.1.4 Load duration curves

Stamhuis

In Figure 12 the LDC of the demand can be seen. There is a peak demand of 283,08 kW which rapidly decreases, as the next demand value is 204,32 kW. After just 96 hours with a demand of 148 kW, the demand curve starts to follow a slope which gradually decreases until the last timestep. The initial peak in demand is not of great concern, as the PV generation is of much higher value (Figure 13). The largest value occurs on 30-07-2022, 08:15-08:30. More importantly, the second highest demand value, including several values in the top 20, occur on 10-12-2022.

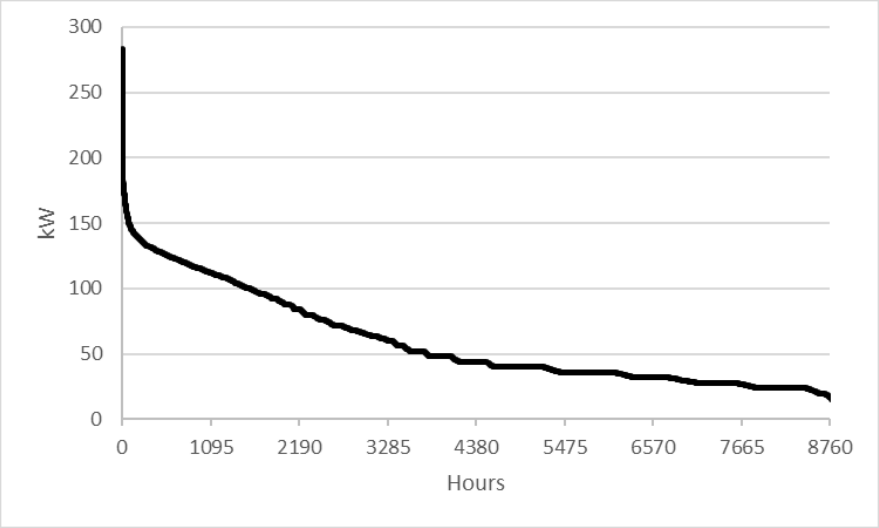

Figure 12 Load duration curve demand Stamhuis

In Figure 13 the LDC of the PV generation can be seen. In this graph the maximum value of 256 kW for Pgrid is relevant as congestion occurs for 2217 hours. Compared to the demand, one could argue that when the demand is synchronized with PV generation the level of congestion reduces. However, the demand is not high enough to reduce the level of congestion below grid limitations. In Figure 14, the demand and PV generation are combined, resulting in Pgrid. The largest value occurs on 22-6-2022, 13:30-13:45.

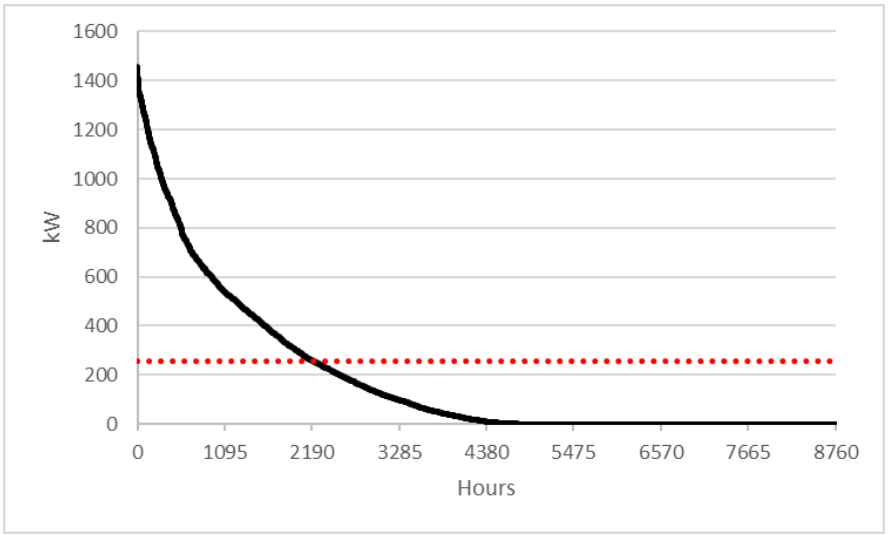

Figure 13 Load duration curve PV generation Stamhuis

Compared to the earlier presented graphs, the duration of PV generation exceeding grid limits is smaller and reduced to 450 hours. A sudden drop in Pgrid around (2/3) of the hours can be noticed, this is due to hourly integer data e.g. Pgrid is either 4 kW, or -4 kW. Peak demand of 283,08 kW does not occur here, as PV is generated in that same timeframe. This is however a random occurrence, as historical PV data on a single timestep is hardly comparable to future PV data on a single timestep. Nevertheless, combining load and generation reduces congestion. The largest positive value occurs on 10-12-2020, 08:15-08:30. The largest negative value occurs on 11-07-2022, 13:30-13:45.

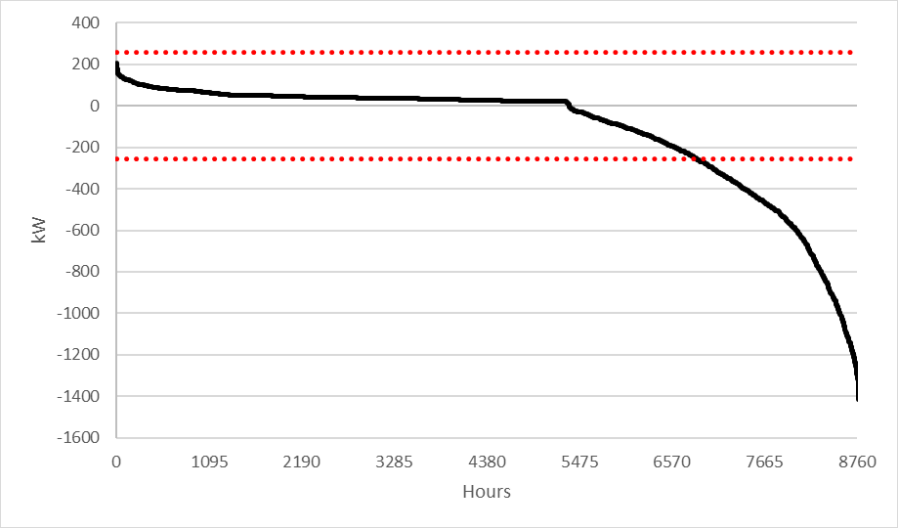

Figure 14 Load duration curve grid power Stamhuis

Warmtebouw

In Figure 15 the LDC of the demand can be seen. In the PV generation and Pgrid graph of Stamhuis the grid limitation can be seen, this limitation is not included for the graphs at Warmtebouw as this threshold is never reached. The grid limitation is 630 kW, and Warmtebouw has a maximum demand of 194,87 kW. The second highest value is 185,32 kW, and after 150 hours with a demand of 145 kW, the demand curve starts to follow a slope which decreases until the last timestep. The highest value occurs on 11-08-2020, 13:30-13:45. In the first 30 values, the months June and August have frequent occurrences.

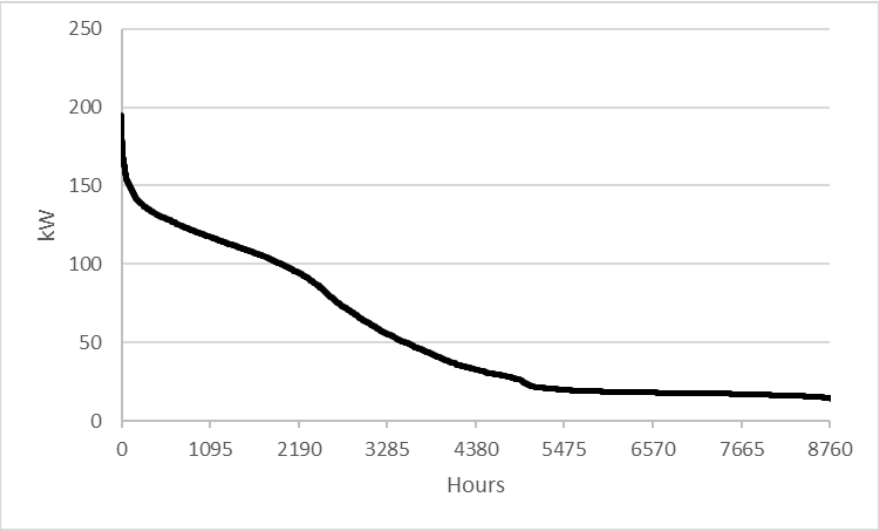

Figure 15 Load duration curve demand Warmtebouw

In Figure 16 the LDC of the PV generation can be seen. There is no clear peak in PV generation, and the generation decreases almost linearly for the most part. In Figure 18 the PV generation between Stamhuis and Warmtebouw is compared. The largest value occurs on 05-05-2020, 13:00-13:15. From the first 30 values, the months May and July have frequent occurrences.

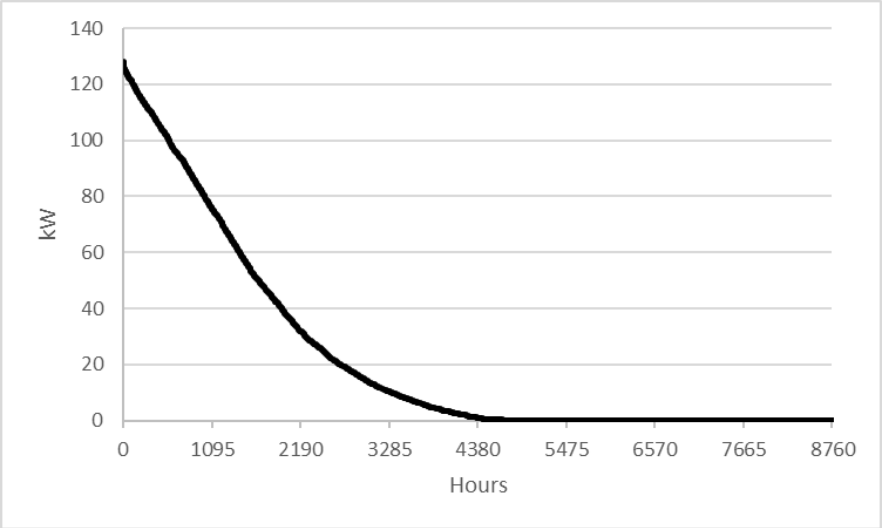

Figure 16 Load duration curve PV Warmtebouw

In Figure 17 the LDC of Pgrid can be seen. Energy consumed from the grid follows a more gradient line compared to only demand, Figure 15. This is because the PV generation fluctuates less compared to Stamhuis. Furthermore, it can be seen that the peak in energy consumed from the grid is larger than energy delivered to the grid, but that the difference is much smaller compared to Stamhuis. This is due to the fact that Warmtebouw has lower PV generation. The highest positive value occurs on 10-03-2020, 09:15. The lowest negative value occurs on 17-05-2020, 13:00-13:15. The highest 30 positive values of Pgrid occur throughout the year, and August has the highest frequency with 8 times.

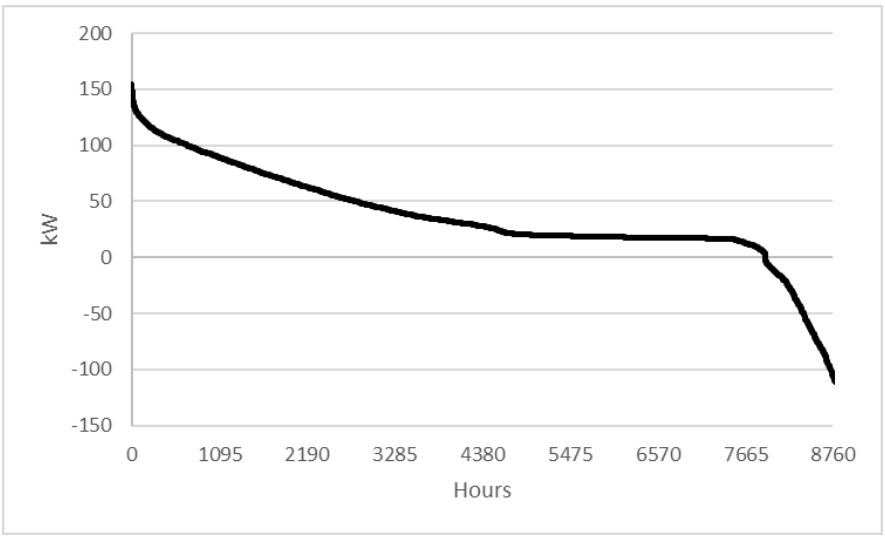

Figure 17 Load duration curve Warmtebouw

Comparison industrial sites

To compare the two industrial sites on demand/PV/Pgrid, the values are normalized. This analysis is important because it directly compares the industrial sites, which are entirely different on demand/PV/Pgrid. Therefore, remarkable data could come to light. In Figure 18 the LDC of the PV generation for both industrial sites can be seen. The industrial sites are located 1.2 km away, so it is expected that the generation profiles follow the same curvature. This is however not the case, and the panels at Stamhuis produce less relative PV generation compared to Warmtebouw. This could be due to the orientation of the panels. The difference is significant and while outside the scope of this thesis, future research could use the PVlib module in Python to determine the cause of this difference.

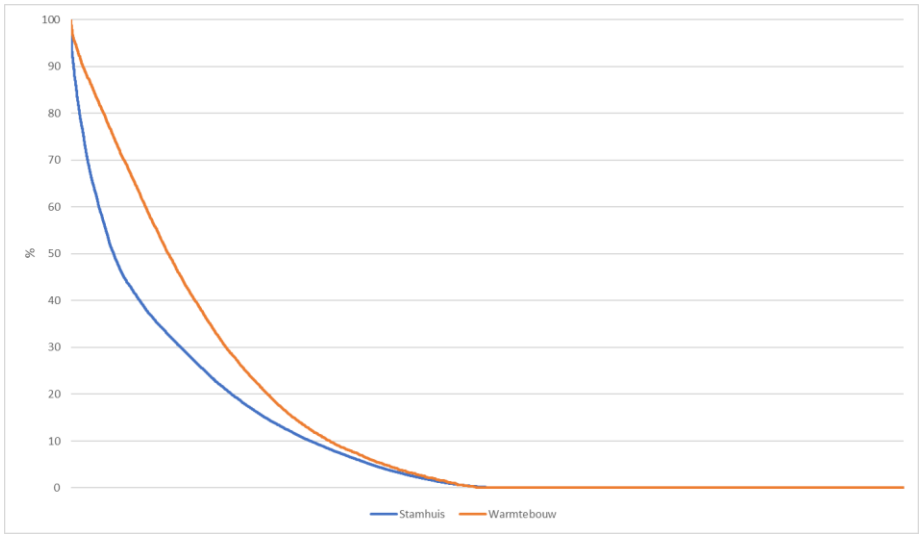

Figure 18 Load duration curve PV comparison

In Figure 19 the LDC of the demand of both industrial sites can be seen. The peak demand of Stamhuis is larger than Warmtebouw on a relative basis. However, for Stamhuis this peak is less relevant, as there is much more PV generation than demand. The demand at Warmtebouw follows a different curvature compared to Stamhuis, and this could be due to the type of energy consuming appliances installed.

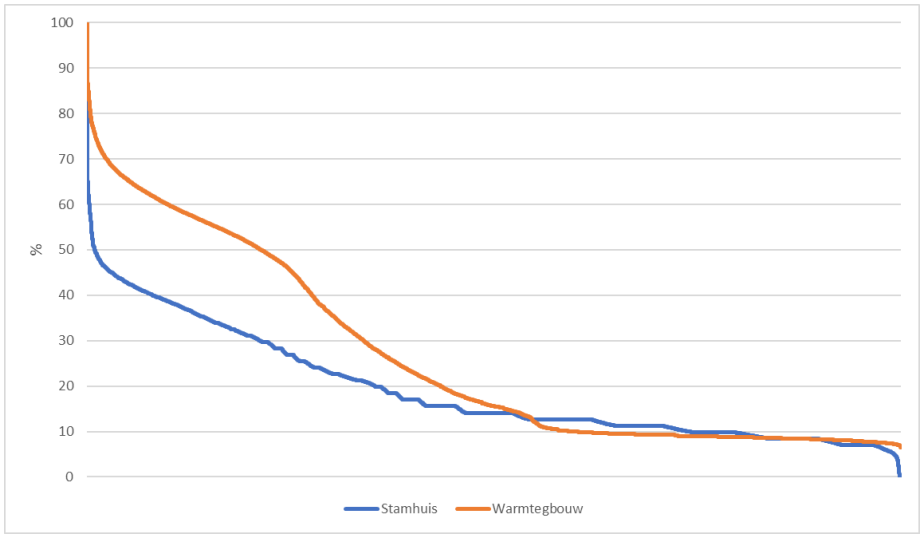

Figure 19 Load duration curve demand comparison

In Figure 20 the LDC of Pgrid of both industrial sites is shown. Stamhuis uses 14.4% of the total Pgrid for grid extraction, and 100% for grid injection. Warmtebouw uses 100% of the total Pgrid for grid injections, and 72% for grid extraction. This figure illustrates that the industrial sites have entirely different demand vs PV generation ratios. Enforcing a grid limitation due to cost will be beneficial for Stamhuis regarding maximum grid injection and for Warmtebouw in equaling grid injection and grid extraction.

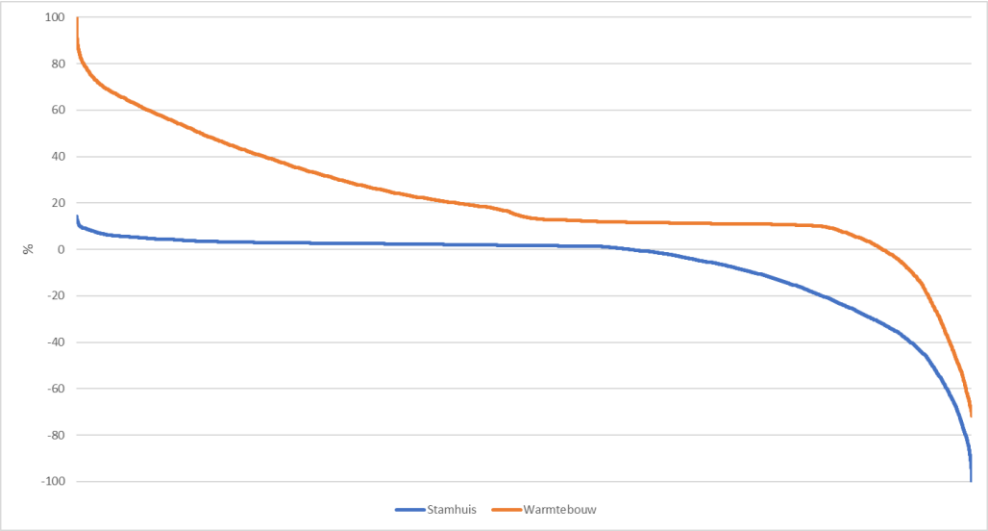

Figure 20 Load duration curve grid power comparison

4.1.5 Contracts SDE and grid electricity supplier

SDE contracts

Stamhuis

Stamhuis receives a subsidy called sustainable energy production and climate transition (SDE). The SDE incentives companies in the sectors industry, mobility, electricity, agriculture, and the build environment to generate renewable energy or apply CO_2 reducing techniques (Netherlands Enterprise Agency, 2022). Fermiweg 24 as well as Fermiweg 28 receive the subsidy. Stamhuis receives two SDE subsidies, one for each group. Each subsidy is awarded over a period of 15 years and is entirely applicable to PV generation. See Table 18 for detailed subsidy information.

Table 18 Stamhuis SDE scheme

	Fermiweg 28	Fermiweg 24
Nominal installed capacity	0,845 MW	0,925 MW
Maximum subsidy tariff	89,00 €/MWh	83 €/MWh
Annual contracted energy	802,75 MWh/year	878,75 MWh/year
15 Year contracted energy	12.041,25 MWh	13.181,25 MWh
15 Year contracted revenue	€ 1.071.672	€ 1.094.044
Start time	1-6-2018	1-6-2018

Warmtebouw

Warmtebouw receives two different SDE subsidy schemes, one for each panel group (Table 19). The received subsidy tariff differs per group and is awarded over a period of 15 years.

The SDE with the starting year of 2017 is based on receiving subsidy over all generated PV. The SDE with the starting year of 2022 is based on splitting the subsidy between injecting generated PV back into the grid, and self-consumption of generated PV. As a result, it does not matter how the energy generated by group B is used. While for group A, it does matter how the energy is used, as it generates more revenues to inject the energy back into the grid. Self-consumption of the energy generates a small amount of revenues. It is expected that this type of subsidy scheme pushes the system to little usage of the BESS, as storing the energy is expensive.

Table 19 Warmtebouw SDE scheme

	Group A	Group B
Nominal installed capacity	0,102 MW	0,171 MW
Maximum subsidy tariff	-	74 €/MWh
Maximum subsidy tariff net supply	46,2 €/MWh	-
Maximum subsidy tariff self-consumption	2,8 €/MWh	-
Annual contracted energy	91,98 MWh/year	162,878 MWh/year
15 Year contracted energy	1.380 MWh	2.443 MWh
15 Year contracted revenue	€ 63.740	€ 180.795
Start time	1-5-2022	26-10-2017

Grid electricity supplier

Warmtebouw

Warmtebouw has a grid electricity contract with Engie. Warmtebouw has a variable tariff depending on the time of the day. The night tariff, or low tariff, is in place between 23:00 and 06:00. The day tariff is between 06:00 and 23:00. See Table 20 for the grid tariffs of Stamhuis and Warmtebouw.

Stamhuis

Stamhuis has a grid electricity contract with Nieuwe Stroom. Stamhuis has a fixed electricity price of 0.0423 €/kWh.

Table 20 Grid tariffs industry sties

Warmtebouw	Low tariff	0,03326 €/kWh
	High tariff	0,04624 €/kWh
Stamhuis	Fixed tariff	0,04230 €/kWh

4.2 Model

The Python code will be a generic model that works with data in csv file format. As mentioned in step 2 of the methodology, the generic model will be the foundation and expanded into a case study specific model. Each scenario will alter small parts of the generic model to make it case study specific and applicable to a different set of input data. Besides, input parameters such as the battery size should be changeable.

4.2.1 Model flow chart

In this section the few models, proposed as in Table 6, are written as a flowchart. Not all models and model alternations are visualized, as most alterations are small, or similar between different models. Therefore, in Table 21 and Table 22 is described what changes in the model compared to the GBM.

Generic model

In Figure 21 Flow chart generic modelFigure 21**Error! Reference source not found.** the generic model is depicted. As input, the model has measurement data data. With this data it is determined if the model can run with the current grid contract, Pgrid. Please note that Pgrid in this case also the grid contract can be. If PV_{gen} exceeds $P_{ch}+P_{gridinj}$ this boundary is pushed upwards and set to the nearest level the model can operate.

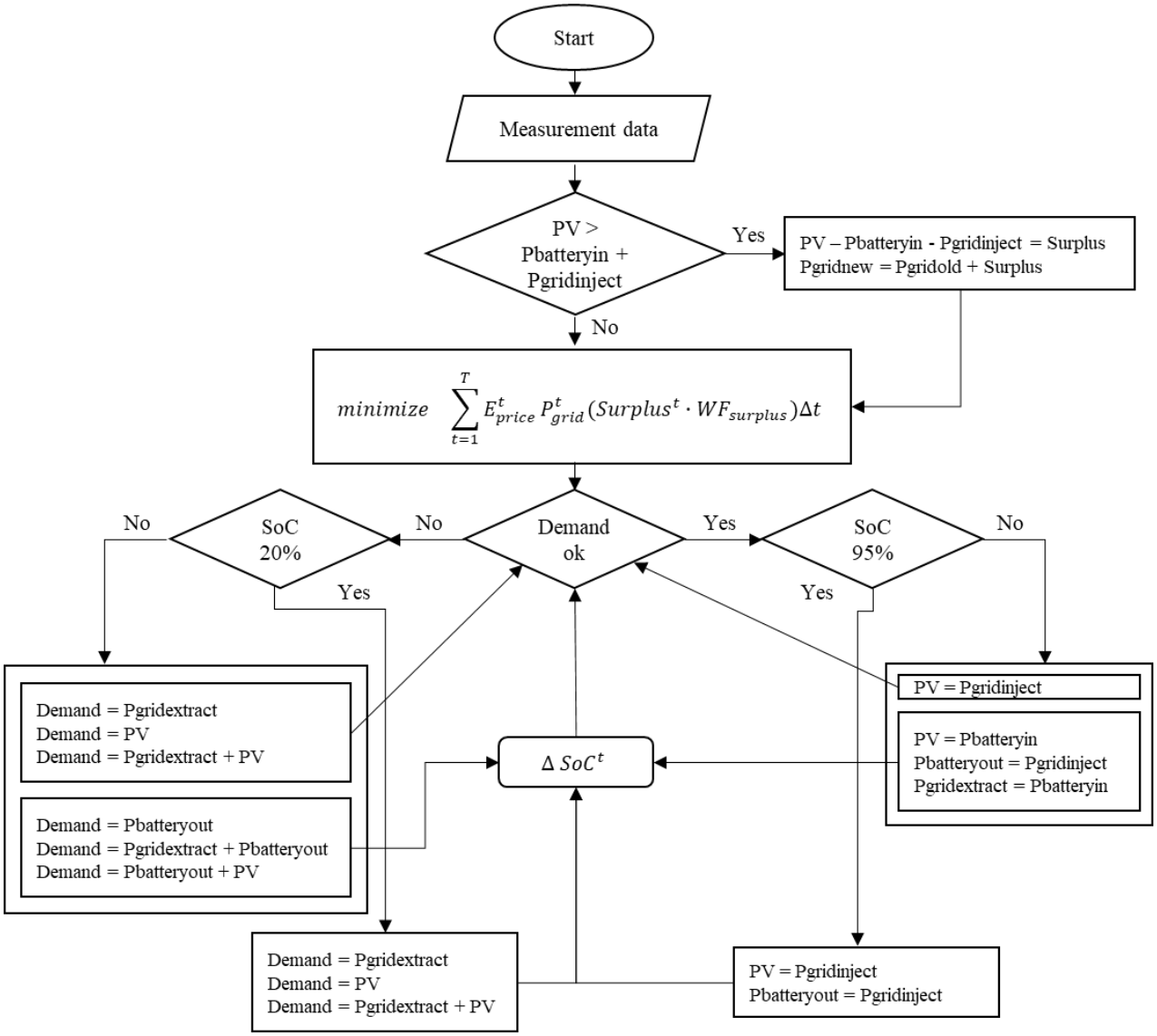

Figure 21 Flow chart generic model

If there is no higher grid connection required, the model solves the objective function. From there, the optimization process cannot be monitored as Gurobi is a shielded module, but depending on the constraints, energy is able to flow several options. Some options use the battery and change the battery SOC, other options do not use the battery. If the battery is completely full or empty, battery energy flow is restricted.

Table 21 Stamhuis model alterations

Stamhuis	**Changes**
GBM + SDE	The objective function changes to equation 20
GBM + SDE + DEG	The objective function changes to equation 20. The piecewise linear constraint is modeled by placing a block between the objective function and demand block. If the costs of the objective function are higher in one timestep than the costs of battery degradation, the model proceeds. Vice versa, the battery is limited in power before proceeding.

	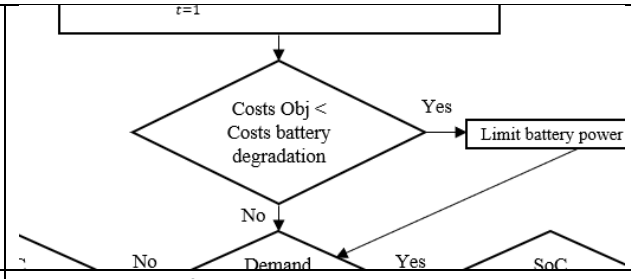
GFM SDE DEG	The objective function changes to equation 29
SCM SDE DEG	The objection function changes to equation 31. See GBM+SDE+DEG for degradation alterations.

Table 22 Warmtebouw model alterations

Warmtebouw	**Changes**
GBM + SDE	The objective function changes to equation 22
GBM + SDE + DEG	The objective function changes to equation 22. See Table 21, GBM+SDE+DEG for degradation alterations.
GFM SDE DEG	The objective function changes to equation 30
SCM SDE DEG	The objection function changes to equation 31 See model See Table 21, GBM+SDE+DEG for degradation alterations.

4.2.2 Results Generic model

The results are categorized by model type and are GBM, GFM and SCM. First the results of the Stamhuis case are discussed, followed by the results of the Warmtebouw case. From the LDC section it can be seen that the PV generation of the 2 industrial sites differs by an order of magnitude. Furthermore, Stamhuis has a fixed grid electricity price, and Warmtebouw has a varying electricity price between night and day. Also, there is a difference in SDE contracts, which impacts the revenues during PV generation. It is interesting to see how these parameters influence the results, because the two industrial sites are not comparable mentioning the previous points. The data points used in the simulation are determined using LDC. The simulation duration can vary between 1 day and 2 weeks. The readability of a graph decreases with increasing duration. A duration of 1 day is used so the model decisions are visualized, and a duration of 2 weeks is used to gather information for results over a prolonged period. In 1 day, 24 hours, there are 96 timesteps of 15 minutes. In 2 weeks, 336 hours, there are 1344 timesteps of 15 minutes. Due to computational hardware limitations, the maximum duration is set to 2 weeks. To see the influence of subsidy and degradation on the models, the generic battery model is described in higher detail compared to the other models. To computing result of a simulation is called a run.

Stamhuis

GBM

The timeframe of this run is: 1 day, 03-06-2020.

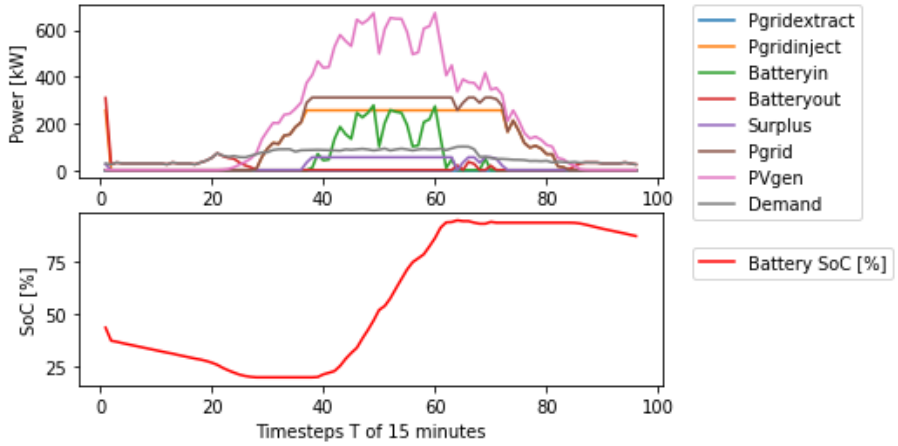

Figure 22 Energy GBM 1-day Stamhuis

From Figure 22 can be seen that during daytime, PV generated energy is injected into the grid. During PV generation, demand is entirely fulfilled by PV. The demand is relatively low compared to the PV generation. There is no incentive to charge the battery with Pgridextract due to a fixed electricity price. Pgridinject reaches the contracted power limit of 256 kW, and the remaining energy flow goes to Pbatteryin. Although the battery is discharged from the start of the run to generate sufficient capacity, the battery has not enough capacity to store the sum of PV energy, and therefore there is surplus energy. There is a discharge peak in the beginning of the run because there is no degradation penalty for heavy charging and discharging. After PV generation decreases below demand, the demand is fulfilled by stored energy in the BESS. There are no positive revenues generated, as there is no method in the GBM to generate these. More importantly, there are no negative revenues, as there is no Pgridextract. By using a short timeframe and starting with SoC 50%, it is not likely Pgridextract will be used if there is excessive PV generation in place.

Now, the day with the largest Pgridinject is taken, 11-07-2020.

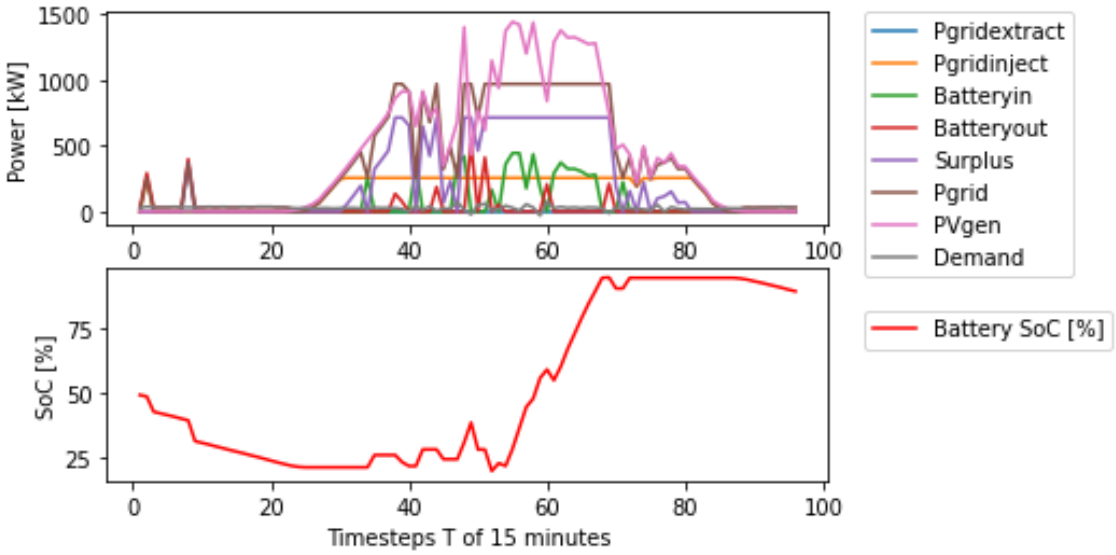

Figure 23 Energy GBM 1-day Stamhuis

From Figure 23 can be seen that there is a large surplus of PV generation. As a result, energy is injected back to the grid, as the battery is insufficient in capacity to consume all energy. The grid contract of 254 kW is exceeded by a surplus of 715 kW, resulting in a new Pgrid of 971 kW. This is below the physical grid connection, although it will raise the grid contract by quite some margin. No positive or negative revenues are being generated. The bottleneck of the system with large amounts of consecutive PV generation is battery capacity, as the battery is not limited by power.

The timeframe of this run is 3 weeks, 01-07-2020 to 21-07-2020.

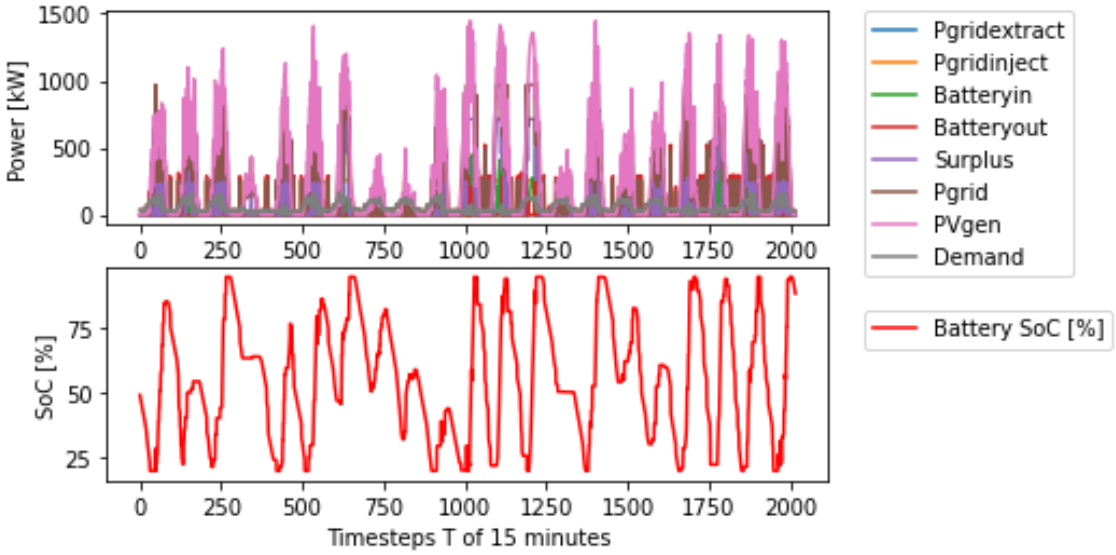

Figure 24 Energy GBM 3-weeks Stamhuis

Figure 24 shows that there is a large variance in PV power, and the high and lows are distributed irregularly. An excess of PV generation compared to demand results in a continuing energy flow of Pbatteryout. During consecutive days of high PV generation, Pbatteryout and Pgridinject are constantly needed to create room for energy in the system which is overloaded with PV generation.

In Figure 25 can be seen that the battery is discharging during the night and charging during the day, and during consecutive days of high PV generation, Pbatteryin power increases. The grid connection increases with surplus energy, and because of the relatively low power of the battery compared to the PV generation, a smaller grid connection is not possible. No positive or negative revenues are generated.

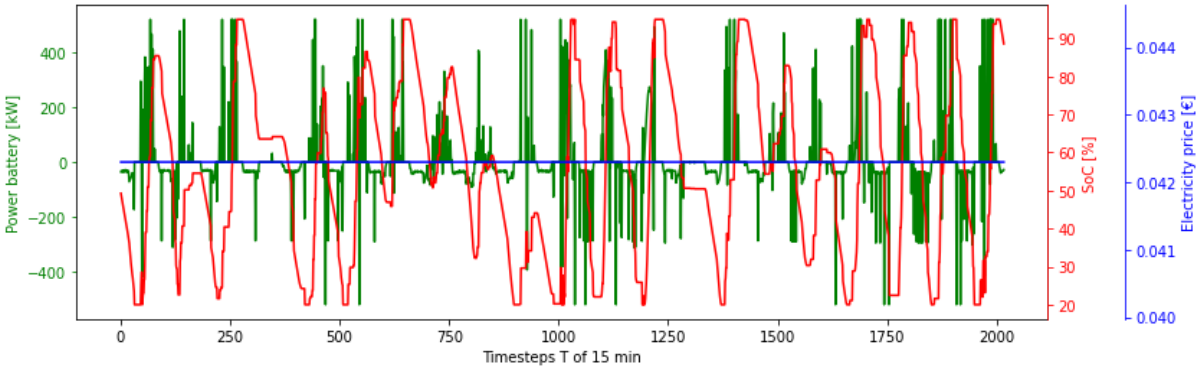

Figure 25 Energy GBM 3-weeks Stamhuis

Table 44 shows the results of the simulation runs. In the second and third run contract congestion occurs. The third run NewPgridMax is 969,5kW, which is lower than the 971,2kW of the second run. While the second run was the annual day with highest PV generation, the battery could consume this energy for the most part. Due to consecutive high PV generation in the third run, the model can optimize and allows more Pbatteryout. In the first run there would be congestion of 322 kW if there was no BESS installed. With a BESS, this is limited to 310 kW. During the second run, peak congestion of 1160 kW without BESS would occur. With a BESS installed, this is reduced to 715,2 kW. In the third run with the BESS installed, peak congestion of 713,5 kW occurs. Reduction of congestion occurs when a BESS system is installed, however the BESS is insufficient in capacity and power to eliminate congestion. Without the installation of PV and BESS, there would be electricity costs to fullfill the demand. These costs are included in the last row of the table. When run 1 and 2 are compared on cyclic costs and demand electricity costs, it can be seen that higher PV generation compared to demand puts less cycle stress on the battery, reducing the degradation costs. As long as there is excessive PV generation compared to demand but not by great margin, the battery is stressed the least, while still mitigating demand electricity costs.

Generic model + SDE

The timeframe of this run is: 1 day, 11-07-2020.

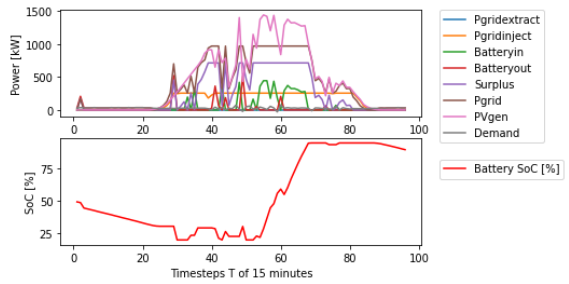

Figure 26 Energy GBM SDE 1-day Stamhuis

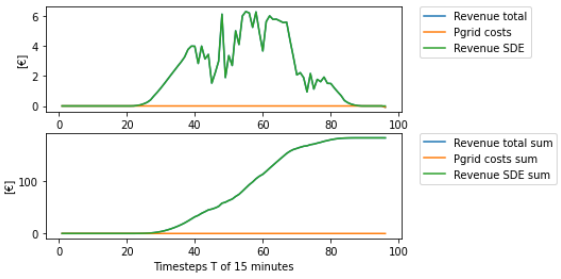

Figure 27 Revenues GBM SDE 1-day Stamhuis

Figure 26 shows the same result as Figure 23**Error! Reference source not found.**. This is due to Stamhuis having an SDE scheme not based on energy injection but based on a PV generation subsidy

scheme. The objective function is equal, see the method section. Figure 27 shows a breakdown of revenues. The top picture shows the revenues per timestep, which highlights the influence of PV generation on SDE subsidy, or grid electricity costs. The system is self-sustainable due to high PV generation and BESS storage, therefore there are no grid costs. In the last timestep the SDE revenues are €183,708.

The timeframe of this run is: 3 weeks, 01-07-2020 to 21-07-2020.

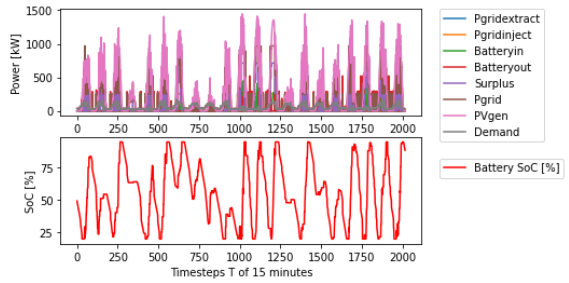

Figure 28 Energy GBM SDE 3-weeks Stamhuis

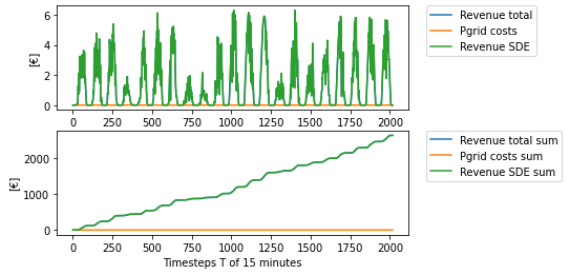

Figure 29 Revenues GBM SDE 3-weeks Stamhuis

Figure 28 Energy GBM SDE 3-weeks StamhuisFigure 28 shows the same result as Figure 24. From the trend the revenues in Figure 29 follow can be deduced that there is more subsidy income on days with more PV generation. In the last timestep the SDE revenues are €2649,58. The degradation costs are lower than the demand electricity costs. It is expected that in the case of Warmtebouw where a new SDE subsidy influences the optimization, the results of GBM and GBM + SDE are not similar.

Generic model + SDE + Degradation

The timeframe of this run is: 1 day, 11-07-2020.

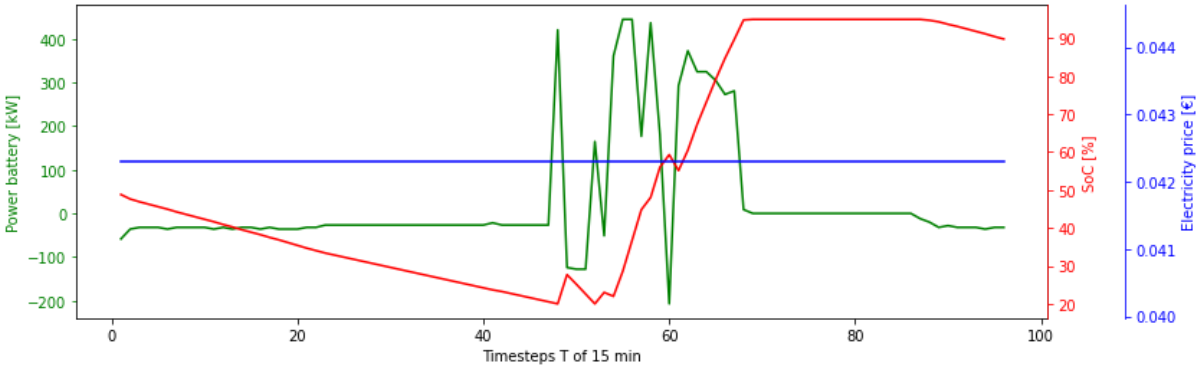

Figure 30 Energy BESS GBM SDE DEG 1-day Stamhuis

In Figure 30 can be seen that the battery discharges at a smaller discharge rate compared to the GBM run, Figure 31. The charts are compared in this segment because they visualize the impact of degradation per delta SoC. Instead of discharging with high power surges, the battery discharges continuously at a lower rate of ~30kW. This process has no influence on the total energy consumed by the battery as the energy in the system is similar, however it changes the control scheme of the battery.

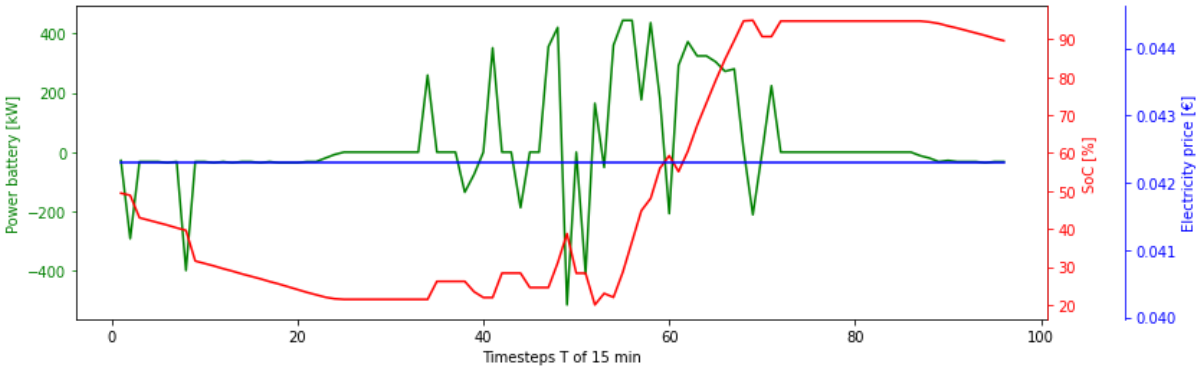

Figure 31 Energy BESS GBM 1-day Stamhuis

The timeframe of this run is: 3 weeks, 01-07-2020 to 21-07-2020.

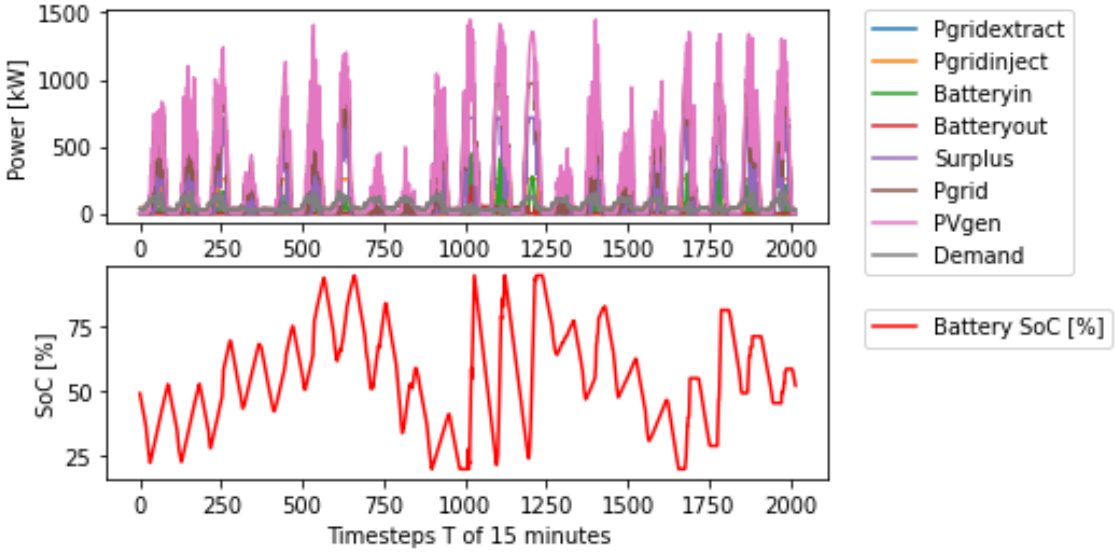

Figure 32 Energy GBM 3-weeks Stamhuis

Figure 32 shows that battery SoC changes in an increased linear way, compared to Figure 28, due to the penalty over a difference in SoC over time. Figure 33 highlights this, as the battery power is quite consistent. No difference in revenues due to SDE occurs. The 3-week results are explained in a direct comparison between the GBM+addon in Table 23.

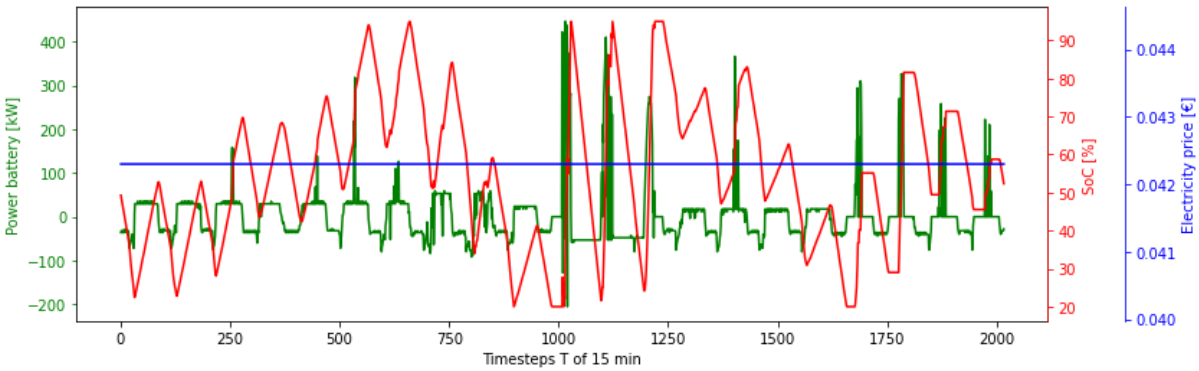

Figure 33 Energy GBM SDE DEG 3-week Stamhuis

In a direct comparison between the runs, it can be seen an equal amount of surplus energy is required in GBM SDE DEG compared to the other model runs. This is due to the limited capacity of the battery. Congestion time increases, as the source of this energy can be from the grid or battery. However, with a lower allowed battery delta SoC, battery energy flow is more controlled and takes longer. Degradation costs decrease when a degradation penalty is applied, showing a battery model without degradation can be drastically optimized without this leading to higher grid connection requirements.

Table 23 Comparison GBM+addons models

Stamhuis		**GBM 3-weeks high**	**GBM SDE 3-weeks high**	**GBM SDE DEG 3-week high**
Pgridextract max	kW	0	0	0
Pgridinject max	kW	256	256	256
Pgrid max	kW	256	256	256
Surplus	kW	713,5	713,5	713,5
New Pgrid max	kW	969,5	969,5	969,5
Pgridextract costs	€	0	0	0
Revenues SDE	€	0	2649,58	2649,58
Revenues total	€	0	2649,58	2649,58
$Congestion_{contract}$	%	31,25	31,35	44,64
Pgrid max dataset	kW	1416	1416	1416
Peak congestion no BESS	kW	1160	1160	1160
Peak congestion BESS	kW	713,5	713,5	713,5
$Congestion_{grid}$	%	0	0	0
Degradation costs	€	176,52	171,34	53,66
Degradation cyclic	%	0,0286	0,0278	0,0087
Demand electricity costs	€	306,52	306,52	306,52

Results of a single day visualize the energy flow throughout the day in a detailed way. Simultaneously, results over a prolonged period of time enable the model to function over a longer time, and give more realistic values. From now on, runs with a duration of 2 weeks are explained in the results, except for 1 day for Warmtebouw, to highlight the influence of a variable electricity price. Each run produces one table, and finally the results of all runs are compared in a single table.

Warmtebouw

GBM

The timeframe of this simulation is: 11-08-2020, 1 day.

Figure 34 shows the battery power, SoC and electricity price. The battery charges when the electricity price is low, and discharges when the electricity price is high. Degradation does not play a role in in this run, which causes the battery to charge at random during the timeframe the electricity price is low.

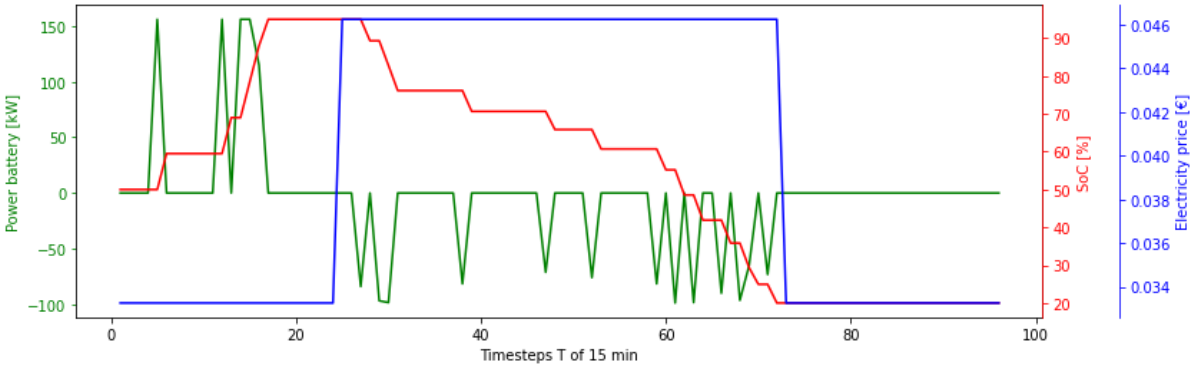

Figure 34 Energy GBM 1-day Warmtebouw

The timeframe of this simulation is: 04-08-2020 until 17-08-2020, 2 weeks.

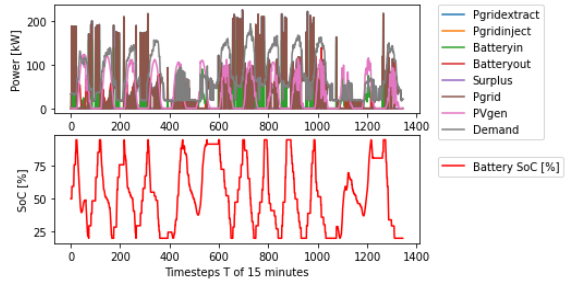

Figure 35 Energy GBM 3-weeks Warmtebouw

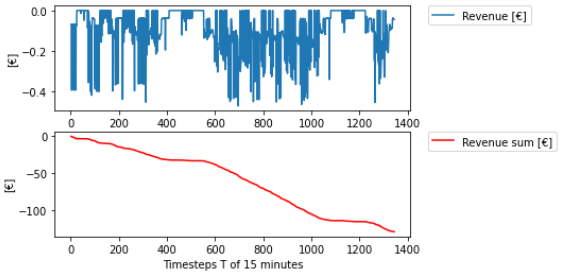

Figure 36 Revenues GBM 3-weeks Warmtebouw

Figure 35 shows that when there is more PV gen than demand (between timestep ~370 and ~580), the battery is charged during this period. Otherwise, the varying price scheme incentivizes the battery to charge. This principle is used past timestep ~580, when there is for consecutive days more demand than generation. In case the battery is depleted, the demand is met with grid energy.

In Table 24 can be seen that the electricity costs are €128,348. The required grid connection is below the maximum grid connection, so no surplus energy occurs. There is a higher grid connection required than the reference value (Pgrid max dataset), and this is due to charging and discharging of the battery. Without BESS, the grid connection has 490,4 kW remaining. With BESS, the grid connection has 403.2 kW remaining.

GBM + SDE

The timeframe of this simulation is: 03-08-2020 until 16-08-2020, 2 weeks.

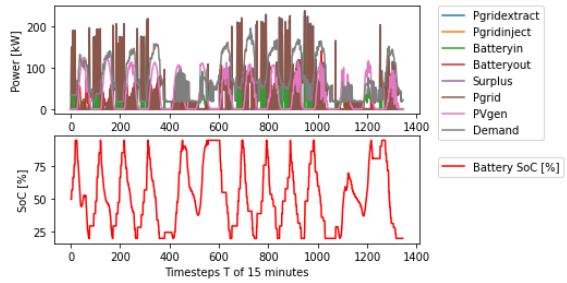

Figure 37 Energy GBM SDE 3-weeks Warmtebouw

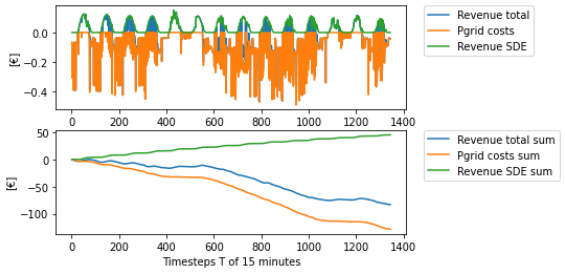

Figure 38 Revenues GBM SDE 3-weeks Warmtebouw

Figure 38 depicts the revenue streams with the GBM plus SDE. The yellow line below shows the electricity costs, which are equal for the GBM and GBM+SDE run. The SDE subsidy schemes generate total income of €45,358. This is however not enough to equal the electricity costs, resulting in a total cost of €82,98. The subsidy scheme based on injecting energy in the grid generates more Pgridinject and thus more Pgridextract, as the latter is the source of this energy. Further results can be seen in Table 24.

GBM + SDE + DEG

The timeframe of this simulation is: 03-08-2020 until 16-08-2020, 2 weeks.

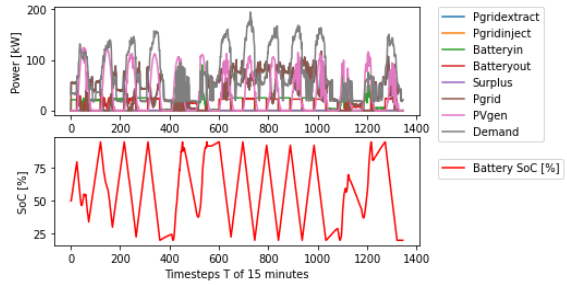

Figure 39 Energy GBM SDE DEG 3-weeks Warmtebouw

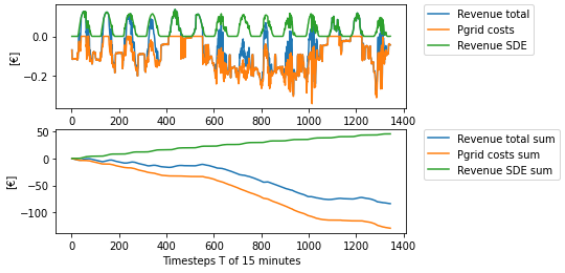

Figure 40 Revenues GBM SDE DEG 3-weeks Warmtebouw

Figure 39**Error! Reference source not found.** shows the energy flow of the run. Compared to Figure 35, the battery SoC ramps up and down gradually due to the degradation penalty. Besides, because these energy flows are not occurring random as before, Pbattery is also lower. Because of this, Pgridmax is lower, and there is more room left in the grid contract. Installing a battery lowers the required grid connection by ~22 kW and reduces the costs by some margin.

Table 24 Comparison GBM+addons Warmtebouw

Warmtebouw		**GBM 2-weeks high**	**GBM SDE 2-weeks high**	**GBM SDE DEG 2-week high**
Pgridextract max	kW	226,8	236,8	117,22
Pgridinject max	kW	67,2	80	45,9
Pgrid max	kW	226,8	236,8	117,22
Surplus	kW	0	0	0
New Pgrid max	kW	0	0	0
Pgridextract costs	€	128,34	128,34	128,8
Revenues SDE	€	0	45,35	45,35
Revenues total	€	-128,34	-82,98	-83,44
$Congestion_{contract}$	%	0	0	0
Pgrid max dataset	kW	139,6	139,6	139,6

Peak congestion no BESS	kW	-490,4	-490,4	-490,4
Peak congestion BESS	kW	-403,2	-393,13	-512,77
$Congestion_{grid}$	%	0	0	0
Degradation costs	€	46,38	45,39	16,49
Degradation cyclic	%	0,0251	0,0245	0,0089
Demand electricity costs	€	256,52	256,52	256,52

Conclusion Warmtebouw + Stamhuis

The results show the type of subsidy scheme and revenues per kWh matter. Revenues per generated kWh have no influence on the results regarding energy flow. Revenues for gridinjection can only be successful if they are stronger than the electricity price, or if this type of scheme is combined with sufficient PV generation compared to demand. The addition of degradation to the model causes a reduction of Pgridmax at both industrial sites. Energy extracted from the grid or injected in the grid is distributed over time, and high peaks are limited. Furthermore, the installation of PV and BESS lead to cost reduction.

4.2.3 Results Grid Fees model

Stamhuis

GFM+SDE+DEG

The timeframe of this simulation is: 03-07-2020 until 16-07-2020, 2 weeks.

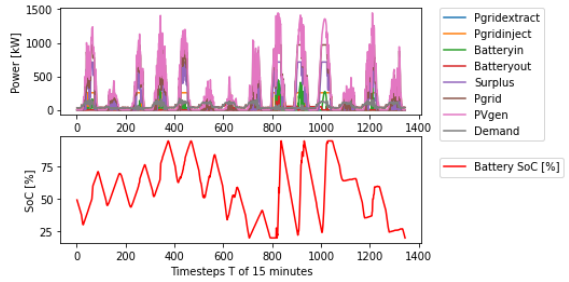

Figure 41 Energy GFM SDE DEG 2-weeks Stamhuis

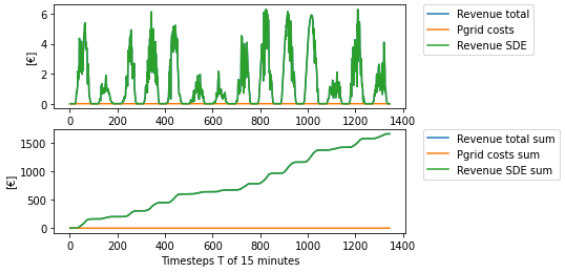

Figure 42 Revenues GFM SDE DEG 2-weeks Stamhuis

Figure 41 shows that, even though there is a large surplus in PV generation, the battery capacity is not entirely utilized. This is emphasized in Figure 43, as the battery is charged and discharged at near constant rates, except for excess PV generation. In that case, more battery power is required. The battery cannot consume all PV generation and surplus energy is required, with New Pgrid max at 969,5 kW. Battery degradation causes a longer requirement of surplus energy, but does not increase New Pgrid max. See Table 25 for detailed results.

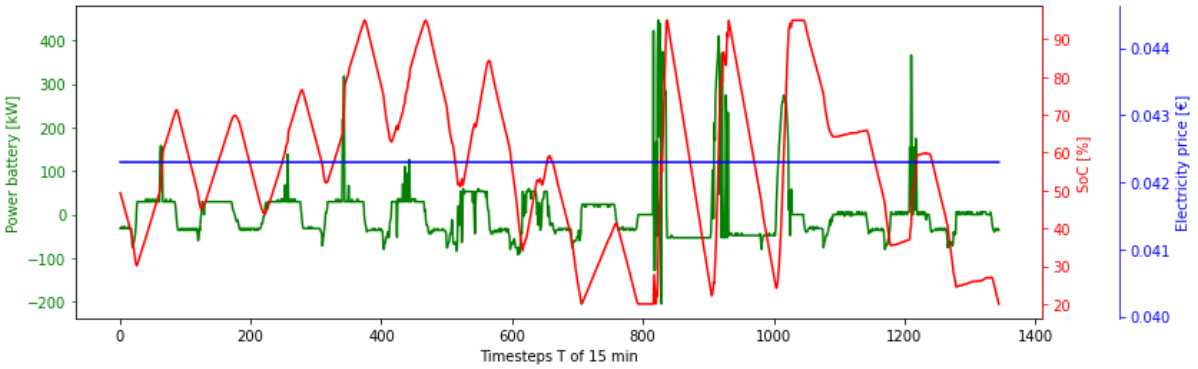

Figure 43 Energy BESS GFM SDE DEG 2-weeks Stamhuis

Table 25 GFM results Stamhuis

Stamhuis		**GFM SDE 2-weeks high**	**GFM SDE DEG 2-week high**
Pgridextract max	kW	0	0
Pgridinject max	kW	256	256
Pgrid max	kW	256	256
Surplus	kW	713,5	713,5
New Pgrid max	kW	969,5	969,5
Pgridextract costs	€	0	0
Revenues SDE	€	1652,51	1652,51
Revenues total	€	1652,51	1652,51
$Congestion_{contract}$	%	27,75	44,41
Pgrid max dataset	kW	1416	1416

Peak congestion no BESS	kW	1160	1160
Peak congestion BESS	kW	713,5	713,5
$Congestion_{grid}$	%	0	0
Degradation costs	€	107,70	39,34
Degradation cyclic	%	0,0174	0,0069
Grid tariff max costs	€	1412,57	1412,57
Grid tariff contract costs	€	928,49	928,49
Grid tariff costs sum	€	2341,06	2341,06
Demand electricity costs	€	204,46	204,46

Warmtebouw

GFM+SDE+DEG

The timeframe of this simulation is: 03-08-2020 until 16-08-2020, 2 weeks.

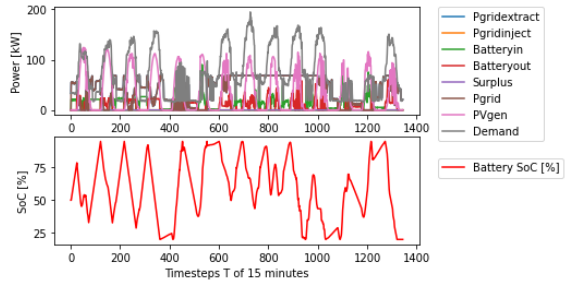

Figure 44 Energy GFM SDE DEG 2-weeks Stamhuis

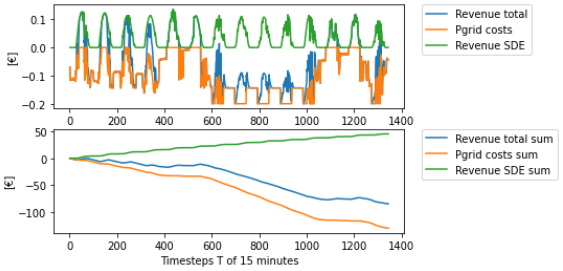

Figure 45 Revenues GFM SDE DEG 2-weeks Stamhuis

Between timesteps 0 until ~400 in Figure 44Figure 47 can be seen that demand is slightly higher than PV generation. Figure 46 shows the battery is charged during the night and low grid tariff. This small deficit in demand and generation shows minimal negative revenues in Figure 45. The subsidy scheme based on grid injection is not strong enough to provide a noticeable share in SDE revenues. A larger battery capacity could increase the amount of energy charged during the night, and excess energy could be injected into the grid, making the SDE scheme more useful. Between timesteps ~1100 until ~1300, more PV is generated than demand, and this subsidy scheme is working as intended. Table 26 shows adding degradation does not change any maximum grid values. The penalty for grid fees is larger than the degradation penalty.

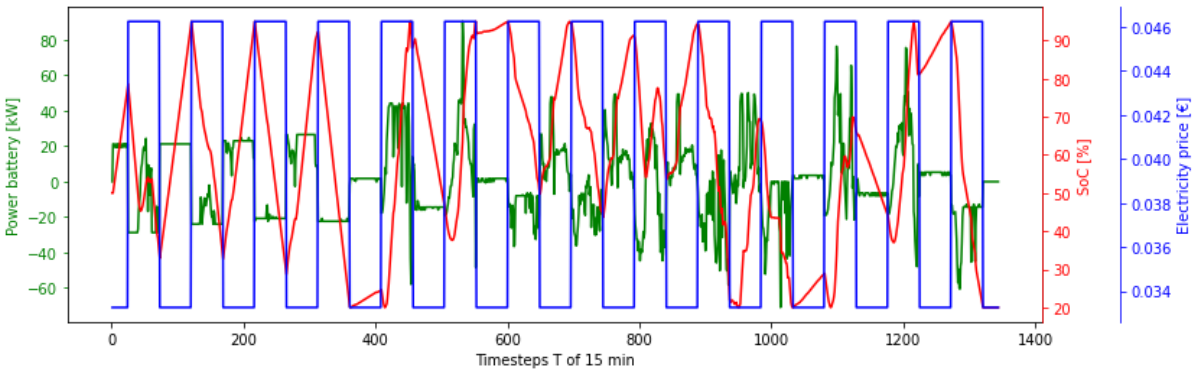

Figure 46 Energy BESS GFM SDE DEG 2-weeks Warmtebouw

Table 26 GFM results Warmtebouw

Warmtebouw		GFM SDE 2-weeks high	GFM SDE DEG 2-week high
Pgridextract max	kW	68,5	68,5
Pgridinject max	kW	68,5	44,3
Pgrid max	kW	68,5	68,5
Surplus	kW	0	0
New Pgrid max	kW	68,5	68,5
Pgridextract costs	€	129,53	130,003
Revenues SDE	€	45,35	45,3585
Revenues total	€	84,17	84,6442
$Congestion_{contract}$	%	0	0
Pgrid max dataset	kW	139,6	139,6
Peak congestion no BESS	kW	-490,4	-490,4
Peak congestion BESS	kW	-561,4	-561,4
$Congestion_{grid}$	%	0	0
Degradation costs	€	22,1991	15,5299
Degradation cyclic	%	0,00012	0,00841
Grid tariff max costs	€	99,91	99,91
Grid tariff contract costs	€	65,67	65,67
Grid tariff costs sum	€	165,58	165,58
Demand electricity costs	€	256,52	256,52

4.2.4 Results Self-Consumption model

For both industrial sites, only the SCM+SDE+DEG results are shown.

Stamhuis

SCM + SDE + DEG

The timeframe of this simulation is: 03-08-2020 to 16-08-2020, 2 weeks.

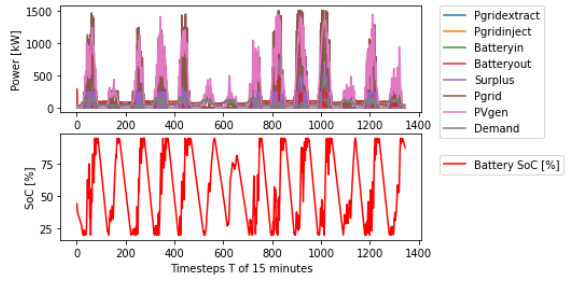

Figure 47 Energy SCM SDE 2-weeks Stamhuis

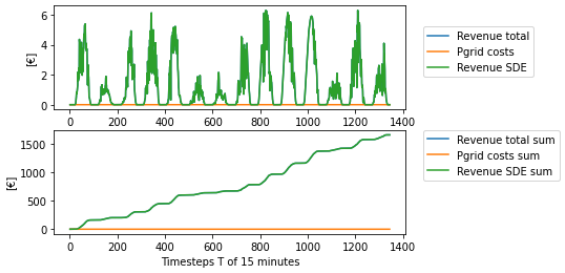

Figure 48 Revenues SCM SDE 2-weeks Stamhuis

By optimizing towards self-consumption whilst having excess PV generation, the battery is being stressed more (Figure 49), as the amount of grid power and max value are restricted. As a result, there are high degradation costs, and the grid connection is used to the physical limit. Significant PV generation excess whilst maintaining as much energy in the system as possible wears the battery down and pushes the maximum grid connection even further. See Table 27 for detailed results.

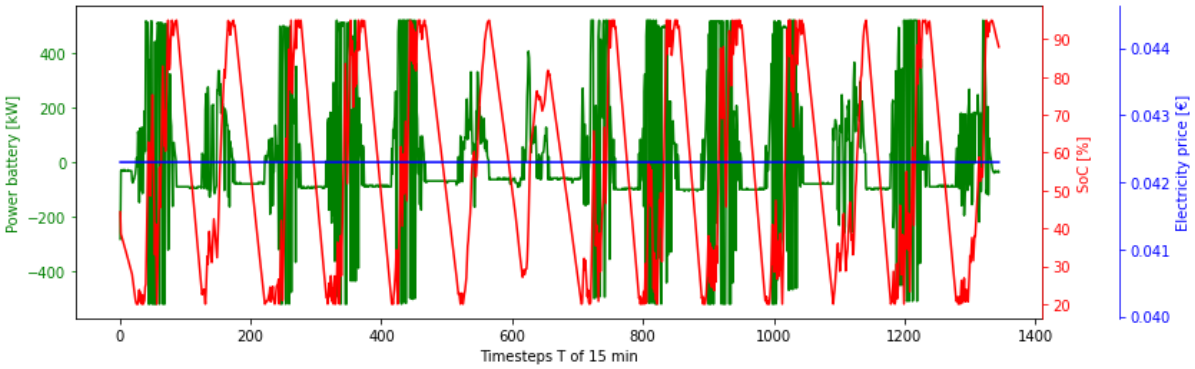

Figure 49 Energy BESS SCM SDE DEG 2-weeks Stamhuis

Table 27 SCM results Stamhuis

Stamhuis		**SCM SDE 2-weeks high**	**SCM SDE DEG 2-week high**
Pgridextract max	kW	0	0
Pgridinject max	kW	256	256
Pgrid max	kW	256	256
Surplus	kW	1244	1244
New Pgrid max	kW	1500	1500
Pgridextract costs	€	0	0
Revenues SDE	€	1652,51	1652,51
Revenues total	€	1652,51	1652,51
$Congestion_{contract}$	%	18,45	18,60
Pgrid max dataset	kW	1416	1416
Peak congestion no BESS	kW	1160	1160
Peak congestion BESS	kW	1244	1244
$Congestion_{grid}$	%	0	0
Degradation costs	€	479,46	439,12
Degradation cyclic	%	0,0779	0,0713
Demand electricity costs	€	204,46	204,46

Warmtebouw

SCM + SDE + DEG

From Figure 52 can be seen that the grid connection is minimized, as there are small amounts of battery power. The battery is not being charged on a regular basis during the night, as it does provide a minimal amount of energy to fulfill the demand. The battery is only charged with excess PV energy, and not during low night grid prices. Consecutive days with more demand than PV, while sometimes the battery can charge with excess PV, shows great potential for self-consumption. See Table 28 for detailed results.

The timeframe of this simulation is: 03-08-2020 until 16-08-2020, 2 weeks.

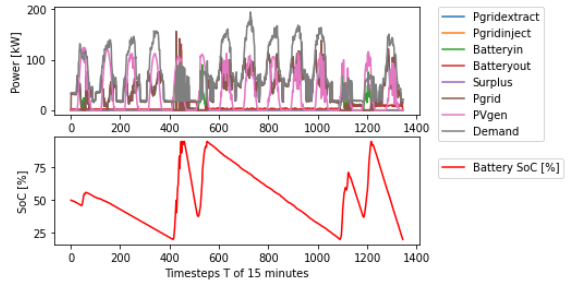

Figure 50 Energy SCM SDE 3-weeks Warmtebouw

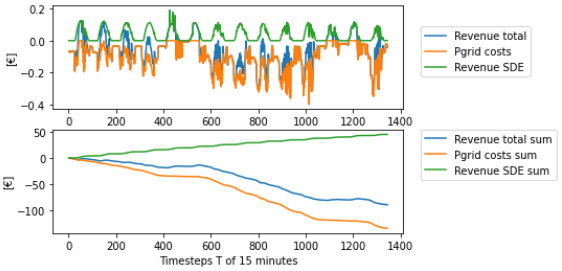

Figure 51 Revenues SCM SDE 3-weeks Warmtebouw

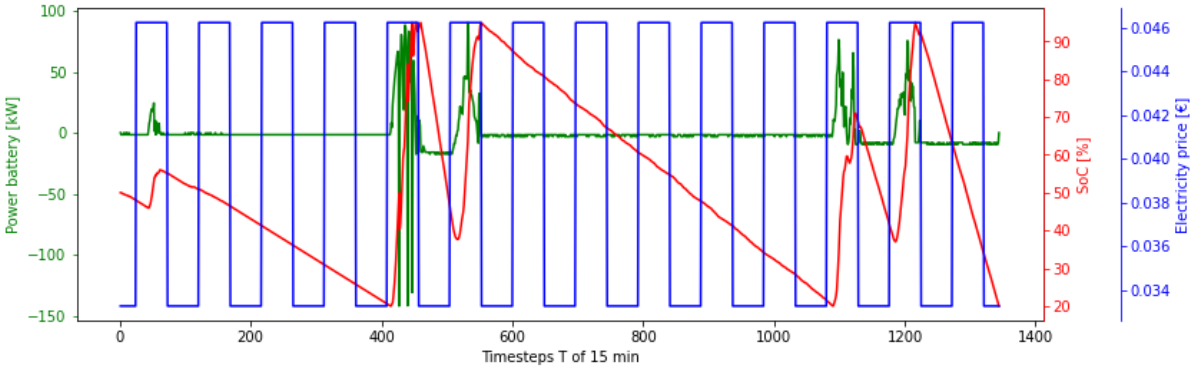

Figure 52 Energy BESS SCM SDE DEG 2-weeks Warmtebouw

Table 28 SCM results Warmtebouw

Warmtebouw		**SCM SDE 2-weeks high**	**SCM SDE DEG 2-week high**
Pgridextract max	kW	139,6	138,0
Pgridinject max	kW	180,2	156,2
Pgrid max	kW	180,2	156,2
Surplus	kW	0	0
New Pgrid max	kW	180,2	156,2
Pgridextract costs	€	134,3	134,9
Revenues SDE	€	45,33	45,33
Revenues total	€	88,99	89,63
$Congestion_{contract}$	%	0	0
Pgrid max dataset	kW	139,6	139,6
Peak congestion no BESS	kW	-490,6	-490,4
Peak congestion BESS	kW	-449,7	-473,7

$Congestion_{grid}$	%	0	0
Degradation costs	€	11,166	6,6315
Degradation cyclic	%	0,006	0,0035
Demand electricity costs	€	256,5	256,5

Direct comparison models

While the models have different objective functions, the goal is to find the optimal BESS strategy to prevent or reduce congestion. First the results of Stamhuis are discussed, afterwards the results of Warmtebouw.

Stamhuis

Table 29 shows the results of the models. As reference, Pgrid max dataset is 1416 kW. Any lower value of New Pgrid max means the model succeeds in reducing congestion. The GBM and GFM succeed in finding a smaller New Pgrid max, the SCM does not. The combination of excessive PV generation, and insufficient battery capacity results in a surplus of 713,5 kW in the GBM and GF models. Peaks in PV generation dominate the results, as the battery capacity is sufficient enough for most of the time. Low degradation costs highlight this, as it means the battery is not used to a large extent.

The current grid contract between Stamhuis and Stedin needs to be expanded during times of large PV generation. However, this does not mean this value of peak power contract is required throughout the year. For instance, during the summer months, the peak power contract could be 1000 kW, and during fall/spring/winter this value is lowered. Another option could be to use the full 1500 kW grid connection to provide FCR service throughout the year, or, to provide FCR services during fall/spring/winter.

Table 29 Direct comparison models Stamhuis

Stamhuis		**GBM SDE DEG 2-weeks high**	**GFM SDE DEG 2-weeks high**	**SCM SDE DEG 2-week high**
Pgridextract max	kW	0	0	0
Pgridinject max	kW	256	256	256
Pgrid max	kW	256	256	256
Surplus	kW	713,5	713,5	1244
New Pgrid max	kW	969,5	969,5	1500
Pgridextract costs	€	0	0	0
Revenues SDE	€	1652,5	1652,5	1652,5
Revenues total	€	1652,5	1652,5	1652,5
$Congestion_{contract}$	%	42,41	44,41	18,60
Pgrid max dataset	kW	1416	1416	1416
Peak congestion no BESS	kW	1160	1160	1160
Peak congestion BESS	kW	713,5	713,5	1244
$Congestion_{grid}$	%	0	0	0
Degradation costs	€	39,3	39,3	439,1
Degradation cyclic	%	0,0063	0,0063	0,0713
Grid tariff max costs	€	1412,5	1412,5	2185,5
Grid tariff contract costs	€	928,4	928,4	1436,5
Grid tariff costs sum	€	2341,0	2341,0	3622,5
Demand electricity costs	€	204,4	204,4	204,4

Warmtebouw

The results of the models show great potential for the battery system. The grid limitation of 600 kW is never reached. For reference, the grid connection required in the dataset is 139,6 kW. Using a BESS lowers this connection to 68,5 kW, when optimized towards grid fees. Comparing the GBM and GFM shows the battery degrades marginally less using GF strategy, and simultaneously lowering Pgrid max. As a result, grid fees are lowered by quite some margin. The Pgridextract costs are almost equal between all models, although the size of the grid connections varies. While the SCM minimizes grid energy and does this in combination with small battery degradation, high Pgrid values make this strategy unfavorable. For the reference model, the total costs would be €593,5, with the GF strategy and technologies installed, this is €265,6.

Warmtebouw can use a grid connection of 68,5 kW. With headroom in the physical grid connection, more PV can be installed. It is however doubtful if a larger grid connection outweighs the extra grid tariff costs. On the other hand, the current SDE subsidies generate more revenues if there is more PV generation compared to demand. On the roof of Warmtebouw, surface area is limited for further PV expansion. Therefore, providing FCR or scaling down entire grid connection capacity would be feasible.

Table 30 Direct comparison models Warmtebouw

Warmtebouw		**GBM SDE DEG 2-weeks high**	**GFM SDE DEG 2-weeks high**	**SCM SDE DEG 2-week high**
Pgridextract max	kW	117,2	68,5	138,0
Pgridinject max	kW	45,90	44,3	156,2
Pgrid max	kW	117,2	68,5	156,2
Surplus	kW	0	0	0
New Pgrid max	kW	0	0	0
Pgridextract costs	€	128,8	130,0	134,9
Revenues SDE	€	45,3	45,3	45,3
Revenues total	€	-83,4	-84,6	-89,6
$Congestion_{contract}$	%	0	0	0
Pgrid max dataset	kW	139,6	139,6	139,6
Peak congestion no BESS	kW	-490,4	-490,4	-490,4
Peak congestion BESS	kW	-512,7	-561,4	-473,7
$Congestion_{grid}$	%	0	0	0
Degradation costs	€	16,49	15,5	6,6315
Degradation cyclic	%	0,0089	0,00841	0,0035
Grid tariff max costs	€	170,8	99,9	227,1
Grid tariff contract costs	€	112,2	65,6	149,5
Grid tariff costs sum	€	283,0	165,5	376,6
Demand electricity costs	€	256,5	256,5	256,5

4.2.5 Results Sensitivity analysis

In the section below the results of the sensitivity analysis are presented. First the electricity price is shown, followed by PV generation and demand. Only the performance parameters of influence on the results are shown. The demand electricity costs are important, as it shows what the costs of electricity would be if no BESS and PV were installed.

Electricity price

Stamhuis

Table 31 shows an increase in electricity price leads to €0 revenues for SDE subsidy. Because the subsidy scheme is based on difference between generation technology price and electricity price, the scheme becomes negative when the electricity price is higher than the generation technology price. With high PV generation and sufficient battery capacity, no grid extract costs are made, while the reference demand costs increase. As a result, the economic benefits are +4.1% with high electricity prices compared to reference. No additional grid fees costs are generated because the required grid connection remains unchanged.

Table 31 Results electricity price Stamhuis

		Reference	**High price**	**Diff.**
Pgridextract costs	€	0	0	
Revenues SDE	€	1652	0	
Demand elec costs	€	204	1933	
Economic benefits	€	1856	1933	+ 4.1 %

Warmtebouw

Table 32 shows there are no SDE revenues with increased electricity price. The economic benefits of the BESS and varying price scheme come to light. The grid electricity costs at night are much lower than the demand electricity costs during daytime, which means the system stores energy at night for using during daytime. This results in economic benefits of +550%. No additional grid fees costs are generated because the required grid connection remains unchanged.

Table 32 Results electricity price Warmtebouw

		Reference	**High price**	**Diff.**
Pgridextract costs	€	130	1031	
Revenues SDE	€	45	0	
Demand elec costs	€	256	2143	
Economic benefits	€	171	1112	+ 550 %

PV generation

As the results show Stamhuis has already excessive PV generation, the analysis is conducted with -20% and +20% PV generation. The results show that Warmtebouw has too little PV generation, and with the installation of more efficient panels or building integrated PV foils, this could increase significantly. Therefore, the analysis is run with 50% more PV generation.

Stamhuis

From Table 33 can be seen that changing PV generation has a linear relationship with benefits. Because the system is limited by battery capacity during high PV peaks, installing more PV results in a higher grid connection, which is related to grid tariff costs. Because there is more PV installed, more revenues from subsidies are generated.

Table 33 Results PV generation Stamhuis

		Diff.	Low gen	Reference	High gen	Diff.
New Pgrid	kW	-25,5%	721	969	1219	+25,5%
Pgridextract costs	€		0	0	0	
Revenues SDE	€	-19,9 %	1322	1652	1983	+19,9 %
Demand elec costs	€		204	204	204	
Grid tariff costs	€	-25,5 %	871	1170	1472	+25.5%
Economic benefits	€	-4,5 %	654	685	715	+4,5%

Warmtebouw

Table 34 shows in case of less PV generation, a larger grid connection is required which rises grid tariff costs, and more energy from the grid energy is required. Besides, less SDE revenues are generated which results in negative benefits. In case of more PV generation, a lower grid connection is required, which means the battery can store this energy without limited by capacity boundaries. Sufficient energy is generated by PV and the SDE scheme based on grid injection is working, as the relative SDE revenue difference is larger compared to the lower generation case. Higher PV generation leads to more economic benefits.

Table 34 Results PV generation Warmtebouw

		Diff.	Low gen	Reference	High gen	Diff.
Pgrid	kW	+39,7%	95	68	55	-19,1%
Pgridextract costs	€	+42,3%	185	130	86	-33,8%
Revenues SDE	€	-51,1%	22	45	70	+55,5%
Demand elec costs	€		256	256	256	
Grid tariff costs	€	+39,3%	115	82	66	-19,4%
Economic benefits	€	-124,8%	-22	88	173	+96%

Demand

Stamhuis

Table 35 shows having lower demand does not mean in necessity there are lower costs. Because of lower demand and still high PV generation, a larger grid connection is required, creating higher grid tariff costs. Compared to the reference scenario there are lower demand electricity costs. However, these benefits are negated by higher grid tariff costs. The battery has insufficient capacity to overcome the deficit in demand and PV generation. This is emphasized in the case of high demand, as this demand reduces the required grid connection and lowers grid tariff costs. It shows high PV generation needs high demand to alleviate insufficient battery capacity.

Table 35 Results demand Stamhuis

		Diff.	Low dem	Reference	High dem	Diff.
New Pgrid max	kW	+3,4%	1002	969	957	-1,2%
Pgridextract costs	€		0	0	0	
Revenues SDE	€		1652	1652	1652	
Demand elec costs	€	-40,1%	122	204	286	+40,1%
Grid tariff costs	€	+3,4	1210	1170	1156	-1,2%
Economic benefits	€	-17,8%	563	685	173	+14,1%

Warmtebouw

In Table 36 the low demand case shows there are more economic benefits. These benefits are contributed by lower required grid connection, more SDE revenues, and lower grid tariff costs. Also, using a BESS with varying price scheme saves demand electricity costs. If there is less PV generation than demand, and the BESS is limited in capacity, the case study benefits from lower demand. In case of high demand, there is not sufficient PV generation and BESS capacity to satisfy demand, and electricity costs rise.

Table 36 Results demand Warmtebouw

		Diff.	Low dem	Reference	High dem	Diff.
Pgrid max	kW	-58,8%	28	68	124	82,2%
Pgridextract costs	€	-67,7%	42	130	228	+75,3%
Revenues SDE	€	+4,4%	47	45	45	
Demand elec costs	€	-39,8%	154	256	359	+40,2%
Grid tariff costs	€	-59,3%	33	82	150	+82,4%
Economic benefits	€	+41,8%	92	6	-125	-71,1%

4.2.6 Results FCR model

In this section the results of the FCR model are presented. As can be seen from Table 11, FCR prices are distributed over a broad range. Because of this, results are produced with different FCR prices. The timeframe which represents the average FCR price is chosen as input parameter of the results presented in this section. To create a comparison between the generic battery model with SDE and degradation, the timeframe is during the summer.

The timeframe of this simulation is: 1 day, 02-08-2020. The average FCR price is €0,02187 [€/kWh].

Stamhuis

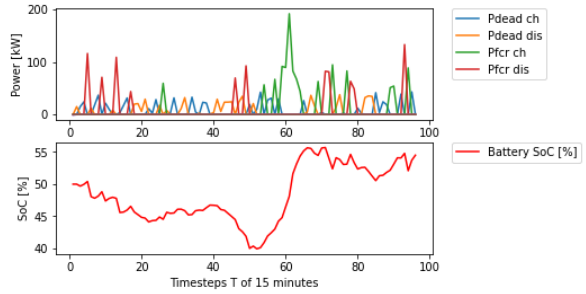

Figure 53 Results energy flow Stamhuis FCR

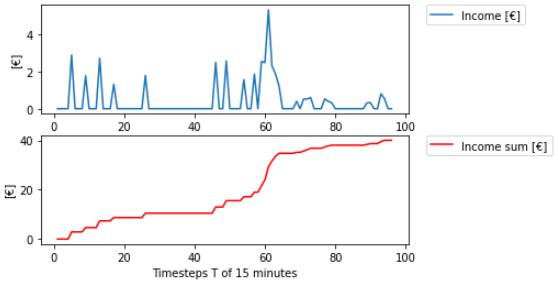

Figure 54 Results revenues Stamhuis FCR

As can be seen in Figure 53 the SoC drops from initial 50% and around timestep 52 rises again. The average grid frequency is 50,00101Hz. As a result, the battery needs to provide a downward service and has to store grid electricity. Therefore, the battery state of charge is 50%> on the last timestep. The battery charges and discharges by 2 separate methods, these are respectively within dead-band zone and whilst providing FCR services. If the grid frequency is in the dead-band zone, no FCR service is required and thus no revenues can be generated. Revenues are generated by charging and discharging during FCR services. The battery cannot provide charge and discharge services simultaneously. In Figure 53 can be seen that energy flow is distributed between Pdeadband charging/discharging and Pfcr charging/discharging on separate timesteps. In Figure 54 the revenue per timestep and cumulative sum of all timesteps can be seen. This results in a total revenue of €40,06 on the last timestep.

Warmtebouw

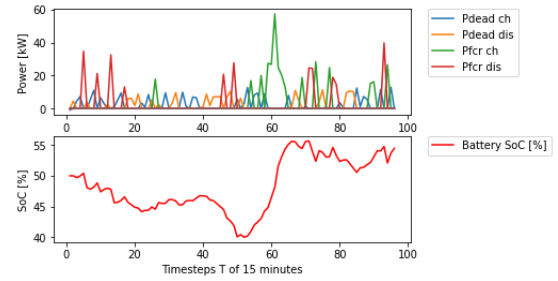

Figure 55 Results energy flow FCR

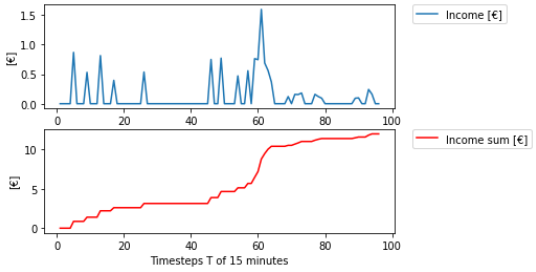

Figure 56 Results revenues FCR

Figure 55 and Figure 56 follow the same pattern as they are based on the grid frequency data and FCR prices, which are constant over the results. The revenues on the last timestep are €11.97. The results are limited by battery power as can be seen from the FCR power equation.

4.2.7 FCR model + Degradation

The timeframe of this simulation is: 1 day, 02-08-2020. The average FCR price is €0,02187 [€/kWh].

Stamhuis

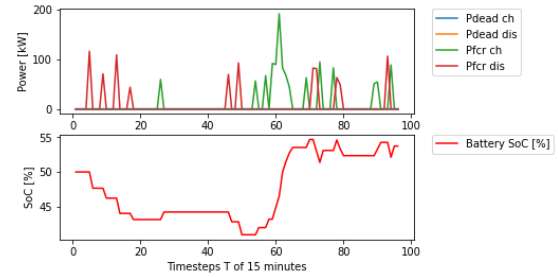

Figure 57 Results energy flow FCR + degradation

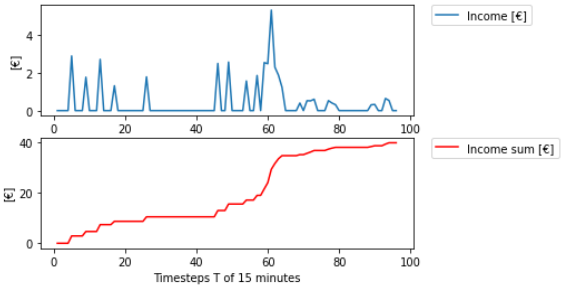

Figure 58 Results revenues FCR + degradation

As can be seen from Figure 57, with battery degradation there is still an energy flow through the battery as opposed to the generic battery model with SDE and degradation. As a result of the degradation penalty, the delta in SoC is limited over a timestep, and the available FCR power is reduced. If a certain delta SoC is exceeded, the degradation costs outweigh the revenues. Charging and discharging during dead-band operation generates negative revenues. There is no optimization done over the dead-band zone, because the dead-band zone is required to maintain a frequency close to 50 Hz. If the dead-band zone would be eliminated from the model and the model would run for a prolonged duration of time, the battery state of charge could reach an upper or lower limit where the battery is not able to provide FCR services. In Figure 58 the revenue per timestep and cumulative sum of all timesteps can be seen. This results in a total revenue of €39,9049 on the last timestep.

Warmtebouw, dead-band

In the previous result the dead-band zone is eliminated from the model. In this result the impact of the elimination of the dead-band zone is reviewed. The industry complex Warmtebouw is chosen because the y-axis has values closer to each other, and the readability is increased. There are 3 results produced: without limitation on the dead-band, with a limitation of 5 [kW] on the dead-band and without dead-band. In Figure 59 the results with 5 kW limitation can be seen, in Figure 60 the results without limitation on dead-band can be seen. The results without limitation on dead-band are discussed below. Minimum and maximum SoC values can be seen in

Table 37.

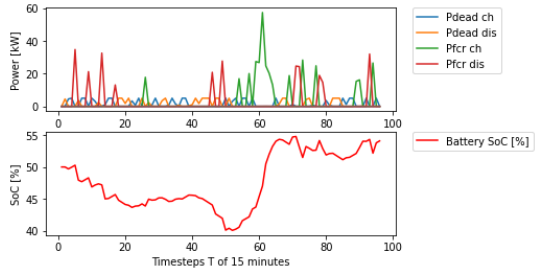

Figure 59 Results limit 5kW dead-band

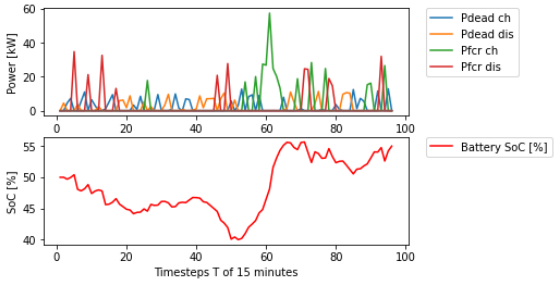

Figure 60 Results no limit dead-band

Using the dead-band does marginally impact the SoC range in this timeframe. While a larger timeframe can be used e.g. multiple days, using a dead-band does not keep the state of charge close to 50%. The reasoning behind this is that with a SoC_0 of 50% and target grid frequency of 50 [Hz], the upper and lower SoC values should remain closer to 50% with dead-band enabled.

Table 37 Dead-band SoC relation

	SoC min %	SoC max %
Without limitation on dead-band	39,98	55,67
With limitation on dead-band	40,04	54,78
Without using dead-band	40,95	54,68

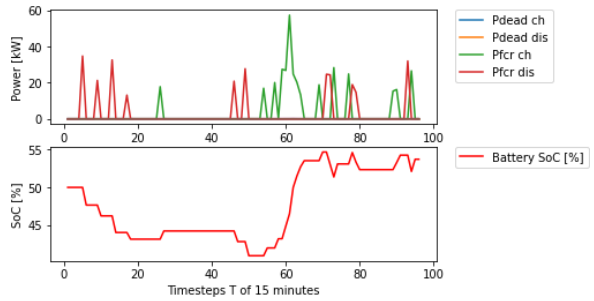

Figure 61 Results no dead-band

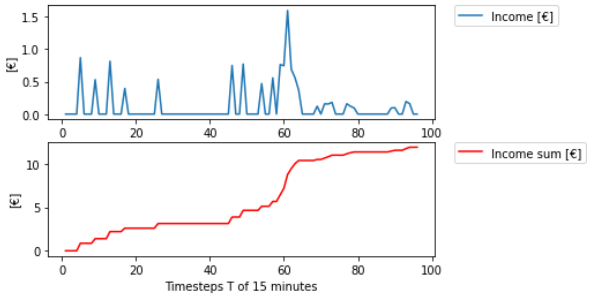

Figure 62 Results revenues no dead-band

In figure the Figure 61 the energy flow is depicted, which follows the same trend as in Figure 57 and is lower due to battery power. In Figure 62 the revenues are depicted and are on the last timestep €11,926, resulting in a difference without degradation of €0,048. The battery charge/discharge power is not high enough for a significant degradation penalty as the SoC_d remains low. This is verified by another result using high FCR prices, see next section.

Warmtebouw, high prices

In this result the upper limit of FCR prices is used, for 1 bidding period of 4 hours this means a price of €121,25. Other bidding periods this day are increased to a daily average of €70,61.

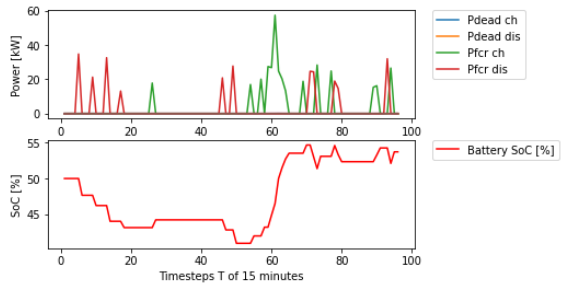

Figure 63 Results energy flow high price

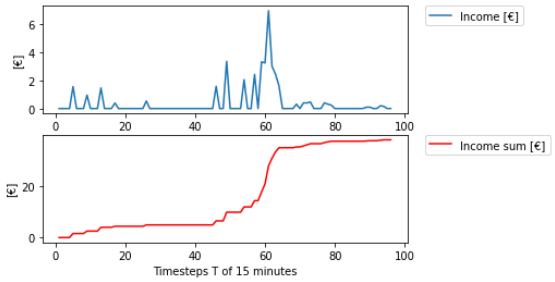

Figure 64 Results revenues high price

The revenues on the last timestep are €37,97 as can be seen in Figure 64. The power flow can be seen in Figure 63 FCR revenues are mainly driven by FCR price. Degradation occurs with higher Pfcr, which is linked to delta SoC, which is the case with higher grid frequency deviations. The frequency of higher grid deviations is limited.

4.2.8 Analysis FCR model + degradation + grid frequency

As a result of the FCR model the revenues are known. The revenues are determined by the FCR price and required FCR power. As frequency deviations are random it is uncertain whether a certain revenue target can be made. However, using the historical grid frequency data, it can be seen that 98% of frequency values are between 49,96557 [Hz] and 50,03615 [Hz]. Using the maximum grid frequency per month (Table 10) and FCR power equation, it is determined how much power is required to provide FCR services, see Table 38

	Stamhuis [kW]		Warmtebouw [kW]		
	Min	Max	Min	Max	Max delta SoC %
January	240,7	275,8	107,9	123,6	31,7
February	287,5	255,3	128,9	114,5	33,1
March	255,3	238,8	114,5	107,1	29,3
April	254,3	247,9	114,3	111,2	29,3
May	243,6	281,4	109,2	126,2	32,4
July	438,5	311,0	196,6	148,4	50,4
August	314,5	256,7	141,0	115,1	36,2
September	293,2	268,0	131,4	120,1	33,7
Average	**291,0**	**269,4**	**130,5**	**120,8**	**33,5**

Table 38. As the battery systems in Stamhuis and Warmtebouw are scaled regarding capacity and charge/discharge rate, instead of *Pfcr*, the delta SoC is used. By reserving a certain delta SoC over 1 timestep for FCR services, the remaining delta SoC over one timestep can be used for other services. It is however redundant to reserve a certain percentage of battery power for FCR if this is only used in an outlier scenario.

Table 38 Min and max FCR power

	Stamhuis [kW]		Warmtebouw [kW]		
	Min	Max	Min	Max	Max delta SoC %
January	240,7	275,8	107,9	123,6	31,7
February	287,5	255,3	128,9	114,5	33,1
March	255,3	238,8	114,5	107,1	29,3
April	254,3	247,9	114,3	111,2	29,3
May	243,6	281,4	109,2	126,2	32,4
July	438,5	311,0	196,6	148,4	50,4
August	314,5	256,7	141,0	115,1	36,2
September	293,2	268,0	131,4	120,1	33,7
Average	**291,0**	**269,4**	**130,5**	**120,8**	**33,5**

See Table 39 for the maximum FCR power when the 98% percentile range as FCR service window is applied.

Table 39 Maximum FCR power 98% percentile range

Stamhuis		Warmtebouw		
Min	Max	Min	Max	Max delta SoC %
149,77	157,25	67,14	70,49	18,08

From Table 39 it can be seen that the maximum charge/discharge rate is 18,08% in 98% of the values. It is redundant to reserve up to 50.4% battery power for FCR. Using a maximum delta SoC of 18,08% and therefore corresponding *Pfcr*, the generic model is analyzed once again. Reserving 18,08% battery

power for FCR services, the new maximum battery power for Stamhuis and Warmtebouw is respectively 712,75 [kW] and 319,51 [kW] for maximum charge/discharge rate and, 427,65 [kW] and 127,81 [kW] for nominal charge/discharge rate.

5. Discussion

5.1 Interpretations

Results of the models cannot directly be compared to other research, as the models work with case-study specific data. However, results regarding subsidy, as well as battery capacity and power can be compared.

For Stamhuis, given the timeframe the subsidy is calculated, the 15-year contracted revenues are much smaller compared to the scheme provided in Table 18. In the SDE contracts it is assumed there are 950 full load hours in a year. However, the 2020 data provides 192 full load hours. Warmtebouw is subjected to the same observations, with 146 full load hours. The SDE schemes are therefore not as profitable as expected. The SDE results provided in the model are in line with the contracts using adjusted full load hours. SDE schemes relieve costs and justify solar investment costs. This revenue stream is however not large enough to recover battery investment costs. From literature this is supported, as multiple sources of income are required for BESS-business cases to be successful (Invest NL, 2021). Using a BESS with large capacity is redundant, as full capacity is rarely used. A lot of capacity is left untouched, and therefore the BESS does not deep cycle frequently, impacting and extending the lifetime of the BESS (Dufo-López & Bernal-Agustín, 2015). The BESS reduces grid connection size and lowers grid tariffs. This is in line with research from Tiemann et al. (2020). Zooming in on the results of the SC model, it is somewhat contrary that reducing grid dependence leads to a larger required grid connection. This is most likely due to a lower sum of energy exchange, but therefore energy spikes are required to satisfy the energy balance at all times. An observation made is that with a large surplus of PV over demand, a fixed price scheme is sufficient, as surplus PV can be stored in the battery. Vice versa, a varying price scheme can charge the battery at night during low costs, and PV during day is used to relieve battery power out, if the objective is to minimize grid costs. Due to high PV generation for the industry site Stamhuis there are no grid costs. This means the optimization towards minimizing grid costs, combined with SDE schemes based on generation, are redundant. Therefore, the only relevant models for Stamhuis are GF and SC. It is still good to run the GBM for Stamhuis, as in different scenarios there can be grid electricity demand.

The results of the FCR model are compromised. With the correct operating strategy, FCR is a feasible revenue stream for BESS. The application of such a control scheme has failed in Gurobi, which means the SoC is uncontrolled, and at a certain moment the battery unable to provide FCR services due to high or low SoC level. Nevertheless, the results show degradation has a small impact on revenues, and this is mainly due to low frequency deviations in which the battery does not have to provide a large amount of power. It is however assumed that while the grid frequency deviates uninterrupted, a fixed average deviation is used for 15 minutes in FCR modelling. When the FCR model performed a run with 10-second data resolution over a period of 4 hours, it showed revenue values which are in line with literature. These results are not included due to time constraints but shows the potential of FCR in the industrial cases Stamhuis and Warmtebouw.

5.2 Limitations

In this research and in the models, assumptions were made which impacts the results. First, the data provided by the industrial sites is in kWh, but in 15-minute resolution. This means power peaks a resolution lower than 15 minutes, e.g. in seconds or minutes are not visible, as they do not exist in the input data in the first place. It is assumed that a given demand/PV generation is constant over this 15-minute resolution, despite energy flows constantly varying. Although 15-minute resolution is recommended for renewable energy sources (Bloch et al., 2019). Second, power flow from the battery can only go one way, e.g. the battery cannot charge and discharge simultaneously. Batteries

experience one current flow, so in reality they cannot be charged and discharged simultaneously. In practice this means excessive PV in relationship to demand cannot flow into the battery, while the battery supplies demand. Over one timestep the battery would charge due to excessive PV, but this concept is taken out due to strange model behavior. As battery capacity is the limiting factor and not power, with the worst-case input data the model is not influence by this choice, but future freak situations could trigger model limitations. It is assumed the grid connection point is the only limiting factor, and therefore no details of cables inside the industrial sites are taken into this research. This is a limitation for precise track of energy flows and discovering bottlenecks. Another model limitation is the set time limit. Gurobi cannot solve towards a certain percentage wherein the model is solved, and the simulation can only be stopped by a time limit. With large files the model is unable to close a 0.03% gap, 99.7% of the 100% ideal result is herein reached. It has been shown that this result is achieved within 1600 seconds; therefore, this is the set time limit. Also, the generic model is simplified from an electrical perspective, and inverter losses are neglected. Furthermore, regarding battery degradation, as stated before large swings in battery SoC increase degradation. Using a piecewise linear constraint, with a maximum delta SoC of ~10% per time step based on battery power, it subdivides delta SoC into smaller steps, resulting in less degradation. Continuing, high dwell time or prolonged low SoC speeds up the degradation process but is not taken into account. Another limitation lies in the optimization concept of using Gurobi. Using Gurobi, potential over a historical timeframe is shown, and because this model knows in advance input data, it can perform actions e.g., optimal strategy of battery SoC. In real time, using real data, this is unknown. Finally, using historical data from the year 2020 gives a somewhat distorted perspective of current reality. The year 2020 was a strange year with an ongoing pandemic. Demand was lower, as the industry sector took a hit and electricity prices were at an all an all-time low (CBS, 2021). Compared to the current situation, a geological conflict drives up the electricity prices to an all-time high (Energiemarktinformatie, 2022), and energy security in Europe is not as obvious as it used to be.

Also, the methodology is adhered to limitations. Validity of the model is challenging, and with this the validation of results. Based on literature the current models are constructed without the validation of results. However, consulting unit checks on all equations does limit the possibility of distorted results.

5.3 Practical limitations

Practical limitations are approached from model perspective and relate to predefined knowledge to use the model. Future users of the model are required to input demand/PV data in 15-minute kWh resolution. Furthermore, battery specifications regarding efficiency, capacity and power are mandatory as well as grid power. For SDE calculations a base amount is required. On the other hand, these values can be filled in according to average values from literature, and only demand/PV data is a real necessity. Regardless of data format, data collection can still be an issue, especially if this data is provided by a 3rd party. The models have become larger during the thesis, and this has especially affected the Gurobi module. Gurobi solves a model by duplicating it into the random access memory (RAM). As a result, large datasets require sufficient RAM for the model to run. It has turned out that running the models with 8GB RAM restricts dataset duration to 2 weeks. It is likely possible to simplify the models, but in the current state and options suffice.

5.4 Future research

Future research should focus on the balance between grid size and battery capacity. In the research gap, Mohamed et al. (2020) proposed congestion can be minimized by operational BESS strategies. It has been confirmed that operational BESS strategies can reduce congestion, albeit congestion optimization does not necessarily mean this favors BESS behavior. Grid congestion is reduced by placing a BESS, and it appears the surplus grid energy e.g., congestion, shifts to the BESS. This is

economically beneficial, however it limits the BESS function to provide other services. The ultimate trade-off has yet to be determined by future research. In future research, the congestion management service GOPACS should be thoroughly reviewed, as with increasing renewable it could play a role in the future. Future case-studies should be more comparative to each other as the industrial sites used in this research were each other's counterparts in day-night scheme, grid contract, SDE contract, battery capacity and magnitude of PV generation. While using counterparts provides more generic information about BESS behavior under certain circumstances, it limits in-depth exploitation of certain scenarios. Besides, it is interesting to see how multiple grid nodes impact the outcome. The industrial sites were not subjected to this, yet in combination with more excessive research on grid fees it could give interesting insights. From literature it can be seen SDE+ subsidy decreased from 2014 to 2019 (Iskandarova et al., 2021). Future case-study specific research should focus on the decreasing prices of these support schemes. The costs analysis could be in more detail, using for example the net present value and payback period, and is recommended for future research.

The current state of the model has been designed for consumers with Python knowledge. The goal is to have an UI which overlays the model, making it applicable to a wider public. An example of this UI could be VICTOR (VIKTOR, 2022). The DT can be created from the current state of the model, and a UI increases usability. In future development of the model, it could be interesting to include PV capacity in the objective function. By doing so, recommendations can be given on possible expansion of PV capacity.

Furthermore, more BESS revenue streams should be researched in greater detail e.g., FCR/FRR, which can be implemented in the DT. Future research can determine an optimal distribution between these grid services and local services using the Pareto front. Besides, the uncertainty analysis was too limited, and more input parameters should be subjected to analysis to increase reliability of results. Finally, it was not possible to create a DT model in this work due to time constraints, and future research should focus on the expansion of the current model and creation of the DT.

5.5 Recommendations

One practical implementation of the model is the usability for other project partners, who cannot be assumed to have Python knowledge or have familiarity with certain quantities and types of data. Developing the model to a DT with UI takes time, yet a preliminary UI would suffice for the partners. A Gurobi license is required for the model to work, so it is recommended that the model runs on a centralized server coupled to UU, which can be accessed by the UI. A similar type of recommendation can be the added functionality of automatic detection of worst-case scenarios in the input dataset. By doing so, an annual dataset can be imported, and possible bottlenecks can be automatically detected. Related to this are the creation of automatic LDC curves and demand/PV/Pgrid graphs over time. Another recommendation is the critical analysis of result types. For this case-study, specific KPI's are constructed, but more or other information can be extracted from the model and potential lies ahead depending on user demands. Recommendations based on model results are further analysis of defining the battery capacity and exploiting of grid fees in detail. It is recommended to expand the FCR model with active SoC management, which makes it applicable for future case-studies.

5.5.1 Stamhuis

The LDC shows that the PV panels at Stamhuis are most likely oriented in a sub optimal way. Based on full load hours, the PV panels at Stamhuis and Warmtebouw generate less SDE income than expected. With future PV expansion it should be kept in mind this has a significant effect on expected SDE revenues. In the case of Stamhuis, installing large amounts of PV does necessarily mean monthly SDE revenues outweigh high grid tariffs driven by large grid connection. Even though using a BESS in this

case is recommended to lower grid tariffs, further BESS services should be exploited in advance to determine battery capacity and power.

The sensitivity analysis shows that a current electricity price makes the SDE scheme redundant, because the grid electricity price is higher than the technology price. It should be determined for future SDE schemes if these are making sense in economic terms. However, a new SDE scheme would be coupled with new PV panels, as the first schedule expires at least in 2032. Seen from the sensitivity based on PV generation, installing more PV generation would not be economical feasible. The battery has insufficient capacity to consume this extra generation, and while the SDE revenues increase, they do not outweigh the extra grid tariff costs. With the current electricity price in mind, it's not recommended to install this extra PV capacity. Besides, even larger PV generation could lead to a higher category grid tariff (appendix B) and require a physical larger grid connection. This recommendation can however change if the demand increases heavily, or a battery with larger capacity is installed. This is based on the demand results, which show that closing the gap between industry demand and PV generation reduces the required grid connection, resulting in lower grid tariff costs. While it should be kept in mind that the annual worst-case scenario is chosen, grid fee costs can be mandatory for a full year. It might be an option for Stamhuis to alter the demand profile, and schedule maximum demand around peak solar hours, especially during summer season.

5.5.2 Warmtebouw

In the case of Warmtebouw, it is recommended that they maximize the amount of PV, to an extent that it surpluses the demand during daytime. By doing so, the SDE++ scheme can work as intended, and more revenues can be generated. However, PV capacity should not exceed the BESS ability to consume this energy, as it creates a trade-off between rising grid fees costs and SDE revenues.

The sensitivity analysis shows that high grid electricity prices with a varying price scheme maximize the economic benefits of the battery. The ability to store energy at night and use during daytime generate significant economic benefits compared to a system without BESS. However, to lower the grid power extract costs, more PV capacity is recommended. This is emphasized by the results of the sensitivity of PV generation. However, SDE revenues give a distorted picture as new installed PV capacity cannot be added to the current contract and high electricity prices have influence on old SDE schemes. At the same time, the grid tariff costs reduce, which means a balance can be found between PV generation and demand. Therefore, it is recommended that Warmtebouw optimizes further expansion of PV capacity against grid tariffs. From the demand sensitivity results can be recommended that Warmtebouw has benefits by installing more energy efficient appliances. The battery is insufficient in capacity to support a change in load profile.

6. Conclusion

A model and alterations to this model have been created to show potential for a BESS system, based on a real-life counterpart, the DT. Development is pushed by seeking an answer to the research question: "*What is the optimal utilization of a BESS using a digital-twin model?*". Mitigation of congestion is herein the target, as the focus lies on local services.

From a methodological standpoint, several sub-research questions are generated to provide building blocks. Battery applications are determined by performing a literature review, and multi-revenue scenarios are created which are in line with this literature review and test BESS operating strategies. These scenarios are tested with models, but before these can be used, an assessment needs to be made regarding the type of data. This data is collected and helps in the process of transforming the GBM to a case-study specific model, which is the foundation of the DT model. For validation of the models, a case-study was performed on the industrial sites Stamhuis and Warmtebouw. Finally, results based on data collection are created and model outputs are generated.

From the case-study performed on Stamhuis and Warmtebouw is can be concluded that the optimal utilization of a BESS is a strategy that includes grid fees, subsidy scheme and electricity costs, and those concepts outweigh the degradation penalty. This holds regardless of industry site PV/demand/grid characteristics. Minimization of grid power does not favor battery degradation, and solely electricity demand costs are outweighed by strategic use of the BESS. Using real measurement data as well as real hardware specific data and physical lay-out, the DT concept comes to light. The grid fees model optimizes to a minimal grid connection for the model to work and using a DT approach, a trade-off between monetary flow and system hardware characteristics is found.

In conclusion, the energy market is a complex market, and these models give a glimpse of ongoing processes. By creating a generic model and adding extra features to this step by step, interactions between complex concepts have been exposed. The scenarios are easily comparable, yet extra or more specific results can be obtained if deemed feasible. It is encouraging to see sufficient battery storage in combination with PV leading to reduction in total and peak grid energy required. While this research does not optimize towards maximum BESS revenues by exploiting more profitable services, it does contribute to the Paris Agreement, and decarbonization of the sector.

Utrecht University

Acknowledgements

Through this way I would like to take some time to reflect on the past period in which I have been conducting my master thesis. I am incredibly grateful for the interesting, educational and most definitely exciting journey I have been on. For over 8 months I have been a part of the CPB project under guidance of Ioannis and Simone. Both of whom have supported me through their incredible flexibility, knowledge and assistance during this process. I would like to thank everyone involved in completing my master's degree and graduating. I couldn't possibly have done this without the help of my supervisors, friends and family. All their infinite patience and willingness to help where possible. Rik, Maurits and Mart for sharing their cleverness and knowledge and helping me out whenever I got stuck. Puck for endlessly motivating me and her curiosity about and proofreading whatever I wrote. I highly appreciate all the support, help and assistance I got and along the road and will forever look back on this period as unbelievably useful and productive and part of my development and growth as a master of energy.

Appendices

Appendix A

These keywords are used in the literature reviews in this report.

BESS	
Libraries	Google Scholar
Keywords	BESS, applications, microgrid, self-consumption, self-sufficiency, services, revenues, technologies, efficiency, aging, materials, PV

Modeling	
Libraries	Google Scholar
Keywords	BESS, efficiency, aging, case-study, microgrid, supply, market, revenues, EV, domestic, storage, industrial, applications, nodes, simulation, PV, demand, constraints, charge/discharge limits

Digital twin	
Libraries	Google Scholar
Keywords	Python, optimization, constraints, industry 4.0, families, concept, fidelity, applications, state-of-the-art, digital twin, digital environment, industry park

Appendix B

Table 40, Table 41, Table 42 show the fixed grid fees from Stedin.

Table 40 Single-use connection fee 2020(Stedin, 2020)

Connection capacity	Connection fee €/connection	Cable tariff €/meter
> 3 x 80 A to 3x 125 A	4210	47,5
> 3 x 125 A to 175 kVA	5330	50,0
> 175 kVA to 630 kVA	36.870	83,0
> 630 kVA to 1000 kVA	38.085	93,0
> 1000 kVA to 1750 kVA	46.700	96,0
> 1750 kVA to 3000 kVA	197.649	130,0

Table 41 Periodical connection fee 2020 (Stedin, 2020)

Connection capacity	Connection category	€/annual	€/month
	LS	32,775	8,7313
> 80 A to 175 kVA	Trafo MS/LS	77,500	6,4583
> 175 kVA to 1750 kVA	MS-distribution	711,500	59,2917
> 1750 kVA to 3000 kVA	Trafo HS+TS/MS	1510,0941	125,8412
> 3000 kVA to 10.000 kVA	Trafo HS+TS/MS	7771,000	647,5833
> 10.000 kVA	TS	Case specific	Case specific

Table 42 Fixed grid fees 2020 (Stedin, 2020)

Transport category	**Contracted power**	**Transport €/month**	**Dubbel tariff normal €/kWh/month**	**Dubbel tariff low €/kWh/month**
LS	to 50 kW	1,50	0.6574	-
Trafo MS/LS	51 to 150 kW	36,75	1.7229	1.4570
MS	151 to 1500 kW	36,75	0.9577	1.4570
Trafo HS+TS/MS reserve	> 1500 kW	230,00	0.926	0.8183
Trafo HS+TS/MS	> 1500 kW	230,00	1.8473	2.3640
TS reserve	> 1500 kW	230,00	0.8157	0.7930
TS	> 1500 kW	230,00	1.6314	2.2908

Appendix C

In Table 43 the contact partners of the project can be seen.

Table 43 Contact partners

Company	Contact person	Job	Description
Berenschot	John Eisses	Consultant	Supervising project schedule
Stamhuis	Harald Kor	Manager Sustainability & Innovation	Contact person
Warmtebouw	Rik Hartog	Energy coach	Contact person

Appendix D

In Table 44 the results of the GBM can be seen. This table is placed here because it shows different time periods next to each other, which does not increase the readability.

Table 44 Results GBM Stamhuis

Stamhuis		**GBM 1-day**	**GBM 1-day high**	**GBM 3-weeks high**
Pgridextract max	kW	0	0	0
Pgridinject max	kW	256	256	256
Pgrid max	kW	256	256	256
Surplus	kW	54,72	715,2	713,5
New Pgrid max	kW	310,72	971,2	969,5
Pgridextract costs	€	0	0	0
Revenues SDE	€	0	0	0
Revenues total	€	0	0	0
$Congestion_{contract}$	%	37,5	46,88	31,25
Pgrid max dataset	kW	588	1416	1416
Peak congestion no BESS	kW	322	1160	1160
Peak congestion BESS	kW	54,72	715,2	713,5
$Congestion_{grid}$	%	0	0	0
Degradation costs	€	6,367	15,42	176,52
Degradation cyclic	%	0,001	0,0025	0,0286
Demand electricity costs	**€**	14,7913	6,95613	306,527

References

Behrangrad, M. (2015). A review of demand side management business models in the electricity market. *Renewable and Sustainable Energy Reviews*, *47*, 270–283.

Bhattacharyya, S., Choudhury, A., & Jariwala, H. R. (2011). Case study on power factor improvement. *International Journal of Engineering Science and Technology (IJEST)*, *3*(12), 8372–8378.

Bloch, L., Holweger, J., Ballif, C., & Wyrsch, N. (2019). Impact of advanced electricity tariff structures on the optimal design, operation and profitability of a grid-connected PV system with energy storage. *Energy Informatics*, *2*(1), 1–19.

Brinkel, N. B. G., Schram, W. L., AlSkaif, T. A., Lampropoulos, I., & van Sark, W. (2020). Should we reinforce the grid? Cost and emission optimization of electric vehicle charging under different transformer limits. *Applied Energy*, *276*, 115285.

Cacuci, D. G., Ionescu-Bujor, M., & Navon, I. M. (2005). *Sensitivity and uncertainty analysis, volume II: applications to large-scale systems*. CRC press.

Calvert, K., & Mabee, W. (2015). More solar farms or more bioenergy crops? Mapping and assessing potential land-use conflicts among renewable energy technologies in eastern Ontario, Canada. *Applied Geography*, *56*, 209–221.

Castillo-Cagigal, M., Caamaño-Martín, E., Matallanas, E., Masa-Bote, D., Gutiérrez, Á., Monasterio-Huelin, F., & Jiménez-Leube, J. (2011). PV self-consumption optimization with storage and Active DSM for the residential sector. *Solar Energy*, *85*(9), 2338–2348.

CBS. (2021). *Martprijzen energie 2000-2020*. https://www.cbs.nl/nl-nl/maatwerk/2021/14/marktprijzen-energie

Choi, J., Lee, J.-I., Lee, I.-W., & Cha, S.-W. (2021). Robust PV-BESS Scheduling for a Grid With Incentive for Forecast Accuracy. *IEEE Transactions on Sustainable Energy*, *13*(1), 567–578.

Chua, K. H., Lim, Y. S., & Morris, S. (2016). Energy storage system for peak shaving. *International Journal of Energy Sector Management*.

Ciocia, A., Amato, A., di Leo, P., Fichera, S., Malgaroli, G., Spertino, F., & Tzanova, S. (2021). Self-Consumption and self-sufficiency in photovoltaic systems: Effect of grid limitation and storage installation. *Energies*, *14*(6), 1591.

Dratsas, P. A., Psarros, G. N., & Papathanassiou, S. A. (2021). Battery energy storage contribution to system adequacy. *Energies*, *14*(16), 5146.

Dufo-López, R., & Bernal-Agustín, J. L. (2015). Techno-economic analysis of grid-connected battery storage. *Energy Conversion and Management*, *91*, 394–404.

Ecker, M., Nieto, N., Käbitz, S., Schmalstieg, J., Blanke, H., Warnecke, A., & Sauer, D. U. (2014). Calendar and cycle life study of Li (NiMnCo) O2-based 18650 lithium-ion batteries. *Journal of Power Sources*, *248*, 839–851.

ECUB. (2021, December 10). *Subsidie voor congestiemanagement en power balancing op utrechtse bedrijventerreinen*. https://www.ecub.nl/cpb

EFRO. (2021). *REACT EU*. Kansen Voor West 2. https://www.kansenvoorwest2.nl/nl/subsidie/react-eu/

Energiemarktinformatie. (2022). *APX Power Spot Exchange*. https://www.energiemarktinformatie.nl/beurzen/elektra/#stockchart_apx

Energievergelijk. (2022). *Netbeheerders overzichtskaart*. https://www.energievergelijk.nl/onderwerpen/netbeheerders

Engeland, K., Borga, M., Creutin, J. D., François, B., Ramos, M. H., & Vidal, J. P. (2017). Space-time variability of climate variables and intermittent renewable electricity production – A review. *Renewable and Sustainable Energy Reviews*, *79*, 600–617. https://doi.org/10.1016/J.RSER.2017.05.046

ENTSOE. (2022a). *Frequency Containment Reserves (FCR)*. https://www.entsoe.eu/network_codes/eb/fcr/

ENTSOE. (2022b). *Prices of actived balancing energy*. https://transparency.entsoe.eu/balancing/r2/pricesOfActivatedBalancingEnergy/show

ENTSO-E, A. C. E. (n.d.). TSOs' proposal for additional properties of FCR in accordance with Article 154 (2) of the Commission Regulation (EU) 2017/1485 of 2 August 2017 establishing a guideline on electricity transmission system operations, 2018. *Online under Https://Consultations. Entsoe. Eu/System-Operations/Synchronous-Area-Operational-Agreement-Policy-1-Lo/Supporting_documents/Article% 20A2_Additional% 20properties% 20of% 20FCR*, *20002*.

Ersdal, A. M., Imsland, L., Uhlen, K., Fabozzi, D., & Thornhill, N. F. (2016). Model predictive load–frequency control taking into account imbalance uncertainty. *Control Engineering Practice*, *53*, 139–150.

Friday Energy. (2022). *Friday Battery Specificaties*. https://friday.energy/friday-battery/

Gowrisankaran, G., Reynolds, S. S., & Samano, M. (2016). Intermittency and the value of renewable energy. *Journal of Political Economy*, *124*(4), 1187–1234.

Groza, E., Kiene, S., Linkevics, O., & Gicevskis, K. (2022). Modelling of Battery Energy Storage System Providing FCR in Baltic Power System after Synchronization with the Continental Synchronous Area. *Energies*, *15*(11), 3977.

Gundogdu, B., Gladwin, D. T., & Stone, D. A. (2017). Battery SOC management strategy for enhanced frequency response and day-ahead energy scheduling of BESS for energy arbitrage. *IECON 2017-43rd Annual Conference of the IEEE Industrial Electronics Society*, 7635–7640.

Gurobi Optimization, L. (2022). *Gurobi*. https://www.gurobi.com/features/academic-named-user-license/

Gurobi Optimization L. (2022). *Sensitivity analysis*. https://www.gurobi.com/documentation/9.5/examples/sensitivity_py.html

Haghnegahdar, A., Razavi, S., Yassin, F., & Wheater, H. (2017). Multicriteria sensitivity analysis as a diagnostic tool for understanding model behaviour and characterizing model uncertainty. *Hydrological Processes*, *31*(25), 4462–4476.

Höök, M., & Tang, X. (2013). Depletion of fossil fuels and anthropogenic climate change—A review. *Energy Policy*, *52*, 797–809.

IBM Corp. (2022). *SPSS*. https://www.ibm.com/support/pages/downloading-ibm-spss-statistics-29

IEA. (2020). *The Netherlands 2020*. https://www.iea.org/reports/the-netherlands-2020

IEA. (2022). *Global Energy Review: CO2 Emissions in 2021*. https://www.iea.org/reports/global-energy-review-co2-emissions-in-2021-2

Invest NL, D. (2021). *Battery energy storage systems in the Netherlands*. https://www.dnv.com/Publications/battery-energy-storage-systems-in-the-netherlands-203632

IPCC. (2022). *Climate Change 2022: Impacts, Adaptation, and Vulnerability. Contribution of Working Group II to the Sixth Assessment Report of the Intergovernmental Panel on Climate Change* .

IRENA. (2021). *Renewable Power Generation Costs in 2020*. https://www.irena.org/-/media/Files/IRENA/Agency/Publication/2021/Jun/IRENA_Power_Generation_Costs_2020.pdf

Iskandarova, M., Dembek, A., Fraaije, M., Matthews, W., Stasik, A., Wittmayer, J. M., & Sovacool, B. K. (2021). Who finances renewable energy in Europe? Examining temporality, authority and contestation in solar and wind subsidies in Poland, The Netherlands and the United Kingdom. *Energy Strategy Reviews*, *38*, 100730.

KNMI. (2022). *Maandsommen zonneschijnduur, normale, anomalieën*. https://www.knmi.nl/nederland-nu/klimatologie/geografische-overzichten/archief/maand/sq

Kobashi, T., Jittrapirom, P., Yoshida, T., Hirano, Y., & Yamagata, Y. (2021). SolarEV City concept: building the next urban power and mobility systems. *Environmental Research Letters*, *16*(2), 024042.

Koch, C., & Maskos, P. (2019). *Passive balancing through intraday trading*.

Lampropoulos, I., Alskaif, T., Schram, W., Bontekoe, E., Coccato, S., & van Sark, W. (2020). Review of energy in the built environment. *Smart Cities*, *3*(2), 248–288.

Lasi, H., Fettke, P., Kemper, H.-G., Feld, T., & Hoffmann, M. (2014). Industry 4.0. *Business & Information Systems Engineering*, *6*(4), 239–242.

Liu, M., Fang, S., Dong, H., & Xu, C. (2021). Review of digital twin about concepts, technologies, and industrial applications. *Journal of Manufacturing Systems*, *58*, 346–361.

Luthander, R., Widén, J., Nilsson, D., & Palm, J. (2015). Photovoltaic self-consumption in buildings: A review. *Applied Energy*, *142*, 80–94.

Magnor, D., Gerschler, J. B., Ecker, M., Merk, P., & Sauer, D. U. (2009). Concept of a battery aging model for lithium-ion batteries considering the lifetime dependency on the operation strategy. *Proceedings of the European Photovoltaic Solar Energy Conference, Hamburg, Germany*, 21–25.

Marchgraber, J., Gawlik, W., & Wailzer, G. (2020). Reducing SoC-Management and losses of battery energy storage systems during provision of frequency containment reserve. *Journal of Energy Storage*, *27*, 101107.

Meindl, B., & Templ, M. (2012). Analysis of commercial and free and open source solvers for linear optimization problems. *Eurostat and Statistics Netherlands within the Project ESSnet on Common Tools and Harmonised Methodology for SDC in the ESS*, *20*.

Moghadam, F. K., Rebouças, G. F. de S., & Nejad, A. R. (2021). Digital twin modeling for predictive maintenance of gearboxes in floating offshore wind turbine drivetrains. *Forschung Im Ingenieurwesen*, *85*(2), 273–286.

Mohamed, A. A. R., Morrow, D. J., Best, R. J., Bailie, I., Cupples, A., & Pollock, J. (2020). Battery energy storage systems allocation considering distribution network congestion. *2020 IEEE PES Innovative Smart Grid Technologies Europe (ISGT-Europe)*, 1015–1019.

Nair, U. R., Sandelic, M., Sangwongwanich, A., Dragičević, T., Costa-Castelló, R., & Blaabjerg, F. (2020). Grid congestion mitigation and battery degradation minimisation using model predictive control in PV-based microgrid. *IEEE Transactions on Energy Conversion*, *36*(2), 1500–1509.

Netherlands Enterprise Agency. (2022, July 13). *Stimulation of sustainable energy production and climate transition (SDE++)*. https://english.rvo.nl/subsidies-programmes/sde

Nyholm, E., Goop, J., Odenberger, M., & Johnsson, F. (2016). Solar photovoltaic-battery systems in Swedish households–Self-consumption and self-sufficiency. *Applied Energy*, *183*, 148–159.

Palensky, P., Cvetkovic, M., Gusain, D., & Joseph, A. (2021). Digital twins and their use in future power systems. *Digital Twin*, *1*(4), 4.

Pang, T. Y., Pelaez Restrepo, J. D., Cheng, C.-T., Yasin, A., Lim, H., & Miletic, M. (2021). Developing a digital twin and digital thread framework for an 'Industry 4.0'Shipyard. *Applied Sciences*, *11*(3), 1097.

PBL Netherlands Environmental Assessment Agency. (2020). *Netherlands Climate and Energy Outlook 2020 – Summary*. https://www.pbl.nl/sites/default/files/downloads/pbl-2020-netherlands-climate-and-energy-outlook-2020-summary-4299.pdf

Puranen, P., Kosonen, A., & Ahola, J. (2021). Technical feasibility evaluation of a solar PV based off-grid domestic energy system with battery and hydrogen energy storage in northern climates. *Solar Energy*, *213*, 246–259.

Python Software Foundation. (2022). *Python*. https://www.python.org/downloads/

Resch, M., Ramadhani, B., Bühler, J., & Sumper, A. (2015). Comparison of control strategies of residential PV storage systems. *Proceedings 9th International Renewable Energy Storage Conference and Exhibition (IRES 2015), Messe Düsseldorf, 9-11 March 2015*, 1–18.

Rijksoverheid. (2022). *Kamerbrief over rol zonne-energy in energietransitie*. https://www.rijksoverheid.nl/documenten/kamerstukken/2022/05/20/zonnebrief

RTE. (2020). *RTE data*. https://www.services-rte.com/en/view-data-published-by-rte.html

RVO. (2022a). *Berekening SDE ++*. https://www.rvo.nl/subsidies-financiering/sde/berekening

RVO. (2022b). *Wetgeving zonne-energie*. https://www.rvo.nl/onderwerpen/zonne-energie/wetgeving

Sevilla, F. R. S., Knazkins, V., Park, C., & Korba, P. (2015). Advanced Control of Energy Storage Systems for PV Installation Maximizing Self-Consumption. *IFAC-PapersOnLine*, *48*(30), 524–528. https://doi.org/10.1016/J.IFACOL.2015.12.433

Shayeghi, E. N. H. (2020). *Sustainable Energy Scheduling of Grid-Connected Microgrid Using Monte Carlo Estimation and Considering Main Grid Penetration Level*.

Shen, P., Ouyang, M., Lu, L., Li, J., & Feng, X. (2017). The co-estimation of state of charge, state of health, and state of function for lithium-ion batteries in electric vehicles. *IEEE Transactions on Vehicular Technology*, *67*(1), 92–103.

Stedin. (2020). *Elektriciteit tarieven 2020*. https://www.stedin.net/zakelijk/betalingen-en-facturen/tarieven#tarieven

Stedin. (2022a). *Liggingsdata kabels en leidingen*. https://www.stedin.net/zakelijk/open-data/liggingsdata-kabels-en-leidingen

Stedin. (2022b). *Stedin tarieven*. https://www.stedin.net/tarieven/download-tarieven

Sulzer, V., Marquis, S. G., Timms, R., Robinson, M., & Chapman, S. J. (2021). Python battery mathematical modelling (PyBaMM). *Journal of Open Research Software*, *9*(1).

TenneT. (2021). *Annual Market Update 2021*. https://www.tennet.eu/fileadmin/user_upload/Company/Publications/Technical_Publications/Annual_Market_Update_2021.pdf

TenneT. (2022). *Dutch ancillary services*. https://www.tennet.eu/markets/dutch-ancillary-services

Tennet. (2022). *Imbalance Pricing System: how are the (directions of) payment determined?* https://www.tennet.eu/fileadmin/user_upload/SO_NL/Imbalance_pricing_system.pdf

Tiemann, P. H., Bensmann, A., Stuke, V., & Hanke-Rauschenbach, R. (2020). Electrical energy storage for industrial grid fee reduction–a large scale analysis. *Energy Conversion and Management*, *208*, 112539.

van Rossum, G. (2007). Python Programming language. *USENIX Annual Technical Conference*, *41*(1), 1–36.

Vartiainen, E., Masson, G., Breyer, C., Moser, D., & Román Medina, E. (2020). Impact of weighted average cost of capital, capital expenditure, and other parameters on future utility-scale PV levelised cost of electricity. *Progress in Photovoltaics: Research and Applications*, *28*(6), 439–453.

VIKTOR. (2022). *Create apps with Python*. https://www.viktor.ai/platform

Xu, B., Oudalov, A., Poland, J., Ulbig, A., & Andersson, G. (2014). BESS control strategies for participating in grid frequency regulation. *IFAC Proceedings Volumes*, *47*(3), 4024–4029.

Yu, W., Patros, P., Young, B., Klinac, E., & Walmsley, T. G. (2022). Energy digital twin technology for industrial energy management: Classification, challenges and future. *Renewable and Sustainable Energy Reviews*, *161*, 112407. https://doi.org/10.1016/J.RSER.2022.112407